8-2011

BIOMARKERS IN THE LOWER HURON SHALE (UPPER DEVONAIN) AS INDICATORS OF ORGANIC MATTER SOURCE, DEPOSITIONAL ENVIRONMENT, AND THERMAL MATURITY

John Kroon
Clemson University, jkroon@clemson.edu

BIOMARKERS IN THE LOWER HURON SHALE (UPPER DEVONAIN) AS INDICATORS OF ORGANIC MATTER SOURCE, DEPOSITIONAL ENVIRONMENT, AND THERMAL MATURITY

A Thesis
Presented to
the Graduate School of
Clemson University

In Partial Fulfillment
of the Requirements for the Degree
Master of Science
Hydrogeology

---

by
John Kroon
August 2011

Accepted by:
Dr. James W. Castle, Committee Chair
Dr. Cindy Lee
Dr. Melissa Riley

ABSTRACT

The Lower Huron Shale (Upper Devonian) is considered the largest shale gas reservoir in the Big Sandy Field in Kentucky and West Virginia. The potential for gas shales, such as the Lower Huron, to produce natural gas is a function of type, amount, and thermal maturation of their organic matter. Twenty-one Lower Huron Shale samples from eight wells located in eastern Kentucky and southern West Virginia were analyzed for biomarker content to interpret biological source of organic matter, depositional environment conditions, and thermal maturity. The following biomarkers were identified: n-alkanes (C_{15} to C_{31}), pristane (Pr), phytane (Ph), steranes (αααR, αααS, αββR, αββS isomers of C_{27} to C_{30} steranes), and hopanes (C_{27}, C_{29}, C_{30} and C_{31} hopanes).

The TAR (terrigenous versus aquatic n-alkanes ratio), n-C_{17}/n-C_{31}, Pr/n-C_{17}, Ph/n-C_{18}, and sterane distribution indicate the source of organic matter in the samples analyzed is predominately marine algae and bacteria. The most source-specific biomarkers identified in the samples were the C_{30} steranes indicative of marine brown algae. The Pr/Ph, Pr/n-C_{17}, Ph/n-C_{18}, Ts/Tm ratios and sterane distribution indicate the samples were deposited in a deep water (>150 m) environment with alternating oxic and anoxic conditions. These results and paleogeographic information support a depositional model involving a seasonally stratified water column.

The C_{27}-20S/(20S+20R), C_{28}-20S/(20S+20R), C_{29}-20S/(20S+20R), C_{28}-αββ/(αββ+ααα), C_{29}- αββ/(αββ+ααα), Ts/(Ts+Tm), and 22S/(22S+22R) ratio values indicate thermal maturities within the early to peak oil generation stages. Contour maps of the biomarker ratio values indicate increasing thermal maturities toward the southeast

within the study area, which corresponds to the direction of increasing maximum burial depth. Biomarker data indicate that gas produced from the Lower Huron Shale in the south-eastern region of the Big Sandy Field has reached a thermal maturity great enough to generate natural gas. Biomarker data indicate that the Lower Huron Shale in the north-western region of the Big Sandy Field was not buried to a great enough depth to generate significant amounts of natural gas. This suggests that gas produced from this area in the Big Sandy Field is biogenic or that thermogenic gas has migrated from more thermally mature areas to the east.

ACKNOWLEDGEMENTS

I would like to thank my advisor, Dr. Castle for providing guidance, time, and helpful suggestions throughout the process of writing this thesis. I would also like to thank my other committee members, Dr. Lee and Dr. Riley for their helpful suggestions and willingness to help.

I would like to thank EQT for graciously providing samples and other useful information needed to complete this research. I would also like to thank the American Association of Petroleum Geologist for providing a grant in aid award to fund some of this research.

TABLE OF CONTENTS

Page

LIST OF TABLES

Page

LIST OF FIGURES

Page

CHAPTER ONE

INTRODUCTION

1.1. Background

Natural gas-producing black shales of Devonian age occur throughout the Appalachian Basin from eastern Tennessee northeastward into Ohio and New York (Milici, 1993). Major production regions of these gas shales occur in southwestern Virginia, eastern Kentucky, southern West Virginia, and southern Ohio. One of these regions is Big Sandy Field in eastern Kentucky and southern West Virginia (Milici et al., 2003). In 2002 the United States Geological Survey estimated total undiscovered gas resources of Big Sandy Field to be 6 trillion cubic feet of gas (Milici et al., 2003). The primary shale gas reservoir of Big Sandy Field is the Upper Devonian Ohio Shale (Hamilton-Smith, 1993). Commercial production of natural gas from shale is dependent on type, amount, and thermal maturity of organic matter found in the source rock (Tissot and Welte, 1978).

Biomarkers are preserved remnants of molecules originally synthesized by organisms with distinctive chemical structures closely related to the biological precursor molecule (Peters et al., 2005; Olcott, 2007). Study of biomarkers is one of only a few ways to directly address origin and history of extractable organic carbon in geological samples. Biomarkers have proven useful for understanding important problems in evolutionary biology, paleobiology, paleoecology, petroleum geology, sedimentary geology, and environmental science (Peters et al., 2005). Biomarkers can vary in abundance from less than one part per million in gas condensates to greater than one part

per hundred in thermally immature rock samples (Peters et al., 2005). Organic geochemical research studying the origin and transformation of biomarkers in modern environments has led to a large number of organic geochemical parameters used to interpret the source of organic matter, environmental conditions during deposition and burial, and thermal maturity of rocks (Peters et al., 2005).

1.2. Research Significance and Objectives

While gas shale reservoirs are becoming an increasingly important economic resource in the United States, there are still many gaps in our understanding of the processes and conditions that generate source beds and reservoirs in shales (Harris, 2005; Piper and Calvert, 2009). Study of these processes and conditions is important to understanding the mechanisms needed to create and preserve gas shale reservoirs through geologic time. Biomarkers may be potentially useful to answer questions surrounding rocks that make up these reservoirs because their complex structures can reveal information about the origin of a that non-biomarker compounds and field observation cannot (Peters et al., 2005). Based on a thorough literature review, no studies were found that attempted to identify biomarkers in Devonian black shale of the Appalachian Basin to address objectives similar to those of this research. The source of oil and gas reserves in Cambrian and Ordovician reservoirs in Ohio was determined by Ryder et al. (1998) using biomarkers in oils produced from these reservoirs and in Ordovician black shale samples from the Appalachian Basin. Brown and Kenig (2004) used biomarkers identified in Middle Devonian through Lower Mississippian black shales of the Illinois and Michigan Basins to assess water column structure during deposition. Schwark and

Empt (2006) identified biomarkers in Ohio Shale samples from the eastern flank of the Cincinnati Arch to assess Paleozoic algal evolution and extinction events. The major objectives of this research were to 1) analyze samples of the Upper Devonian Lower Huron Shale member of the Ohio Shale from eastern Kentucky and southern West Virginia to determine if biomarkers are present and identify biomarkers; 2) interpret biological origin of the biomarkers identified; 3) use the biomarkers to interpret environmental conditions represented by the samples analyzed; and 4) use the biomarkers to interpret thermal maturity of the samples.

1.3. Organization of Thesis

This thesis is organized into four chapters including the Introduction (Chapter 1) and Conclusions (Chapter 4). The two body chapters of this thesis are written and formatted as independent manuscripts intended for submission to scientific journals for review and publication. Therefore, it was necessary to repeat some material and data throughout the chapters. The manuscripts are:

Chapter 2: Organic Matter Source and Depositional Environment of the Lower Huron Shale (Upper Devonian): A Biomarker Approach

Chapter 3: Thermal Maturity Interpretations of Lower Huron Shale (Upper Devonian), Eastern Kentucky and Southern West Virginia, Using Biomarker Maturity Ratios

The second chapter focuses on determining the biological source of organic matter in the samples analyzed and depositional conditions that led to preservation of the organic matter. The third chapter concentrates on using ratios of biomarkers identified in the

samples analyzed to interpret thermal maturity. Representative chromatograms of some of the samples analyzed are included in the appendix.

1.4. References

Brown, T., and Kenig, F., 2004, Water column structure during deposition of Middle Devonian-Lower Mississippian black and green/gray shales of the Illinois and Michigan Basins: A biomarker approach: Palaeogeography, Palaeoclimatology, Palaeoecology, v. 215, p. 59-85.

Hamilton-Smith, T., 1993, Gas exploration in the Devonian shales of Kentucky: Kentucky Geological Survey Bulletin, Bulletin 4, Series XI, http://kgs.uky.edu/kgsweb/PubsSearching/MoreInfo.asp?titleInput=40&map=0**,** 10/26/2009.

Harris, N.B., 2005, The deposition of organic-carbon-rich sediments: models, mechanisms, and consequences—introduction: *In* Harris, N.B. ed, The Deposition of Organic-carbon-rich Sediments: Models, Mechanisms, and Consequences, Special Publication, Society for Sedimentary Geology, Tulsa, p. 1–5.

Milici, R.C., Ryder, R.T., Swezey, C.S., Charpentier, R.R., Cook, T.A., Crovelli, R.A., Klett, T.R., Pollastro, R.M., and Schenk, C.J., 2003, Assessment of undiscovered oil and gas resources of the Appalachian Basin Province, 2002: United States Geological Survey Fact Sheet FS-009-03.

Milici, R.C., 1993, Autogenic gas (self-sourced) from shales- An example from the Appalachian Basin: *In* Howell, D.G., ed, The future of energy gases: U.S. Geological Survey Professional Paper 1570, p. 253-278.

Olcott, A.N., 2007, The utility of lipid biomarkers as paleoenvironmental indicators: Palaios, v. 22, p. 111-113.

Peters, K.E., Walters, C.C., Moldowan, J.M., 2005, The Biomarker Guide: Volume 1 Biomarkers and Isotopes in the Environment and Human History: New York, Cambridge University Press.

Piper, D.Z., and Calvert, S.E., 2009, A marine biogeochemical perspective on black shale deposition: Earth Science Reviews, v. 95, p. 63-96.

Ryder, R.T., Burruss, R.C., and Hatch, J.R., 1998, Black shale source rocks and oil generation in the Cambrian and Ordovician of the Central Appalachian Basin, USA: American Association of Petroleum Geologist Bulletin, v. 82, p. 412-441.

Schwark, L., and Empt, P., 2006, Sterane biomarkers as indicators of Palaeozoic algal evolution and extinction events: Palaeogeography, Palaeoclimatology, Palaeoecology, v. 240, p. 225-236.

Tissot, B.P. and Welte, D.H., 1978, Petroleum formation and occurrence: Berlin, Springer-Verlag, 699 p.

CHAPTER TWO

ORGANIC MATTER SOURCE AND DEPOSITIONAL ENVIRONMENT OF THE LOWER HURON SHALE (UPPER DEVONIAN): A BIOMARKER APPROACH

2.1 Abstract

N-alkanes (C_{15} to C_{31}), pristane (Pr), phytane (Ph), steranes (αααR, αααS, ααβR, ααβS isomers of C_{27} to C_{30} steranes), and hopanes (C_{27} hopanes and C_{29} to C_{31} hopanes) were identified in eighteen of twenty-one Lower Huron Shale (Upper Devonian) samples from eight wells located in eastern Kentucky and southern West Virginia. Biomarker ratios (terrigenous versus aquatic ratio, n-C_{17}/n-C_{31}, Pr/n-C_{17}, Ph/n-C_{18}) and sterane distribution indicate the source of organic matter in the samples was predominately marine algae and bacteria. The C_{30} steranes indicative of marine brown algae were the most source-specific biomarkers identified. Pr/Ph, Pr/n-C_{17}, Ph/n-C_{18}, and 18α(H)-22,29,30-trisnorneohopane/17α(H)-22,29,30-trisnorhopane (Ts/Tm) ratios indicate the samples represent deposition in an environment with alternating oxic and anoxic conditions. The sterane distribution indicates deposition in a deep water (> 150 m) environment. A depositional model is proposed for the Lower Huron Shale involving the establishment and breakdown of a seasonal thermocline. During the warm season, anoxic bottom waters allowed accumulation of phosphorous and nitrogen due to anaerobic decomposition of organic matter. As seasonal temperatures cooled, the thermocline broke down and mixing of shallow water and deep water occurred, allowing the bottom water to become oxic and increasing algal productivity in the shallow water due to upwelling of phosphorous and nitrogen.

2.2. Introduction

Black shales have long intrigued geologists due to their widespread distribution at certain times in the geologic past and early recognition as a major source rock for oil and gas deposits (Piper and Calvert, 2009). Black shales of Middle Devonian to Early Mississippian age span North America from western Canada to the southeastern United States (Ettensohn, 1994). A thorough understanding of the depositional environment responsible for accumulation and preservation of these black shales can reduce oil and gas exploration risk and, therefore, is economically important (Magoon and Dow, 1994). This investigation focused on interpreting depositional conditions represented by the Lower Huron Shale Member of the Upper Devonian Ohio Shale, which is the primary shale gas reservoir of Big Sandy Field, in the Appalachian Basin. In 2002 the United States Geological Survey estimated the total undiscovered gas resources of Big Sandy Field to exceed 6 trillion cubic feet (Milici et al., 2003).

Tyson (1987) listed five factors that are important controls of black shale deposition: sediment texture and grain size, water depth, sedimentation rate, rate of organic matter supply, and bottom water oxygenation. Several different depositional environments have been proposed for the organic rich Devonian black shales of the Appalachian Basin. Rich (1951) suggested the Ohio Shale was deposited in the anoxic portion of a marine basin at depths greater than 100 m based on presence of fine stratifications, abundant organic matter, and phosphate nodules. A shallow water environment (less than 30 to 40 m) was proposed by Conant and Swanson (1961) for the Devonian Chattanooga Shale (Ohio Shale equivalent in Tennessee) based on presence of

a basal unconformity, shallow water sedimentary features, linguloid brachiopods, and overlying sediments of deep water origin. Lineback (1968) suggested the New Albany Shale (Ohio Shale equivalent in Illinois Basin) was deposited in a widespread inland sea with generally shallow water depth (less than 30 to 40 m) and local areas of greater depth (up to 100 m) based on sedimentologic and paleoecologic evidence.

Bottom water oxygenation has been a focus of depositional environment studies of black shales in the Appalachian Basin. Ettensohn et al. (1988) and Kepferle (1989) suggested Devonian black shale in Kentucky was deposited in an anaerobic environment produced by depth-related stratification of basin water based on the identification of aerobic, dysaerobic, and anaerobic strata. Based on carbon, sulfur, and iron relationships, Beier and Hayes (1989) suggested that some black shale intervals of the New Albany Shale were deposited under oxygenated conditions during a time of high organic productivity. Alego el al. (1995) suggested black shale deposition during the Middle to Late Devonian resulted from elevated productivity driven by an increase in terrestrially derived nutrients delivered to the basin by rivers causing anoxic conditions.

More recent depositional interpretations of Upper Devonian black shales in the Appalachian Basin focus on the interdependent roles of sedimentation, primary biological productivity, and microbial decomposition (Murphy et al., 2000). Based on inorganic geochemical data Murphy et al. (2000) suggested that the Devonian Geneseo Formation of western New York was deposited in an environment in which the formation and breakdown of a seasonal thermocline caused water column stratification and mixing, coincident with decrease in a siliclastic input. Sageman et al. (2003) suggested based on

inorganic geochemical data that Middle to Upper Devonian black shales of western New York were deposited in an environment in which biological productivity was increased from upwelling of bio-limiting nutrient due to the establishment and breakdown of seasonal thermoclines.

Sedimentary organic matter found in black shales can provide indicators of depositional environments (Peters et al., 2005a). Organic matter in black shales contains compounds, known as biomarkers, which are preserved remnants of molecules originally synthesized by organisms with distinctive chemical structures closely related to the biological precursor molecule (Peters et al., 2005a; Olcott, 2007). Organic geochemical research on origin and transformation of biomarkers in the environment has led to a large number of organic geochemical parameters which can be used to interpret the source of organic matter, environmental conditions during deposition and burial, and thermal maturity of rocks (Peters et al., 2005a). The biomarker components of a sediment extract reflect precursor compounds in the organisms that contributed organic matter at the time of sediment deposition, and therefore, can provide valuable information about the environmental conditions during deposition Numerous researchers have interpreted depositional environment conditions of black shales from biomarker data (Obermajer et al., 1997; Pancost et al., 1998; Obermajer et al., 1999; Marynowski et al., 2000; Kotarba and Clayton, 2003; Forster et al., 2004). Diverse approaches have been used previously to interpret the paleoenvironmental conditions responsible for accumulation and preservation of black shales in the Appalachian Basin. Obermajer et al. (1997) used biomarkers identified in Middle Devonian Marcellus and Upper Devonian Kettle Point

black shales in southern Ontario to assess the source rock potential of those units. The source of oil and gas reserves in Cambrian and Ordovician reservoirs in Ohio was determined by Ryder et al. (1998) by identifying biomarkers in oils produced from these reservoirs and in Ordovician black shale samples from the Appalachian Basin. Brown and Kenig (2004) used biomarkers identified in Middle Devonian through Lower Mississippian black shales of the Illinois and Michigan Basins to assess water column structure during deposition. Paleozoic algal evolution and extinction events were determined by Schwark and Empt (2006) from biomarkers in Ohio Shale samples from the eastern flank of the Cincinnati Arch. However, based on a thorough literature review, no published papers were found that attempted to identify biomarkers in Devonian black shale of the Appalachian Basin in order to interpret depositional environment.

Biomarker analysis has the potential to be very useful in understanding depositional environments of the Ohio Shale and the origin of organic matter in major shale gas reservoirs of the eastern United States. Therefore, the objectives of this study were to 1) identify biomarkers in the Lower Huron Shale member of the Ohio Shale in eastern Kentucky and southern West Virginia; 2) interpret biologic source of organic matter in the Lower Huron Shale using the biomarkers identified; and 3) interpret depositional environment of the Lower Huron Shale using the biomarkers identified. Well drilling and completions of the Ohio Shale most commonly target the Lower Huron Shale member due to its high total organic carbon content and abundant natural fractures (Nuttal et al., 2005). Cutting samples were analyzed from eight horizontal wells recently drilled into the Lower Huron Shale for natural gas production.

2.3 Geological Setting

The Appalachian Basin is a foreland basin that developed during the late Proterozoic and Paleozoic (Roen, 1993). The basin trends northeast and is approximately 1500 km in length and 150 to 500 km in width. It extends from the Adirondack Mountains in the north to the Black Warrior Basin in the south. To the northwest the Findlay and Algonquin Arches separate the Appalachian Basin from the Michigan Basin, and to the west the Cincinnati Arch separates it from the Illinois Basin (Roen, 1993) (Figure 2.1A). The Appalachian Basin consists of Paleozoic strata ranging from 600 to 900 m thick along the Cincinnati Arch to more than 13,700 m thick to the east in Central Pennsylvania (de Witt and Milici, 1989). Sedimentation in the basin was influenced by three major orogenies: the Taconian (Middle to Late Ordovician), the Acadian (Early to Middle Devonian), and the Alleghenian (Late Carboniferous to Permian) (Moody et al., 1987). The Upper Devonian interval is referred to as the Ohio Shale east of the Cincinnati Arch in eastern Kentucky and southern West Virginia and is subdivided into five recognizable members: Cleveland Shale, Three Lick Bed, Upper Huron Shale, Middle Huron Shale, and Lower Huron Shale (Figure 2.2) (Hamilton-Smith, 1993). The Lower Huron Shale is grayish-black, brownish-black, and black shale interbedded with minor green-gray shale (Hamilton-Smith, 1993). It contains zones of spheroidal to ellipsoidal dolomitic limestone nodules and septaria and a few beds of limestone from 2.5 to 10.0 cm. thick (de Witt et al., 1993). In the study area the Lower Huron Shale ranges in thickness from 24 to 43 m.

Conant and Swanson (1961) and Lineback (1968) proposed depositional models for the Chattanooga Shale (Ohio Shale equivalent in Tennessee) and the New Albany Shale (Ohio Shale equivalent in Illinois Basin) involving black shale deposition in shallow (<100 m) water depths based on sedimentologic and paleoecologic evidence. Based on stratigraphic evidence Ettensohn et al. (1988) and Kepferle (1989) proposed depositional models for Devonian-Mississippian black shale sequences in Kentucky involving permanent pycnoclines with constantly anoxic bottom water.

2.4. Methods

2.4.1. Biomarker Identification

2.4.1.1. Sampling

Twenty-one samples were collected and analyzed from drill cuttings from eight recently drilled horizontal wells targeting the Lower Huron Shale (Figure 2.1B; Table 2.1). The wells were drilled using air, preventing the samples from being contaminated by organic rich drilling muds. Rock cuttings were collected during the drilling process in 3 to 10 meter intervals and consist of chipped rock fragments and powder. In each well one to four samples weighing 75 grams each were selected from the horizontal section of the well. Selection criteria included high organic carbon content, determined using the gamma and density logs for each well, and spacing of samples in the well bore.

2.4.1.2. Sample Preparation

Samples were prepared in four batches of five samples each with one procedural blank in each batch. Samples were ground to a fine powder using a ceramic mortar and pestle. Between samples the mortar and pestle were cleaned with hot tap water and

rinsed with DI water, methanol (MeOH), and dichloromethane (DCM). The sequential extraction procedure for the powdered sample and instrumental analysis of extract for biomarker detection follows the methodology of Brocks et al. (2003), Forster et al. (2004), and Sherman et al. (2007) (Table 2.2).

Soluble organic matter was extracted from 75 g of the powdered samples ultrasonically with a Fisher Sonic Dismembrator Model 300 for 30 min in 40 ml DCM (HPLC grade), and the extract was collected. Forty ml additional DCM was added to the powdered sample and the ultrasonication process was repeated. Extracts were combined. Copper pellets (Fisher Scientific C-430 Copper Metal) were placed in a 14 mm O.D. chromatography tube plugged with cotton wool. The copper was rinsed with 37% hydrochloric acid until it reached a bright color. The copper was then rinsed with DI water, methanol, and DCM seven times each. Five g of the acid activated copper was added to the vials containing the combined extracts and stirred for 8 h to remove elemental sulfur. The extracts were filtered (Whatman 44 filter paper) to remove the copper, and the filtrates were then reduced to 1 ml under a stream of ultra pure (99.998%) nitrogen gas. Fifty ml of n-pentane (HPLC Grade) was added to the extracts and allowed to sit 8 h to precipitate asphaltenes. The extracts were filtered (Whatman 44 filter paper) to remove the asphaltenes and the asphaltene free extract was evaporated to dryness under a stream of ultra pure nitrogen gas.

The extracts were separated into saturated (compounds with no double or triple bonds) and aromatic (compounds with one or more benzene ring) fractions by liquid chromatography using Pasteur pipettes. Silica gel (3 g) was activated by heating at 110

°C for 8 h. The activated silica gel was cooled, and 5 ml hexane (HPLC grade) was added to make a slurry. Pasteur pipettes were plugged with cotton wool and filled with the slurry. The asphaltene free extracts were dissolved in 1 ml DCM and added to the top of the column. Saturated hydrocarbons were eluted with hexane (4 ml) and aromatic hydrocarbons with hexane:DCM (1:1 v/v, 4 ml). The fractions were evaporated to dryness and dissolved in 1 ml DCM and put in autosampler vials for analysis. An extraction variability of 1.6% was determined using three samples spiked with a 5β-cholane standard.

2.4.1.3. Instrumental Analyses

2.4.1.3.1 Gas Chromatography-Flame Ionization Detection (GC-FID)

GC analyses were performed on the saturated hydrocarbon fraction in order to obtain normal (n)-alkanes, pristane, and phytane data with a Hewlett Packard 5890 Series II gas chromatograph equipped with a FID and autosampler. N-alkanes are compounds consisting of carbon and hydrogen in which the carbon atoms are arranged linearly (Peters et al., 2005a) (Figure 2.3). Pristane and phytane are acyclic isoprenoid hydrocarbons (Figure 2.3) that are created by the phytyl side chain of chlorophyll a in phototrophic organisms and bacteriochlorophyll a and b in purple sulfur bacteria (Peters et al., 2005a). Samples (1.0 µl of each) were injected in splitless mode with helium as the carrier gas onto a Zebron ZB-5 column (30 m x 0.25 mm inner diameter, 0.25 µm film thickness). The helium flow rate was set at 1.0 ml/min. The flow rate of the air and hydrogen were 300 ml/min and 30 ml/min respectively. The injector was programmed for 250 °C and the detector for 310 °C. The oven was programmed at 40°C (2 min) and

heated to 310°C at 4°C/min, with a final hold time of 15 min. The amounts of n-alkanes, pristane, and phytane were determined from the integrated area of the chromatogram peak of each compound.

2.4.1.3.2 Gas Chromatography-Mass Spectroscopy-Mass Spectroscopy

Gas chromatography-mass spectroscopy-mass spectroscopy (GC-MS-MS) analyses was performed on the saturated fraction in order to obtain sterane and hopane biomarker data with a Varian Model 4000 GC/MS/MS equipped with an autosampler. Sterane is a class of tetracyclic saturated biomarkers derived from sterols in eukaryotic cells, and hopane is a class of pentacyclic saturated biomarkers derived from plasma membranes in prokaryotic cells (Peters et al., 2005a) (Figure 2.3). Parent/daughter transitions were analyzed in MS-MS mode with a collision energy of 70EV (Table 2.3). The samples (1.0 µl of each) were injected in splitless mode with helium as the carrier gas (1.0 ml/min flow rate) onto a Restek Rtx-5 column (30 m x 0.25 mm inner diameter, 0.25 µm film thickness). The GC oven was programmed at 40°C (2 min) and heated to 310°C at 4°C/min, with a final hold time of 15 min. The amounts of steranes and hopanes identified were determined from the integrated area of the chromatogram peak of each compound.

2.4.1.4 Distribution of Biomarkers Identified in the Samples

The samples analyzed were characterized based on abundance of the biomarkers identified in each. The most abundant n-alkane, most abundant sterane, and most abundant hopane were determined in each sample based on integrated peak areas of the compounds identified. Also, the most abundant n-alkane between n-C_{16} to n-C_{18} and the

most abundant n-alkane between n-C_{27} to n-C_{33} were determined in each sample. The distribution of steranes identified in the samples was determined based on the percentage of each sterane (C_{27}, C_{28}, and C_{29}) making up the total of C_{27} to C_{29} steranes.

2.4.2 Determination of Biological Source of Organic Matter

The identification of source-specific biomarkers is used to interpret the biological source of organic matter. The carbon skeleton of biomarkers is identical or slightly altered relative to the structure of their precursor compounds generated by living organisms (Peters et al., 2005a). Some biomarkers indicate a general biological source (e.g. marine plankton) and others indicate a highly specific biological source (e.g. certain families of brown algae). The biological source of the organic matter in the Lower Huron Shale was evaluated based on the terrigenous versus aquatic ratio (TAR), pristane/n-heptadecane (Pr/n-C_{17}), phytane/n-dotriacontane (Ph/n-C_{18}), n-C_{17}/n-C_{31}, and the distribution of C_{27} to C_{30} steranes. Ratio values were calculated using peak areas of compounds. N-alkanes, pristane, and phytane standards were run and equivalent peak areas were obtained indicating a similar response factor for each standard. Brocks et al. (2003) showed that it is suitable to use uncorrected peak areas of steranes and hopanes to calculate ratios.

2.4.3. Depositional Environment Interpretations

Biomarkers are used to interpret depositional environment based on the known physiological, biological, and environmental limitations of organisms from which the biomarkers originated (Peters et al., 2005b). Different depositional environments are characterized by distinctive and unique assemblages of biomarkers (Peters et al., 2005b).

The depositional environment of the Lower Huron Shale was interpreted based on the Pr/Ph ratio, Pr/n-C_{17} versus Ph/n-C_{18}, 18α(H)-22,29,30-trisnorneohopane/17α(H)-22,29,30-trisnorhopane (Ts/Tm), and the distribution of C_{27} to C_{29} steranes. Ratio values were calculated using peak areas of compounds.

2.5. Results

2.5.1. Biomarkers Identified

2.5.1.1. N-alkanes and Isoprenoids

N-alkanes ranging from n-C_{10} to n-C_{31}, pristane, and phytane were identified in all samples except C3650, D5000, and D7270 (Table 2.4). The distributions based on integrated peak areas of n-alkanes and isoprenoids identified in each sample are listed in Table 2.5. The most abundant n-alkane in ten of the samples is n-C_{12}. N-C_{13}, n-C_{14}, and n-C_{16} are the most abundant n-alkane in two samples each, and n-C_{15} is the most abundant n-alkane in one sample. The aquatic range of n-alkanes is defined as n-alkanes with 16 to 18 carbon atoms because they typically originate from aquatic algae and cyanobacteria (Peters et al., 2005a). The most abundant component in the aquatic range of n-alkanes is n-C_{16} in seventeen samples. The land plant range of n-alkanes is defined as n-alkanes with 27 to 33 carbon atoms because they orginate from waxes typical of land plants (Peters et al., 2005a). The most abundant component in the land plant range of n-alkanes is n-C_{27} in fourteen samples. Pristane is the most abundant isoprenoid in all of the samples analyzed where isoprenoids were detected.

2.5.1.2. Steranes

The ααα*R*, ααα*S*, αα*β*R, and αα*β*S isomers of cholestane (C_{27} sterane), 24-methylcholestane (C_{28} sterane), 24-ethylcholestane (C_{29} sterane), and 24-propycholestane (C_{30} sterane) were identified in all samples except C3650, D5000, and D7270 (Table 2.6). The distributions based on integrated peak areas of steranes identified in each sample are listed in Table 2.5. The isomers of cholestane (C_{27}) are the most abundant sterane isomers comprising 28-64% of the total C_{27} to C_{29} steranes, followed by 24-ethylcholestane (C_{29}) comprising 14-51%, and 24-methylcholestane (C_{28}) comprising 12-44% (Table 2.5). 5α(H),14α(H),17α(H)-Cholestane-20S (C_{27}ααα-S) is the most abundant sterane isomer in eight samples (Table 2.5).

2.5.1.3. Hopanes

The following hopanes were identified in all samples except C3650, D5000, and D7270: 18α(H)-22,29,30-trisnorneohopane (Ts), 17α(H)-22,29,30-trisnorhopane (Tm), 17α(H),21β(H)-30-norhopane (C_{29}H), 18α(H)-norneohopane (C_{29}Ts), 17α(H),21β(H)-hopane (C_{30}H), 17α(H),21β(H)-homohopane-22S (C_{31}H-S), and 17α(H),21β(H)-homohopane-22R (C_{31}H-R) (Table 2.6). The distributions based on integrated peak areas of hopanes identified in each sample are listed in Table 2.5. C_{29}H is the most abundant hopane in all samples where hopanes were detected (Table 2.5).

2.5.2. Biological Source of Organic Matter

2.5.2.1. N-alkane Parameters

The use of n-alkanes to evaluate organic matter source is based on short chain alkanes (n-C_{15} to n-C_{19}) being derived from marine algae and long chain alkanes (n-C_{25} to

n-C_{31}) being derived from land plant waxes (Peters et al., 2005b). The TAR ratio is defined as: (n-C_{27} + n-C_{29} + n-C_{31})/(n-C_{15} + n-C_{17} + n-C_{19}). Values >1 for this parameter indicate more land plant sources than marine algae sources and low values (<1) indicate more marine algae sources than land plant sources. TAR values for the analyzed samples range from 0.10 to 0.33 (Table 2.7), which indicates that the biological source of organic matter in the Lower Huron Shale is dominated by marine algae. A simplified parameter that reflects the relative contribution of marine algae versus land plants to preserved organic matter is the ratio of n-C_{17}/n-C_{31}. Higher values (>2) for this parameter indicate more marine algae sources than land plant sources, and low values (<2) indicate more land plant sources than marine algae sources (Forster et al., 2004). N-C_{17}/n-C_{31} values range from 3.30 to 40.0 for the samples analyzed (Table 2.7). These high values (>2) indicate the source of organic matter is dominated by marine algae, which is consistent with the TAR values. Degradation of organic matter in sedimentary systems can alter the n-alkane distribution causing errors in the TAR and n-C_{17}/n-C_{31} source signals by enriching the more stable land derived n-alkanes through loss of the more labile algal derived n-alkanes (Forster et al., 2004). The predominant marine algal signature in the TAR and n-C_{17}/n-C_{31} parameters suggests conditions conducive to preservation were present with little microbial degradation.

2.5.2.2. Pr/n-C17 versus Ph/n-C18

The relationship between the Pr/n-C_{17} and Ph/n-C_{18} biomarker parameters has been shown to be related to the type (I, II, II/III) of kerogen in sedimentary organic matter (Obermajer et al., 1999). A scatter plot of Pr/n-C_{17} versus Ph/n-C_{18} indicates that

kerogen in the samples analyzed can be classified as type II (Figure 2.4). Type II kerogen is defined as having a hydrogen to carbon ratio greater then 1.25, an oxygen to carbon ratio between 0.03 and 0.18, and originates from mixtures of zooplankton, phytoplankton, and bacterial debris in marine sediments (Tissot and Welte, 1978).

2.5.2.3. Sterane Parameters

The use of the distribution of C_{27} to C_{29} regular steranes in determining biological source of organic matter is based on observations that C_{27} steranes originate predominantly from marine algae; C_{28} steranes from yeast, fungi, bacterial plankton, and algae; and C_{29} steranes from land plants (Peters et al., 2005b). The relationship between sterane composition and biological source of ancient sediments was developed by Huang and Meinschein (1979) and Volkman (2003). A ternary plot of the C_{27} to C_{29} regular steranes indicates that marine algae and bacteria are the dominant biological sources of organic matter in the samples analyzed (Figure 2.5A).

The ratio of C_{29} αααR to C_{27} αααR steranes (C_{29}/C_{27}) can be used to interpret the contribution of marine algae to preserved organic matter relative to the contribution of land plants (Samuel et al., 2009). Low values (<1) of this ratio indicate more algal sources than land plant sources, and high values (>1) indicate more land plant sources than algal sources (Peters et al., 2005b). The C_{29}/C_{27} values range from 0.13 to 0.88 (Table 2.7) for the samples analyzed, indicating that the organic matter is dominated by marine algal sources relative to land plant sources. Additional evidence from steranes identified in the samples analyzed for dominance of marine algal sources is the presence

of C_{30} steranes, which are diagnostic of marine chrysophyte algal contribution to preserved organic matter (Samuel et al., 2009).

2.5.3 Depositional Environment Interpretations

2.5.3.1. Biomarker Parameters

Redox conditions at the time of sediment deposition were interpreted from three biomarker parameters: Pr/Ph, Pr/n-C_{17} versus Ph/n-C_{18}, and Ts/Tm. The distribution of C_{27} to C_{29} steranes was used to interpret deep marine (>150 m) versus shallow marine and lacustrine depositional environments at the time of sediment deposition.

2.5.3.1.1. Pr/Ph

The ratio of pristane to phytane can be used as an indicator of redox conditions in ancient sediments (Didyk et al., 1978). Pristane and phytane may originate from the oxidation or reduction, respectively, of the phytol side chain of chlorophyll, which is controlled by oxic or anoxic conditions during sedimentation (Hughes et al., 1995). Pr/Ph ratio values greater than 3.0 indicate oxic conditions, values below 1.0 indicate anoxic conditions, and values between 1.0 and 3.0 indicate alternating oxic and anoxic conditions (Didyk et al., 1978).

The Pr/Ph ratio values range from 1.14 to 1.69 in the samples analyzed (Table 2.7). These values indicate the Lower Huron Shale was deposited in alternating oxic and anoxic conditions. Some researchers (ten Haven et al., 1987) have raised objections to interpreting redox conditions from the Pr/Ph ratio, suggesting possible sources other than chlorophyll for pristane and phytane and possible influence of thermal maturity on the ratio. However, redox interpretations using the Pr/Ph ratio are consistent with

interpretations using other biomarker redox indicators (Pr/n-C_{17} versus Ph/n-C_{18} and Ts/Tm) in this study.

2.5.3.1.2. Pr/n-C_{17} versus Ph/n-C_{18}

Redox conditions at the time of sediment deposition can be inferred from log-log plots of Pr/n-C_{17} and Ph/n-C_{18} (Lijmbach, 1975). The Pr/n-C_{17} versus Ph/n-C_{18} plot for the samples analyzed indicates sediment deposition in an environment with alternating oxidizing and reducing conditions (Figure 2.6), which is consistent with Pr/Ph and Ts/Tm redox interpretations in this study.

2.5.3.1.3. Ts/Tm

Oxidizing conditions in the depositional environment favor preservation of Tm over Ts, while reducing conditions favor preservation of Ts over Tm (Moldowan et al., 1986). Ts/Tm values greater than 2.0 indicate predominately anoxic conditions, values less than 1.0 indicate predominately oxidizing conditions, and values between 1.0 and 2.0 indicate alternating oxic and anoxic conditions (Solevic et al., 2008). Ts/Tm values in the samples analyzed range from 1.20 to 3.75 except for a value of 7.40 in one sample (Table 2.7). The Ts/Tm value is between 1.0 and 2.0 in 11 of the 18 samples analyzed indicating alternating oxic and anoxic conditions. This interpretation is consistent with interpretations from Pr/Ph and Pr/n-C_{17} versus Ph/n-C_{18} redox indicators in this study. The Ts/Tm value in the remaining seven samples is greater than 2.0 indicating predominately anoxic conditions during deposition, which is not consistent with the other biomarker redox indicators. This inconsistency may be the result of the Ts/Tm values greater than 2.0 having been altered by thermal maturation causing Tm to be converted to

Ts (Peters et al., 2005b). However, these samples are not from areas where thermal maturity is expected to be highest in the study area. These seven samples could also be representative of sediment deposition during the warm season when anoxic conditions persisted in deep (> 150 m) water due to a seasonal thermocline.

2.5.3.1.4. Sterane Distribution

The distribution of C_{27} to C_{29} steranes can be used to interpret if sediment was deposited in deep marine (>150 m) environments, shallow marine (<150 m) environments, or lacustrine environments (Huang and Meinschein, 1979). Regions depicting the distribution of steranes in sediment from different depositional environments are shown on a ternary diagram of C_{27} to C_{29} sterane (Figure 2.5B). Distribution of steranes in the samples analyzed plot in the deep marine region of the diagram indicating deposition in water at least 150 m deep (Figure 2.5B).

2.5.3.2. Depositional Model

Biomarker data indicate a depositional model for the Lower Huron Shale in which algal productivity was high during each cool season and organic matter was preserved in anoxic bottom waters during each warm season, which resulted in high organic carbon content in the Lower Huron Shale. We interpret that a thermocline developed during each warm season and then broke down during each cool season. The Pr/Ph values, Pr/n-C_{17} versus Ph/n-C_{18} crossplot, and Ts/Tm values in the samples analyzed indicate oxic and anoxic conditions, which supports interpretation of a seasonal thermocline. The distribution of C_{27} to C_{29} steranes in the samples analyzed indicates that the Lower Huron Shale in the study area represents deposition in water deeper than

150 m. We interpret that deep anoxic bottom water during each warm season allowed for preservation of organic matter and anaerobic decomposition, which separated phosphorus and nitrogen from carbon in the organic matter and produced carbon dioxide (Figure 2.7). During each cool season, the thermocline was broken down as shallow water cooled and mixed with deep water. Mixing brought oxygen into deep water causing oxic conditions as indicated by the Pr/Ph values, Pr/n-C_{17} versus Ph/n-C_{18} crossplot, and Ts/Tm values in the samples analyzed. Phosphorus, nitrogen, and carbon dioxide were transported to the shallow water causing an elevation in algal productivity due to increased nutrient availability. In modern environments increased nutrient supply due to cool season breakdown of the thermocline favors development of algal blooms (Barnes and Hughes, 1982). In the western part of the South China Sea (average depth 1060 m) algal blooms have been observed during the winter due to upwelling of nutrient-rich cold water (Espenshade, 1984; Wang et al., 2008). Dwivedi et al. (2008) documented algal blooms during the winter in the Arabian Sea (average depth 2734 m) due to upwelling of nutrient rich cold water (Espenshade, 1984). *Phaeocystis* (marine phytoplanktonic algae) can bloom in tropical to polar waters in nutrient enriched areas (Schoemann et al., 2005). The n-alkane and sterane biomarkers in the samples analyzed indicate an environment dominated by marine organisms (mainly algae) and support the interpretation of algal blooms in response to increased nutrient supply. A seasonal thermocline model for deposition of the Lower Huron Shale is consistent with interpretations by Murphy et al. (2000) and Sageman et al. (2003), who suggested that Upper Devonian black shales in western New York represent deposition in alternating oxic and anoxic conditions caused

by establishment and then breakdown of a seasonal thermocline. Other environmental factors such as monsoon winds and large scale ocean circulation could also have played a role in creating alternating oxic and anoxic conditions (Wang et al., 2008).

Paleogeography of the Appalachian Basin and seasonal stratification of modern oceans support a seasonal thermocline depositional model for the Lower Huron Shale. During Late Devonian time the Appalachian Basin was located at approximately 30 to 35° south of the equator (Scotese and McKerrow, 1990) within a subtropical zone (Ettensohn, 1992). Paleoclimatic indicators suggest warm and seasonably variable temperatures, arid to semi-arid conditions, and frequent storm activity (Witzke and Heckel, 1988). Modern subtropical oceans are characterized by a warm season with a thin mixed layer and shallow thermocline (20-40 m), and during the cool season the thermocline is broken down and intensity of mixing increases (Sageman et al., 2003). The Red Sea (average depth 490 m) is a modern example of this (Espenshade, 1984; Lindell and Post, 1995). During summer, the Red Sea is stratified due to a thermocline and the shallow water is depleted of nutrients. During winter, the thermocline deteriorates and mixing occurs for several months, enriching the shallow water with nutrients (Lindell and Post, 1995).

2.6. Conclusions

Biomarkers identified in the samples analyzed provide consistent interpretation of the source of organic matter in the samples and depositional conditions represented by the samples. Based on the TAR ratio, n-C_{17}/n-C_{31}, Pr/n-C_{17}, Ph/n-C_{18}, and sterane distribution, the biological source of preserved organic matter in the Lower Huron Shale

is interpreted to represent predominately marine algae and bacteria. The presence of C_{30} steranes in samples analyzed indicates contribution by brown algae to the organic matter. Pr/n-C_{17} and Ph/n-C_{18} indicate organic matter in the samples analyzed is composed of type II kerogen, which can be the source of both oil and gas. Redox conditions during deposition represented by the samples analyzed were assessed using Pr/Ph, n-C_{17}/n-C_{31}, Pr/n-C_{17}, and Ts/Tm ratios, which indicate alternating oxic and anoxic conditions. Sterane distributions in the samples indicate deposition in deep waters (>150 m).

Biomarker data from the Lower Huron Shale support establishment and breakdown of a seasonal thermocline during deposition. During the warm season of a subtropical climate, anoxic bottom waters persisted and allowed accumulation of phosphorus and nitrogen due to anaerobic decomposition of organic matter. As seasonal temperatures cooled, the thermocline broke down resulting in mixing of the shallow and deep waters, which allowed bottom waters to become oxic and increased algal productivity due to the upwelling of phosphorus and nitrogen.

2.7. References

Alego, T.J., Berner, R.A., Maynard, J.B., and Scheckler, S.E., 1995, Late Devonian oceanic anoxic events and biotic crises: "Rooted" in the evolution of vascular land plants?: Geological Society of America Today, v. 5, p. 64-66.

Barnes, R.S.K. and Hughes, R.M., 1982, An Introduction to Marine Ecology: Oxford, Blackwell Scientific Publications, 339 p.

Beier, J.A. and Hayes, J.M., 1989, Geochemical and isotopic evidence for paleoredox conditions during deposition of the Devonian-Mississippian New Albany Shale, southern Indiana: Geological Society of America Bulletin, v. 101, p.774-782.

Brocks, J.J., Buick, R., Logan, G., and Summons, R.E., 2003, Composition and syngeneity of molecular fossils from the 2.78 to 2.45 billion-year-old Mount

Bruce Supergroup, Pilbara Craton, Western Australia: Geochimica et Cosmochimica Acta, v. 67, p. 4289-4319.

Brown, T., and Kenig, F., 2004, Water column structure during deposition of Middle Devonian-Lower Mississippian black and green/gray shales of the Illinois and Michigan Basins: A biomarker approach: Palaeogeography, Palaeoclimatology, Palaeoecology, v. 215, p. 59-85.

Conant, L. C., and Swanson, V. E., 1961, Chattanooga Shale and related rocks of central Tennessee and nearby areas: U.S. Geological Survey Professional Paper 357.

de Witt, W., Jr., and Milici, R.C., 1989, Energy resources of the Appalachian orogen *in* Hatcher, R.D., Jr., Thomas, W.A., and Viele, G.W., eds., The Geology of North America, v. F-2, the Appalachian-Ouachita Orogen in the United States: Geological Society of America, p. 495-510.

de Witt, W.J., Roen, J.B., and Wallace, L.G., 1993, Stratigraphy of Devonian black shales and associated rocks in the Appalachian Basin: *In* Roen, J.B. and Kepferle, R.C., eds., Petroleum Geology of the Devonian and Mississippian Black Shale of Eastern North America, volume 1909: U.S. Geological Survey Bulletin, p. B1-B57.

Didyk, B.M., Simoneit, B.R.T., Brassell, S.C., and Eglinton, G., 1978, Organic geochemical indicators of palaeoenvironmental conditions of sedimentation: Nature, v. 272, p. 216-222.

Dwivedi, R.M., Raman, M., Babu, K.N., Singh, S.K., Vyas, N.K., and Matondkar, S.G., 2008, Formation of algal bloom in the northern Arabian Sea deep waters during January-March: a study using pooled in situ and satellite data: International Journal of Remote Sensing, v. 29, p. 4537-4551.

Espenshade, E.B., 1984, Goode's World Atlas: Chicago, Rand McNally & Company.

Ettensohn, F.R., Miller, M.L., Dillman, S.B., Elam, T.D., Geller, K.L., Swager, D.R., Markowitz, G., Woock, R.D., and Barron, L.S., 1988, Characterization and implications of the Devonian-Mississippian black shale sequence, eastern and central Kentucky, U.S.A.—pycnoclines, transgression, regression, and tectonism: *In* McMillan, N.J., Embry, A.F., and Glass, D.J., eds., Devonian of the World: Proceedings of the Second International Symposium on the Devonian System: Canadian Society of Petroleum Geology Memoir 14, v. 2, p. 323-345

Ettensohn, F.R., 1992, Controls on the origin of the Devonian-Mississippian oil and gas shales, east central United States: Fuel, v.71, p. 1487-1493.

Ettensohn, F.R., 1994, Marine, organic-rich, dark-shale deposition on North American parts of Pangea, Carboniferous to Jurassic, effects of supercontinent organization *in* Glass, D.J., Pangea; Global Environments and Resources: Memoir Canadian Society of Petroleum Geologist, v. 17, p. 743-762.

Forster, A., Sturt, H., Meyers, P.A., and the Leg 207 Shipboard Scientific Party, 2004, Molecular biogeochemistry of Cretaceous black shales from the Demerara Rise: Preliminary shipboard results from sites 1257 and 1258, Leg 207: *In* Erbacher, J., Mosher, D.C., Malone, M.J., et al., Proceedings of the Ocean Drilling Program, Initial Reports: v. 207, p. 1-22.

Hamilton-Smith, T., 1993, Gas exploration in the Devonian shales of Kentucky: Kentucky Geological Survey Bulletin, Bulletin 4, Series XI, http://kgs.uky.edu/kgsweb/PubsSearching/MoreInfo.asp?titleInput=40&map=0**,** 10/26/2009.

Huang, W., and Meischein, W.G., 1979, Sterols as ecological indicators: Geochimica et Cosmochimica Acta, v. 43, p. 739-745.

Hughes, W.B., Holba, A.G., and Dzou, L.I.P., 1995, The ratios of dibenzothiophene to phenanthrene and pristane to phytane as indicators of depositional environment and lithology of petroleum source rocks: Geochimica et Cosmochimica Acta, v. 59, p. 3581-3598.

Kotarba, M.J. and Clayton J.L., 2003, A stable carbon isotope and biological marker study of Polish bituminous coals and carbonaceous shales: Coal Geology, v. 55, p. 73-94.

Kepferle, R.C., 1989, A depositional model and basin analysis for the gas-bearing black shale (Devonian and Mississippian) in the Appalachian Basin, *in* Roen, J.B. and Kepferle, R.C. eds, Petroleum Geology of the Devonian and Mississippian Black Shale of Eastern North America, v. 1909: U S Geological Survey Bulletin, p. F1-F23.

Lijmbach, G.W.M., 1975, On the origin of petroleum: Proceedings of Ninth World Petroleum Congress: Geology, v.2, p. 357-369.

Lindell, D. and Post, A.F., 1995, Ultraphytoplankton succession is triggered by deep water mixing in the Gulf of Aqaba (Eilat), Red Sea: Limnology and Oceanography, v. 40, p. 1130-1141.

Lineback, J. A., 1968, Subdivisions and depositional environment of the New Albany Shale (Devonian-Mississippian) in Indiana: American Association of Petroleum Geologists Bulletin, v. 52, p. 1291-1303.

Magoon, L.B. and Dow, W.G., 1994, The petroleum system *in* Magoon, L.B. and Dow, W.G., The Petroleum System-from Source to Trap, American Association of Petroleum Geologist Memoir, p. 3-24.

Marynowski, L., Narkiewicz, M., and Grelowski, C., 2000, Biomarker as environmental indicators in a carbonate complex, example from the Middle to Upper Devonian, Holy Cross Mountains, Poland: Sedimentary Geology, v. 137, p. 187-212.

Milici, R.C., Ryder, R.T., Swezey, C.S., Charpentier, R.R., Cook, T.A., Crovelli, R.A., Klett, T.R., Pollastro, R.M., and Schenk, C.J., 2003, Assessment of undiscovered oil and gas resources of the Appalachian Basin Province, 2002: United States Geological Survey Fact Sheet FS-009-03.

Moldowan, J.M., Sundararaman, P., and Schoell, M., 1985, Sensitivity of biomarker properties to depositional environment and/or source input in Lower Toarcian of SW-Germany: Organic Geochemistry, v. 10, p. 915-926.

Moody, J. R., Kemper J. R., Johnston I. M., and Elkin R. R., 1987, The geology and the drilling and production history of the Upper Devonian shale of Whitley, Knox, Bell, and Harlan counties, southeastern Kentucky: Kentucky Geological Survey, publication prepared for the Gas Research Institute, 30 p.

Murphy, A.E., Sageman, B.B., Hollander, D.J., Lyons, T.W., and Brett, C.E., 2000, Black shale deposition and faunal overturn in the Devonian Appalachian basin: Clastic starvation, seasonal water-column mixing, and efficient biolimiting nutrient recycling: Paleooceanography, v. 15, p. 280-291.

Nuttal, B.C., Eble, C.F., and Drahovzal, J.A, 2005, Analysis of Devonian Black Shales in Kentucky for potential carbon dioxide sequestration and enhanced natural gas production: Kentucky Geological Survey, Report DE-FC26-02NT41442.

Obermajer, M., Fowler, M.G., Goodarzi, F., and Snowdon, L.R., 1997, Organic petrology and organic geochemistry of Devonian black shales in southwestern Ontario, Canada: Organic Geochemistry, v. 26, p. 229-246.

Obermajer, M., Fowler, M.G., and Snowdon, L.R., 1999, Depositional environment and oil generation in Ordovician source rocks from southwestern Ontario, Canada: Organic geochemical and petrological approach: American Association of Petroleum Geologist Bulletin, v. 83, p. 1426-1453.

Olcott, A.N., 2007, The utility of lipid biomarkers as paleoenvironmental indicators: Palaios, v. 22, p. 111-113.

Pancost, R.D., Freeman, K.H., Patzkowsky, M.E., Wavrek, D.A., and Collister, J.W., 1998, Molecular indicators of redox and marine photoautotroph composition in the late Middle Ordovician of Iowa, U.S.A.: Organic Geochemistry, v. 29, p. 1649-1662.

Peters, K.E., Walters, C.C., Moldowan, J.M., 2005a, The Biomarker Guide: Volume 1 Biomarkers and Isotopes in the Environment and Human History: New York, Cambridge University Press.

Peters, K.E., Walters, C.C., Moldowan, J.M., 2005b, The Biomarker Guide: Volume 2 Biomarkers and Isotopes in Petroleum Exploration and Earth History: New York, Cambridge University Press.

Piper, D.Z., and Calvert, S.E., 2009, A marine biogeochemical perspective on black shale deposition: Earth Science Reviews, v. 95, p. 63-96.

Rich, J. L., 1951, Probable fondo origin of Marcellus-Ohio-New Albany-Chattanooga bituminous shale: American Association of Petroleum Geologists Bulletin, v. 35,. p. 2017-2040.

Roen, J.B., 1993, Introductory review—Devonian and Mississippian black shales, eastern North America, *in* Roen, J.B. and Kepferle, R.C., eds., Petroleum Geology of the Devonian and Mississippian Black Shale of Eastern North America, volume 1909: U.S. Geological Survey Bulletin, p. A1-A8.

Ryder, R.T., Burruss, R.C., and Hatch, J.R., 1998, Black shale source rocks and oil generation in the Cambrian and Ordovician of the Central Appalachian Basin, USA: American Association of Petroleum Geologist Bulletin, v. 82, p. 412-441.

Sageman, B.B, Murphy, A.E, Werne, J.P., Ver Straeten, C.A., Hollander, D.J., and Lyons, T.W., 2003, A tale of shales: The relative roles of production, decomposition, and dilution in the accumulation of organic-rich strata, Middle-Upper Devonian, Appalachian basin: Chemical Geology, v. 195, p. 229-273.

Samuel, O.J., Cornfor, C., Jones, M., Adekeye, O.A., and Akande, S.O., 2009, Improved understanding of the petroleum systems of the Niger Delta Basin, Nigeria: Organic Geochemistry, v. 40, p. 461-483.

Schoemann, V., Becquevort, S., Stefels, J., Rousseau, V., and Lancelot, C., 2005, *Phaeocystis* blooms in the global ocean and their controlling mechanisms: A review: Journal of Sea Research, v. 53, p. 43-66.

Schwark, L., and Empt, P., 2006, Sterane biomarkers as indicators of Palaeozoic algal evolution and extinction events: Palaeogeography, Palaeoclimatology, Palaeoecology, v. 240, p. 225-236.

Scotese, C.R. and McKerrow, W.S., 1990, Revised world maps and introduction *in* McKerrow, W.S. and Scotese, C.R., Paleozoic Paleogeography and Biogeography: Geological Society Memoir, v. 12, p. 1-21.

Sherman, L.S., Waldbauer, J.R., and Summons, R.E., 2007, Improved methods for isolating and validating indigenous biomarkers in Precambrian rocks: Organic Geochemistry, v. 38, p. 1987-2000.

Solevic, T., Stojanovic, K., Bojese-Koefoed, J., Nytoft, H.P., Jovancicevic, B., and Vitorovic, D., 2008, Origin of oils in the Velebit oil-gas field, SE Pannonian Basin, Serbia – Source rocks characterization based on biological marker distributions: Organic Geochemistry, v. 39, p. 118-134.

ten Haven, H.L., de Leeuw, J.W., Rullkotter, J., and Sinnninghe Damste, J.S., 1987, Restricted utility of the pristane/phytane ratio as a paleoenvironmental indicator: Nature, v. 330, p. 641-643.

Tisot, B.P. and Welte, D.H., 1978, Petroleum Formation and Occurrence: Berlin, Springer-Verlag, 699 p.

Tyson, R.V., 1987, The genesis and palynofacies characteristics of marine petroleum source rocks *in* Brooks, J.R.V. and Fleet, A.J., Marine Petroleum Source Rocks: Geological Society Special Publication, v. 26, p. 47-68.

Volkman, J.K., 2003, Sterols in microorganisms: Applied Microbiology and Biotechnology, v. 60, p. 496-506.

Wang, S., Tang, D., He, F., Fukuyo, Y., and Azanza, R.V., 2008, Occurrences of harmful algal blooms (HABs) associated with ocean environments in the South China Sea: Hydrobiologia, v. 596, p. 79-93.

Witzke, B.J. and Heckel, P.H., 1988, Paleoclimatic indicators and inferred Devonian paleoatitudes of Euramerica *in* Mcmillan, N.J., Embry, A.F., Glass, D.J., Devonian of the World: Canadian Society of Petroleum Geologist, Memoir, v. 14, p. 49-63.

Table 2.1: Samples and depth of samples analyzed.

Well	County	Sample Number	MD[1]	TVD[2]
A	Floyd	A3440	3440 (1049)	2959 (902)
A	Floyd	A4640	4640 (1414)	2968 (905)
A	Floyd	A6100	6100 (1859)	2971 (906)
B	Pike	B4050	4050 (1234)	3923 (1196)
B	Pike	B5350	5350 (1631)	3971 (1210)
C	Perry	C3470	3470 (1058)	3372 (1028)
C	Perry	C3650	3650 (1113)	3423 (1043)
D	Mingo	D5000	5000 (1524)	4964 (1513)
D	Mingo	D6030	6030 (1838)	5169 (1576)
D	Mingo	D7270	7270 (2216)	5173 (1578)
E	Pike	E4060	4060 (1237)	3910 (1192)
E	Pike	E5160	5160 (1573)	3958 (1206)
E	Pike	E6340	6340 (1932)	3968 (1209)
E	Pike	E7100	7100 (2164)	3987 (1215)
F	Letcher	F4125	4125 (1257)	4036 (1230)
G	Logan	G4640	4640 (1414)	4513 (1376)
G	Logan	G6260	6260 (1908)	4570 (1393)
G	Logan	G7100	7100 (2164)	4566 (1392)
H	Knott	H3720	3720 (1134)	3486 (1063)
H	Knott	H5310	5310 (1618)	3519 (1073)
H	Knott	H6600	6600 (2012)	3537 (1078)

[1]Measured depth in feet (m) from ground level along length of wellbore

[2]True vertical depth in feet (m) from ground level to sample location

Table 2.2: Steps of biomarker extraction and detection from whole rock sample.

	Method	Purpose	Procedure
1	Ultrasonication	Extract organic matter	Ultrasonicate 75 g of crushed sample for 30 min in 40 ml of dichloromethane (DCM). Filter to remove crushed sample, collect extract, and repeat with additional 40 ml DCM
2	Sulfur and asphaltene removal	Remove elemental sulfur and asphaltenes	Rinse Cu pellets with 37% hydrochloric acid (HCL) until Cu reaches bright color. Then rinse with deionized (DI) water, then methanol, then DCM. Add 5 g of the activated Cu to vial containing extract and stir 8 h. After stirring filter to remove Cu. Reduce Cu free extract to 1 ml under nitrogen gas. Add 50 ml of n-pentane and allow to sit 8 h to precipitate asphaltenes. Filter extract to remove asphaltenes. Collect asphaltene free extract and reduce to 1 ml.
3	Column chromatography	Fractionate extracted organic matter	Activate silica gel by heating for 8 hours at 110°C. Mix silica gel with hexane to form slurry. Plug Pasteur pipette with cotton wool and fill with slurry. Add extract to top of column. Elute fractions of increasing polarity by sequential elution with 4 ml hexane (saturated fraction) then 2 ml hexane/2 ml DCM (aromatic fraction). Collect the eluated fractions in clean vials, evaporate to dryness, and then dissolve in 1 ml DCM.
4A	Gas chromatography (GC)/flame ionization detection (FID)	Separate and identify biomarkers	With a Phenomenex ZB-5 column (30m x 0.25mm x 0.25µm) installed in the gas chromatograph (GC), program the oven for a 2 min hold at 40°C, and then heat to 310°C at 4°C/min with a final hold time of 15 min. Use helium as the carrier gas.
4B	GC/mass spectroscopy (MS)/MS	Separate and identify biomarkers	With a Restek Rtx-5MS column (30m x 0.25mm x 0.25µm) installed in the GC, program the oven for a 2 min hold at 40°C and then heat to 310°C at 4°C/min with a final hold time of 15 min. Use helium as the carrier gas. Set transfer line at 280°C and the mass spectrophotometer (MS) source at 230°C. Acquire electron impact mass spectra at 70 eV in MS/MS mode.

Procedures modified from Sherman et al. (2007), Forster et al. (2004), and Brocks et al. (2003)

Extraction variability = ±1.6% and Detection limit = 1 ppb

Table 2.3: Parent to daughter transitions analyzed using GC/MS/MS for sterane and hopane detection in this investigation.

Biomarker	*Parent Ion (m/z)	*Daughter Ion (m/z)
C_{27} Steranes	372	217
C_{28} Steranes	386	217
C_{29} Steranes	400	217
C_{30} Steranes	414	217
C_{27} Hopanes	370	191
C_{29} Hopanes	398	191
C_{30} Hopanes	412	191
C_{31} Hopanes	426	191

m/z = mass to charge ratio
*Peters et al. (2005a)

Table 2.4: N-alkane and isoprenoid biomarkers identified in samples analyzed with FID and characteristics of each. All biomarkers listed were identified in all samples analyzed except samples C3650, D5000, and D7270.

Biomarker	Abbreviation	Molecular Formula	Weight (amu)	*Possible Origin
n-Alkanes				
n-Decane	n-C_{10}	$C_{10}H_{22}$	142	Variable
n-Undecane	n-C_{11}	$C_{11}H_{24}$	156	Variable
n-Dodecane	n-C_{12}	$C_{12}H_{26}$	170	Variable
n-Tridecane	n-C_{13}	$C_{13}H_{28}$	184	Variable
n-Tetradecane	n-C_{14}	$C_{14}H_{30}$	198	Variable
n-Pentadecane	n-C_{15}	$C_{15}H_{32}$	212	Marine algae
n-Hexadecane	n-C_{16}	$C_{16}H_{34}$	226	Algae, Bacteria
n-Heptadecane	n-C_{17}	$C_{17}H_{36}$	240	Marine algae
n-Octadecane	n-C_{18}	$C_{18}H_{38}$	254	Algae, Bacteria
n-Nonadecane	n-C_{19}	$C_{19}H_{40}$	268	Marine algae
n-Icosane	n-C_{20}	$C_{20}H_{42}$	282	Algae, Bacteria
n-Henicosane	n-C_{21}	$C_{21}H_{44}$	296	Marine algae
n-Docosane	n-C_{22}	$C_{22}H_{46}$	310	Algae, Bacteria
n-Tricosane	n-C_{23}	$C_{23}H_{48}$	324	Nonmarine algae
n-Tetracosane	n-C_{24}	$C_{24}H_{50}$	338	Nonmarine algae
n-Pentacosane	n-C_{25}	$C_{25}H_{52}$	352	Nonmarine algae
n-Hexacosane	n-C_{26}	$C_{26}H_{54}$	366	Plant waxes
n-Heptacosane	n-C_{27}	$C_{27}H_{56}$	380	Nonmarine algae
n-Octacosane	n-C_{28}	$C_{28}H_{58}$	394	Plant waxes
n-Nonacosane	n-C_{29}	$C_{29}H_{60}$	408	Nonmarine algae
n-Triacontane	n-C_{30}	$C_{30}H_{62}$	422	Plant waxes
n-Hentriacontane	n-C_{31}	$C_{31}H_{64}$	436	Plant waxes
Isoprenoids				
Pristane	Pr	$C_{19}H_{40}$	268	Purple sulfur bacteria
Phytane	Ph	$C_{20}H_{42}$	282	Purple sulfur bacteria

*Peters et al. (2005a)
amu = atomic mass unit

Table 2.5: Characteristics of n-alkane, sterane, and hopane biomarkers identified in samples analyzed.

Sample	MAC Alkane[1]	Cmax Aquatic[2]	Cmax Waxes[3]	MAC Sterane[4]	MAC Hopane[5]	27%[6]	28%[7]	29%[8]
A3440	n-C_{13}	n-C_{16}	n-C_{28}	$C_{27}\alpha\beta\beta$-R	$C_{29}H$	41	25	34
A4640	n-C_{12}	n-C_{16}	n-C_{27}	$C_{27}\alpha\beta\beta$-S	$C_{29}H$	38	26	36
A6100	n-C_{12}	n-C_{16}	n-C_{27}	$C_{27}\alpha\beta\beta$-S	$C_{29}H$	64	21	15
B4050	n-C_{14}	n-C_{16}	n-C_{27}	$C_{27}\alpha\alpha\alpha$-S	$C_{29}H$	41	44	15
B5350	n-C_{13}	n-C_{16}	n-C_{27}	$C_{28}\alpha\beta\beta$-R	$C_{29}H$	41	40	19
C3470	n-C_{15}	n-C_{16}	n-C_{27}	$C_{28}\alpha\beta\beta$-R	$C_{29}H$	28	36	36
C3650	nd	nd	nd	nd	nd	nd	nd	nd
D5000	nd	nd	nd	nd	nd	nd	nd	nd
D6030	n-C_{21}	n-C_{17}	n-C_{27}	$C_{28}\alpha\alpha\alpha$-S	$C_{29}H$	28	43	29
D7270	nd	nd	nd	nd	nd	nd	nd	nd
E4060	n-C_{12}	n-C_{16}	n-C_{28}	$C_{27}\alpha\beta\beta$-S	$C_{29}H$	41	28	31
E5160	n-C_{12}	n-C_{16}	n-C_{27}	$C_{27}\alpha\beta\beta$-S	$C_{29}H$	49	29	22
E6340	n-C_{14}	n-C_{16}	n-C_{27}	$C_{27}\alpha\alpha\alpha$-S	$C_{29}H$	39	20	41
E7100	n-C_{12}	n-C_{16}	n-C_{27}	$C_{27}\alpha\beta\beta$-S	$C_{29}H$	46	20	34
F4125	n-C_{16}	n-C_{16}	n-C_{28}	$C_{27}\alpha\alpha\alpha$-S	$C_{29}H$	48	38	14
G4640	n-C_{16}	n-C_{16}	n-C_{27}	$C_{27}\alpha\alpha\alpha$-S	$C_{29}H$	56	17	27
G6260	n-C_{12}	n-C_{16}	n-C_{28}	$C_{27}\alpha\alpha\alpha$-S	$C_{29}H$	37	12	51
G7100	n-C_{12}	n-C_{16}	n-C_{27}	$C_{27}\alpha\alpha\alpha$-S	$C_{29}H$	42	19	39
H3720	n-C_{12}	n-C_{16}	n-C_{27}	$C_{27}\alpha\alpha\alpha$-S	$C_{29}H$	36	28	36
H5310	n-C_{12}	n-C_{16}	n-C_{27}	$C_{27}\alpha\alpha\alpha$-S	$C_{29}H$	45	41	14
H6600	n-C_{12}	n-C_{16}	n-C_{27}	$C_{29}\alpha\alpha\alpha$-R	$C_{29}H$	41	27	32

[1] Most abundant n-alkane identified in sample

[2] Most abundant n-alkane between n-C_{16} and n-C_{18} in sample

[3] Most abundant n-alkane between n-C_{27} and n-C_{33} in sample

[4] Most abundant sterane identified in sample

[5] Most abundant hopane identified in sample

[6] $(C_{27}\alpha\alpha\alpha(S+R) + C_{27}\alpha\beta\beta(S+R))/(\sum C_{27}$ to $C_{29}\ \alpha\alpha\alpha(S+R) + \alpha\beta\beta(S+R))$

[7] $(C_{28}\alpha\alpha\alpha(S+R) + C_{28}\alpha\beta\beta(S+R))/(\sum C_{27}$ to $C_{29}\ \alpha\alpha\alpha(S+R) + \alpha\beta\beta(S+R))$

[8] $(C_{29}\alpha\alpha\alpha(S+R) + C_{29}\alpha\beta\beta(S+R))/(\sum C_{27}$ to $C_{29}\ \alpha\alpha\alpha(S+R) + \alpha\beta\beta(S+R))$

nd = not detected (below detection limit)

Table 2.6: Sterane and hopane biomarkers identified in samples analyzed with GC/MS/MS and characteristics of each. All biomarkers listed were identified in all samples analyzed except samples C3650, D5000, and D7270.

Biomarker	Abbreviation	Molecular Formula	Weight (amu)	*Source
C_{27} Steranes				
5α(H),14α(H),17α(H)-Cholestane-20S	C_{27}ααα-S	$C_{27}H_{48}$	372	Marine algae
5α(H),14β(H),17β(H)-Cholestane-20R	C_{27}αββ-R	$C_{27}H_{48}$	372	Marine algae
5α(H),14β(H),17β(H)-Cholestane-20S	C_{27}αββ-S	$C_{27}H_{48}$	372	Marine algae
5α(H),14α(H),17α(H)-Cholestane-20R	C_{27}ααα-R	$C_{27}H_{48}$	372	Marine algae
C_{28} Steranes				
5α(H),14α(H),17α(H)-24-Methylcholestane-20S	C_{28}ααα-S	$C_{28}H_{50}$	386	Lacustrine phytoplankton
5α(H),14β(H),17β(H)-24-Methylcholestane-20R	C_{28}αββ-R	$C_{28}H_{50}$	386	Lacustrine phytoplankton
5α(H),14β(H),17β(H)-24-Methylcholestane-20S	C_{28}αββ-S	$C_{28}H_{50}$	386	Lacustrine phytoplankton
5α(H),14α(H),17α(H)-24-Methylcholestane-20R	C_{28}ααα-R	$C_{28}H_{50}$	386	Lacustrine phytoplankton
C_{29} Steranes				
5α(H),14α(H),17α(H)-24-Ethylcholestane-20S	C_{29}ααα-S	$C_{29}H_{52}$	400	Land plants
5α(H),14β(H),17β(H)-24-Ethylcholestane-20R	C_{29}αββ-R	$C_{29}H_{52}$	400	Land plants
5α(H),14β(H),17β(H)-24-Ethylcholestane-20S	C_{29}αββ-S	$C_{29}H_{52}$	400	Land plants
5α(H),14α(H),17α(H)-24-Ethylcholestane-20R	C_{29}ααα-R	$C_{29}H_{52}$	400	Land plants
C_{30} Steranes				
5α(H),14α(H),17α(H)-24-Propylcholestane-20S	C_{30}ααα-S	$C_{30}H_{54}$	414	Marine algae
5α(H),14β(H),17β(H)-24-Propylcholestane-20R	C_{30}αββ-R	$C_{30}H_{54}$	414	Marine algae

Table 2.6 continued

5α(H),14β(H),17β(H)-24-Propylcholestane-20S	C_{30}αββ-S	$C_{30}H_{54}$	414	Marine algae
5α(H),14α(H),17α(H)-24-Propylcholestane-20R	C_{30}ααα-R	$C_{30}H_{54}$	414	Marine algae
C_{27} Hopanes				
18α(H)-22,29,30-Trisnorneohopane	Ts	$C_{27}H_{46}$	370	Cyanobacteria, Proteobacteria
17α(H)-22,29,30-Trisnorhopane	Tm	$C_{27}H_{46}$	370	Cyanobacteria, Proteobacteria
C_{29} Hopane				
17α(H),21β(H)-30-Norhopane	C_{29}H	$C_{29}H_{50}$	398	Cyanobacteria, Proteobacteria
18α(H)-Norneohopane	C_{29}Ts	$C_{29}H_{50}$	398	Cyanobacteria, Proteobacteria
C_{30} Hopane				
17α(H),21β(H)-Hopane	C_{30}H	$C_{30}H_{52}$	400	Cyanobacteria, Proteobacteria
C_{31} Hopane				
17α(H),21β(H)-Homohopane-22S	C_{31}H-S	$C_{31}H_{54}$	426	Cyanobacteria, Proteobacteria
17α(H),21β(H)-Homohopane-22R	C_{31}H-R	$C_{31}H_{54}$	426	Cyanobacteria, Proteobacteria

*Peters et al. (2005a)
amu = atomic mass unit

Table 2.7: Organic matter source and depositional environment biomarker parameter values in the samples analyzed.

Sample	TAR	$n\text{-}C_{17}/n\text{-}C_{31}$	$Pr/n\text{-}C_{17}$	$Ph/n\text{-}C_{18}$	C_{29}/C_{27}	Pr/Ph	Ts/Tm
A3440	0.14	14.04	0.70	0.52	0.56	1.67	1.22
A4640	0.10	40.00	0.68	0.51	0.35	1.69	7.40
A6100	0.10	28.58	0.58	0.45	0.19	1.66	1.55
B4050	0.26	7.51	0.49	0.49	0.22	1.22	3.00
B5350	0.10	34.63	0.44	0.44	0.67	1.30	3.75
C3470	0.33	3.57	0.59	0.49	0.47	1.38	1.80
D6030	0.26	22.68	0.42	0.57	0.26	1.22	1.60
E4060	0.30	3.30	0.49	0.47	0.56	1.25	1.45
E5160	0.20	9.20	0.47	0.45	0.20	1.31	3.55
E6340	0.18	9.63	0.45	0.43	0.83	1.28	1.20
E7100	0.21	20.10	0.45	0.47	0.56	1.14	1.80
F4125	0.28	4.54	0.54	0.53	0.42	1.24	1.87
G4640	0.18	10.66	0.42	0.35	0.44	1.28	3.20
G6260	0.22	5.95	0.41	0.36	0.25	1.18	1.40
G7100	0.23	7.64	0.42	0.35	0.69	1.24	2.64
H3720	0.20	13.32	0.51	0.50	0.65	1.32	1.36
H5310	0.23	5.38	0.52	0.50	0.13	1.27	1.83
H6600	0.19	11.28	0.50	0.44	0.88	1.34	2.20

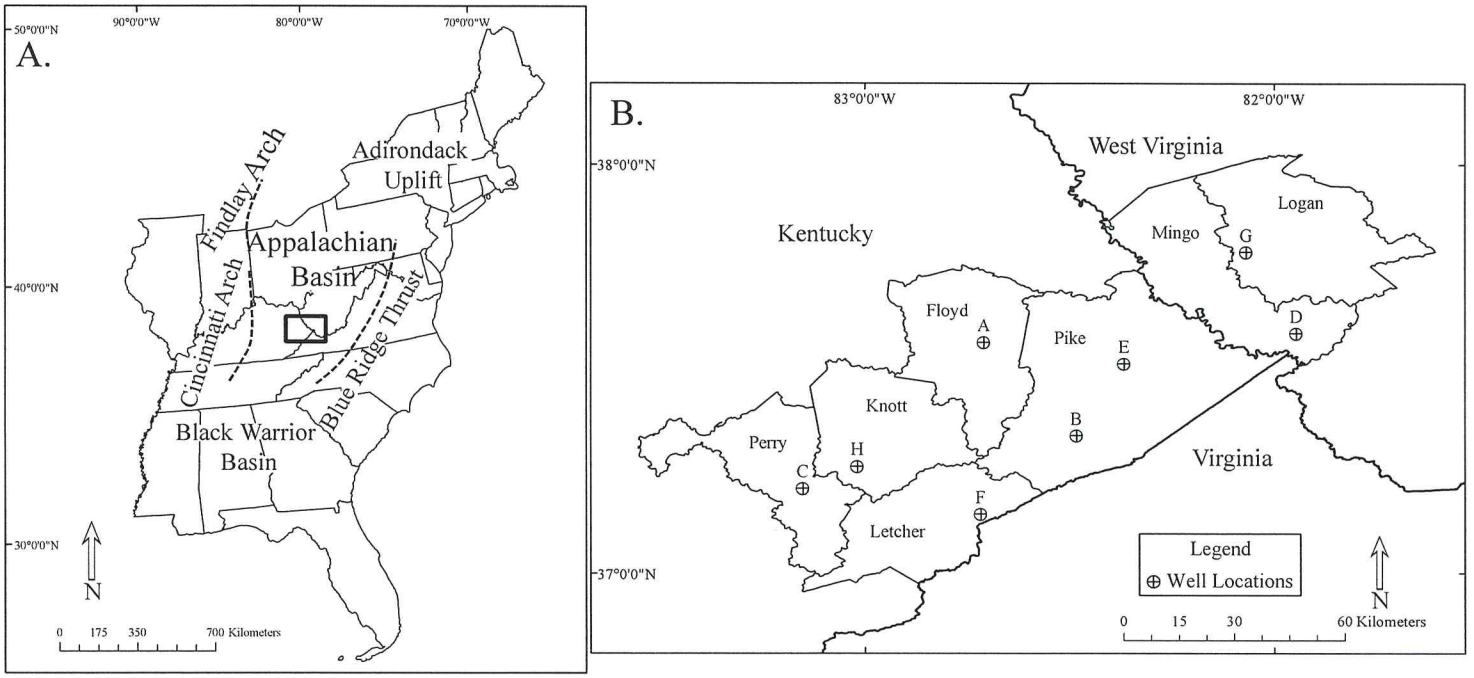

Figure 2.1: A = Major structural features of eastern United States (modified from Roen, 1993) and location of study area map. B = Sample locations with states and counties labeled.

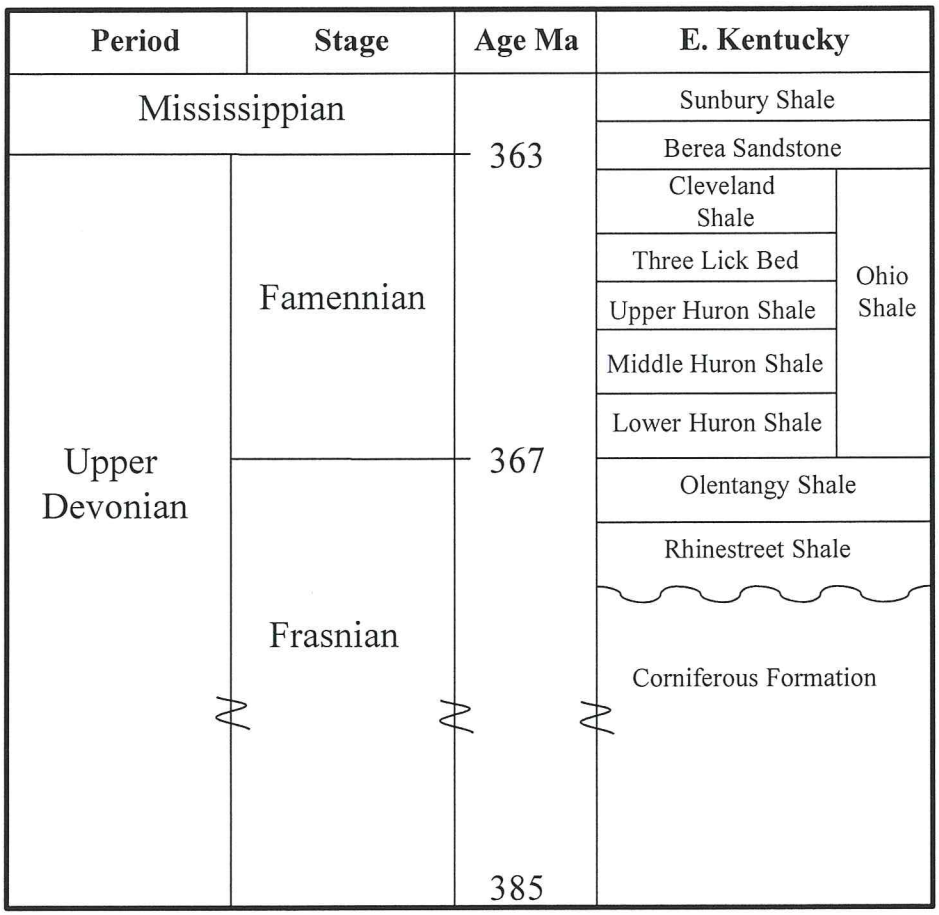

Figure 2.2: Upper Devonian and Lower Mississippian stratigraphy of eastern Kentucky and southern West Virginia (modified from Hamilton-Smith, 1993 and de Witt et al., 1993).

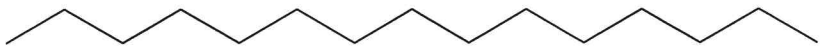

n-pentadecane (n-C_{15})

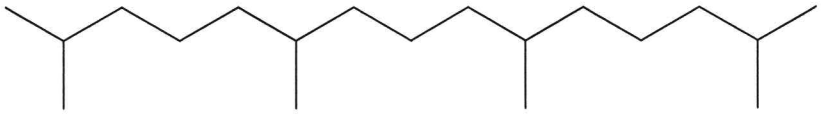

Pristane (Pr)

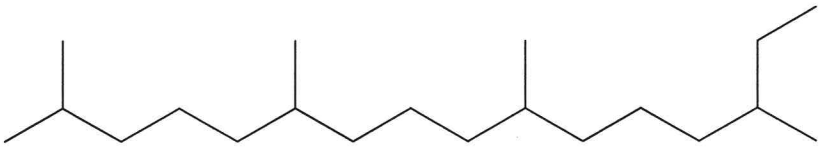

Phytane (Ph)

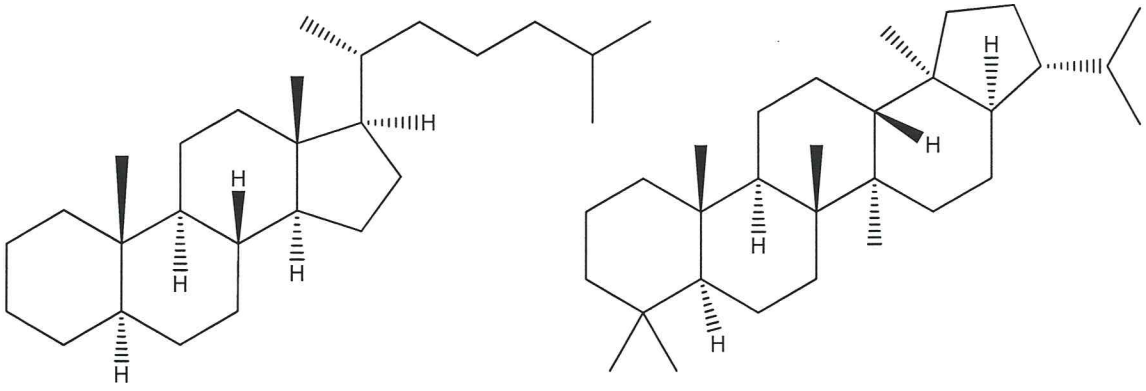

C_{27} Sterane C_{30} Hopane

Figure 2.3: General structures of biomarkers identified in samples. N-pentadecane structure represents structure of n-alkanes.

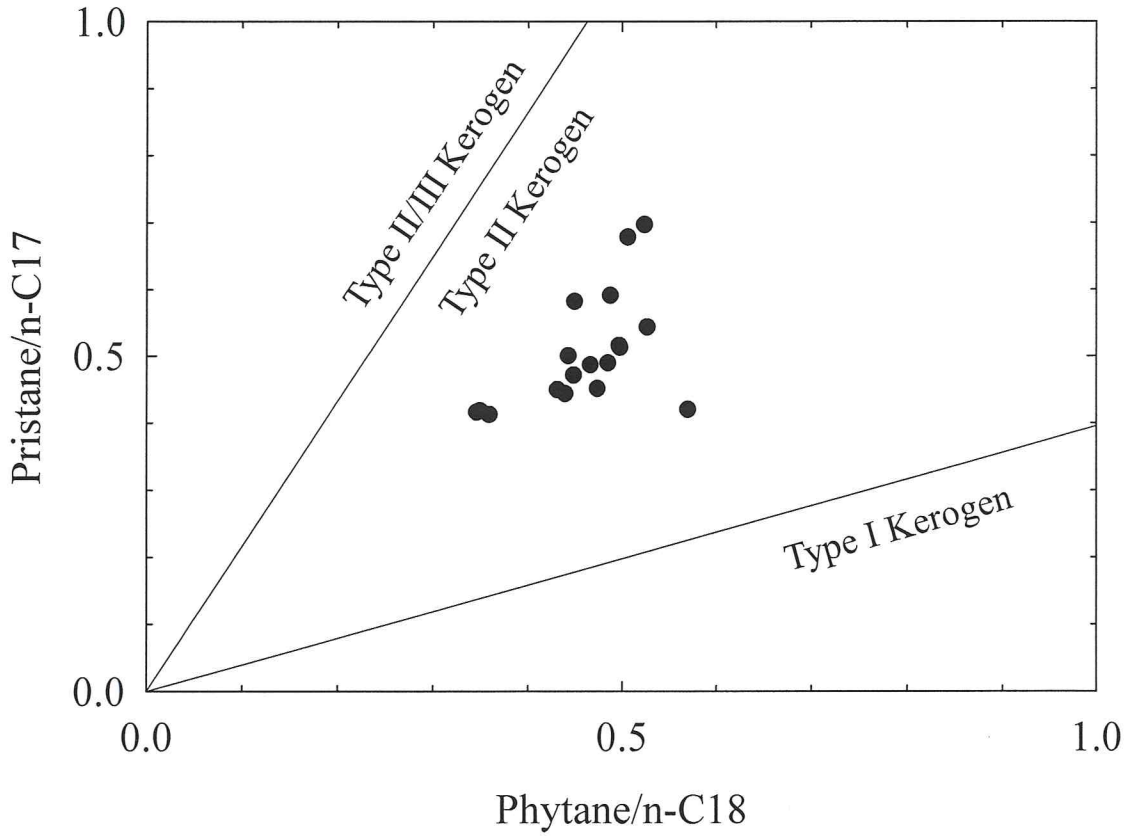

Figure 2.4: Pristane/n-C_{17} versus Phytane/n-C_{18} indicating samples analyzed contain type II kerogen. Kerogen types are defined by Tissot and Welte (1978) as: Type I – Hydrogen:carbon ratio > 1.25, oxygen:carbon ratio < 0.15, and tends to produce oil; Type II – Hydrogen:carbon ratio < 1.25, oxygen:carbon ratio 0.03 to 0.18, and tends to produce oil and gas; and Type III – Hydrogen:carbon ration < 1.00, oxygen:carbon ratio 0.03 to 0.3, and tends to produce coal and gas. Regions of different kerogen types are from Obermajer et al. (1999).

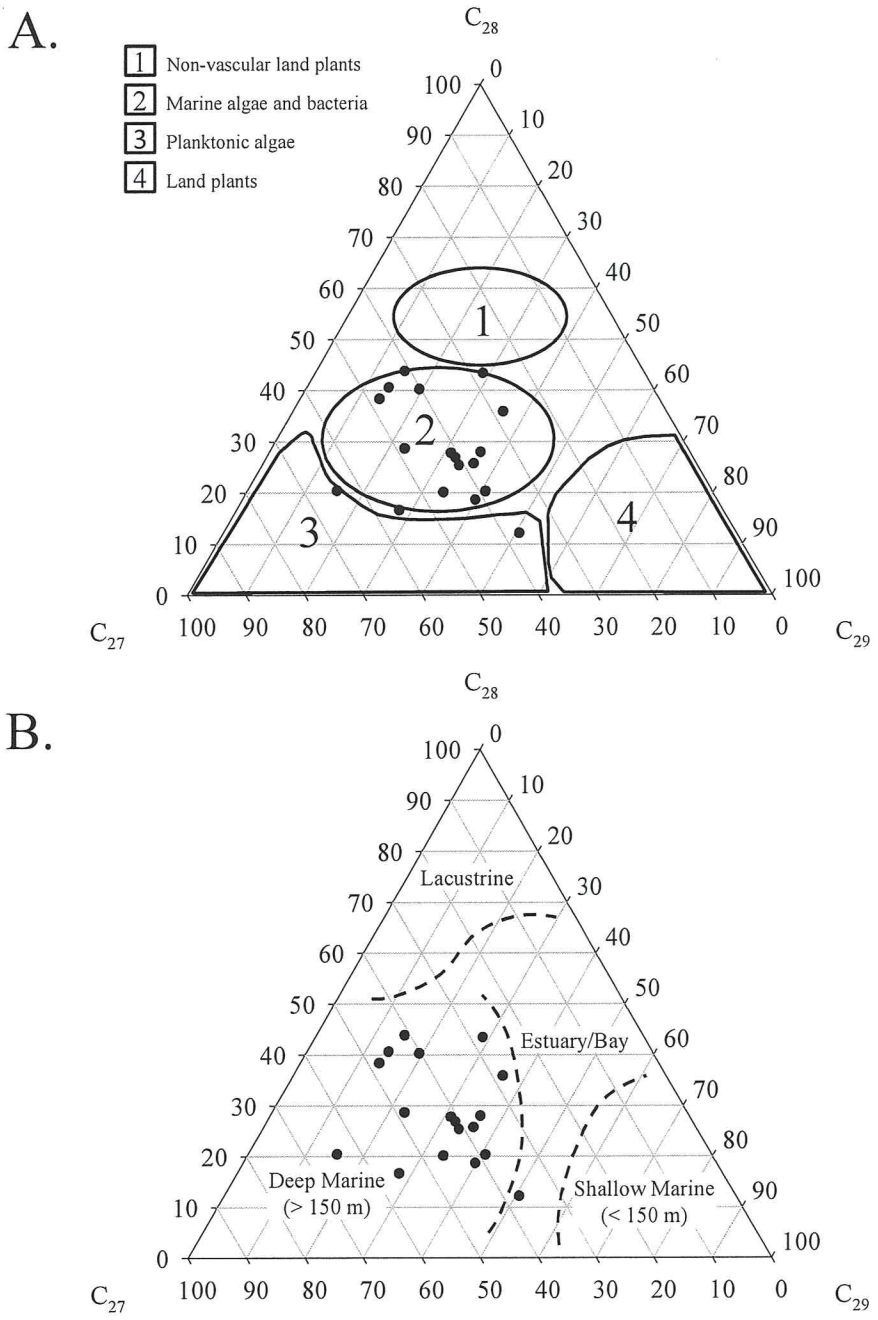

Figure 2.5 Ternary diagrams of C_{27} to C_{29} steranes indicating organic matter source and depositional environment of samples analyzed. Plotted values are the percentage of each sterane (C_{27}, C_{28}, and C_{29}) making up the total of C_{27} to C_{29} steranes. A. Indicates organic matter is dominated by algal and bacterial organic matter sources. B. Indicates sediment was deposited in a deep marine (> 150 m) environment. Organic matter source regions and depositional environment regions are from Huang and Meinschein (1979).

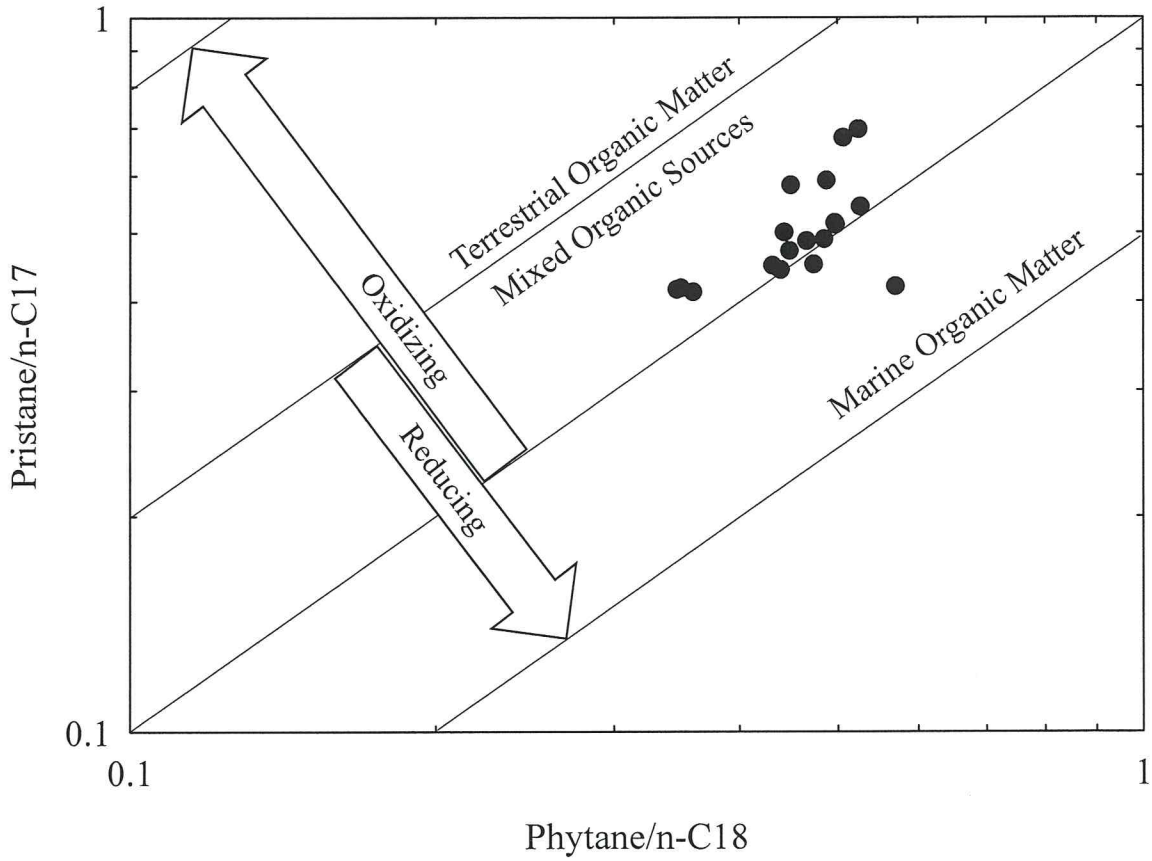

Figure 2.6: Pristane/n-C_{17} versus Phytane/n-C_{18} indicating sediment deposition occurred in alternating reducing and oxidizing conditions. Regions of oxidizing and reducing conditions and organic matter sources are from Lijmbach (1975).

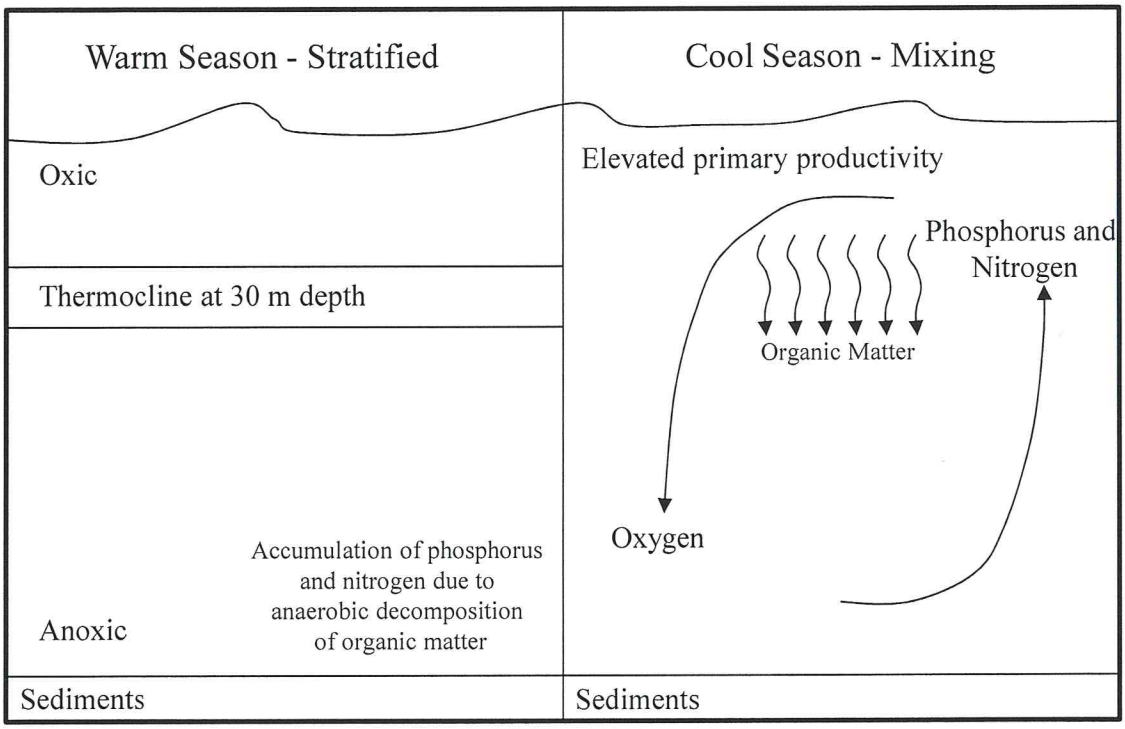

Figure 2.7: Conceptual diagram of the proposed depositional model for the Lower Huron Shale. Water depth is approximately 150 m. The left side shows conditions during the warm season when the water column is stratified separating oxic shallower and anoxic deeper waters. Bio-limiting nutrients are accumulated in the deep water due to anaerobic decomposition of organic matter. The right side shows conditions during the cool season when the shallow and deeper waters mix due to breakdown of the thermocline bringing bio-limiting nutrients to shallow water and elevating algal productivity. The 3 to 10 meter interval represented by each sample is larger than the stratigraphic thickness of warm season/cool season fluctuations. Therefore, depositional conditions of both the cool season and warm season can be represented within each sample.

CHAPTER THREE

THERMAL MATURITY INTERPRETATIONS OF LOWER HURON SHALE (UPPER DEVONIAN), EASTERN KENTUCKY AND SOUTHERN WEST VIRGINIA, USING BIOMARKER MATURITY RATIOS

3.1. Abstract

The Lower Huron Shale Member of the Ohio Shale (Upper Devonian) is considered the largest shale gas reservoir in the Big Sandy Field in Kentucky and West Virginia. The potential for gas shales, such as the Lower Huron, to produce natural gas is a function of type, amount, and thermal maturation of their organic matter. Twenty-one Lower Huron Shale samples from eight wells in the Big Sandy Field were analyzed for biomarker content to interpret thermal maturity. The following biomarkers were identified: n-alkanes (C_{15} to C_{31}), pristane (Pr), phytane (Ph), steranes (αααR, αααS, ααβR, ααβS isomers of C_{27} to C_{30} steranes), and hopanes (C_{27}, C_{29}, C_{30} and C_{31} hopanes).

Thermal maturities within the early to peak oil generation stages for the samples analyzed are indicated by ratio values for C_{27}-20S/(20S+20R), C_{28}-20S/(20S+20R), C_{29}-20S/(20S+20R), C_{28}-αββ/(αββ+ααα), C_{29}- αββ/(αββ+ααα), Ts/(Ts+Tm), and 22S/(22S+22R). Contours maps of Pr/n-C_{17}, Ph/n-C_{18}, C_{28}-20S/(20S+20R), C_{29}-20S/(20S+20R), C_{28}-αββ/(αββ+ααα), C_{29}- αββ/(αββ+ααα), Ts/(Ts+Tm), and 22S/(22S+22R) ratio values indicate an increase in thermal maturity toward the southeast within the study area.

Biomarker data suggest that gas produced from the Lower Huron Shale in the south-eastern region of the Big Sandy Field has reached a thermal maturity great enough to generate natural gas. Biomarker data indicate that the Lower Huron Shale in the north-

western region of the Big Sandy Field was not buried to a great enough depth to generate significant amounts of gas. This suggests that gas produced from this area in the Big Sandy Field is biogenic or that thermogenic gas has migrated from more thermally mature areas to the east.

3.2. Introduction

Although black shales represent a major source rock for oil and gas reserves in the world, they are among the least understood of all sedimentary rocks (Wignall, 1994; Harris, 2005; Piper and Calvert, 2009). Accurate and reliable measurement of thermal maturity, the degree to which heat-driven reactions have converted kerogen to hydrocarbon, is useful in characterizing the thermal and burial history of source rocks and understanding the origin and distribution of oil and gas reserves (Tissot and Welte, 1978). Thermal maturity interpretations can provide information on the quality and quantity of hydrocarbons that may have been generated and, coupled with basin modeling, can help simulate basin evolution and petroleum generation, expulsion, and migration. This study focuses on interpreting the thermal maturity of the Upper Devonian Ohio Shale, which is the primary shale gas reservoir of the Big Sandy Field, in the Appalachian Basin (Figure 3.1). In 2002 the United States Geological Survey estimated the total undiscovered gas resources of the Big Sandy Field to be 6 trillion cubic feet of gas (Milici et al., 2003).

Vitrinite reflectance (R_o) is the most commonly measured thermal maturity parameter in pre-Pennsylvanian age noncarbonate rocks of the Appalachian Basin (Rowan, 2006 and Repetski et al., 2008). Numerous researchers have published R_o data for black shales in the Appalachian Basin. R_o data for the Ohio Shale in eastern

Kentucky and southern West Virginia show a southeastward increase from 0.50 to 2.20% in a study by Curtis and Faure (1997) and from 0.50 to 2.00% in a study by Repetski et al. (2008). R_o data from within eastern Kentucky show a southeastward increase from 0.49 to 1.00% (Hamilton-Smith, 1993). These R_o data suggest that the Ohio Shale reached a level of thermal maturity adequate for abundant oil generation ("oil window" is 0.6 to 1.3% R_o) at most places in eastern Kentucky and southern West Virginia. However, R_o values from a previous study of Devonian black shale are lower than R_o values in overlying Pennsylvanian coal beds in eastern Kentucky and southern West Virginia (Repetski et al., 2008). These low R_o values in Devonian shale may be related to vitrinite suppression or retardation, which can lead to underestimation of the true thermal maturity (Price and Barker, 1985; Carr, 2000). Suppression of vitrinite reflectance may occur in rocks with high total organic carbon content that is rich in liptinite dominated kerogens (Price and Barker, 1985). Retardation of vitrinite reflectance may be caused by generation of overpressure in a sedimentary basin (Carr, 2000).

Detailed studies of sedimentary organic matter found in black shales can provide a variety of indicators that can be used to interpret thermal maturity (Peters et al., 2005a). Organic matter in black shales contains compounds, known as biomarkers, which are preserved remnants of molecules originally synthesized by organisms with distinctive chemical structures closely related to the biological precursor molecule (Peters et al., 2005a and Olcott, 2007). Organic geochemical research studying the origin and transformation of biomarkers in the environment has led to a large number of organic

geochemical parameters used to interpret the source of organic matter, environmental conditions during deposition and burial, and thermal maturity of rocks (Peters et al., 2005a). Thermal maturity interpretations from biomarker data have proven to be accurate and reliable for organic matter that has not undergone microbial degradation (Requejo et al., 1997; Peters et al., 2005b; Shen and Huang, 2007; Arfaoui et al., 2007). Based on a thorough literature review, no studies were found that attempted to identify biomarkers in Upper Devonian black shale of the Appalachian Basin to interpret thermal maturity. Obermajer et al. (1997) used biomarkers identified in Middle Devonian Marcellus and Upper Devonian Kettle Point black shales in southern Ontario to assess the source rock potential of those units. Brown and Kenig (2004) used biomarkers identified in Middle Devonian through Lower Mississippian black shales of the Illinois and Michigan Basins to assess water column structure during deposition. Schwark and Empt (2006) identified biomarkers in Ohio Shale samples from the eastern flank of the Cincinnati Arch to assess Paleozoic algal evolution and extinction events.

Biomarkers are potentially very useful in understanding thermal maturity of the Ohio Shale and origin of the large volume of natural gas contained within the shale. Also, biomarker data may help elucidate previous estimates of thermal maturity of the Ohio Shale based on vitrinite reflectance. Therefore, the objectives of this research were: 1) identify biomarkers in the Lower Huron Shale member of the Ohio Shale in eastern Kentucky and southern West Virginia; 2) interpret thermal maturity of the samples using the biomarkers identified; and 3) compare thermal maturity interpretations using biomarker data to published interpretations based on R_o values. The Lower Huron Shale

was selected for study because drilling and completions of the Ohio Shale most commonly target the Lower Huron Shale due to its high total organic carbon content and abundant natural fractures (Nuttall et al., 2005). Cutting samples were analyzed from eight horizontal wells recently drilled into the Lower Huron Shale for natural gas production.

3.3. Geologic Setting

The Appalachian Basin is a foreland basin that developed during the late Proterozoic and Paleozoic (Roen, 1993). The basin trends northeast and is approximately 1500 km in length and 150 to 500 km in width. It extends from the Adirondack Mountains in the north to the Black Warrior Basin in the south. To the northwest the Findlay and Algonquin Arches separate the Appalachian Basin from the Michigan Basin, and to the west the Cincinnati Arch separates it from the Illinois Basin (Roen, 1993) (Figure 3.1A). The Appalachian Basin consists of Paleozoic strata ranging from 600 to 900 m thick along the Cincinnati Arch to more than 13,700 m thick to the east in Central Pennsylvania (de Witt and Milici, 1989). Sedimentation in the basin was influenced by three major orogenies: the Taconian (Middle to Late Ordovician), the Acadian (Early to Middle Devonian), and the Alleghenian (Late Carboniferous to Permian) (Moody et al., 1987). As a result of the Acadian Orogeny and subsequent erosion of the mountains, the Catskill Delta developed. The Upper Devonian shales are interpreted to have accumulated basinward of the Catskill Delta in an epeiric sea with periodic anoxic bottom waters caused by depth related stratification (Kepferle, 1989) or the establishment and breakdown of seasonal thermoclines (Sageman et al., 2003). The Upper Devonian

interval is referred to as the Ohio Shale east of the Cincinnati Arch in eastern Kentucky and southern West Virginia and is subdivided into five recognizable members: Cleveland Shale, Three Lick Bed, Upper Huron Shale, Middle Huron Shale, and Lower Huron Shale (Figure 3.2) (Hamilton-Smith, 1993).

The Lower Huron Shale is grayish-black, brownish-black, and black shale interbedded with minor green-gray shale (Hamilton-Smith, 1993). It contains zones of spheroidal to ellipsoidal dolomitic limestone nodules and septaria and a few beds of limestone from 2.5 to 10.0 cm. thick (de Witt et al., 1993). In the study area the Lower Huron Shale ranges in thickness from 24 to 43 m.

3.4. Methods

3.4.1. Biomarker Identification

3.4.1.1. Sampling

Twenty-one samples were collected and analyzed from drill cuttings from eight recently drilled horizontal wells targeting the Lower Huron Shale (Figure 3.1B; Table 3.1). The wells were drilled using air, preventing the samples from being contaminated by organic rich drilling muds. Rock cuttings were collected during the drilling process in 3 to 10 meter intervals and consist of chipped rock fragments and powder. In each well one to four samples weighing 75 grams each were selected from the horizontal section of the well. Selection criteria included high organic carbon content, determined using the gamma and density logs for each well, and spacing of samples in the well bore.

3.4.1.2. Sample Preparation

Samples were prepared in four batches of five samples each with one procedural blank in each batch. Samples were ground to a fine powder using a ceramic mortar and pestle. Between samples the mortar and pestle were cleaned with hot tap water and rinsed with DI water, methanol (MeOH), and dichloromethane (DCM). The sequential extraction procedure for the powdered sample and instrumental analysis of extract for biomarker detection follows the methodology of Brocks et al. (2003), Forster et al. (2004), and Sherman et al. (2007) (Table 2.2).

Soluble organic matter was extracted from 75 g of the powdered samples ultrasonically with a Fisher Sonic Dismembrator Model 300 for 30 min in 40 ml DCM (HPLC grade), and the extract was collected. Forty ml additional DCM was added to the powdered sample and the ultrasonication process was repeated. Extracts were combined. Copper pellets (Fisher Scientific C-430 Copper Metal) were placed in a 14 mm O.D. chromatography tube plugged with cotton wool. The copper was rinsed with 37% hydrochloric acid until it reached a bright color. The copper was then rinsed with DI water, methanol, and DCM seven times each. Five g of the acid activated copper was added to the vials containing the combined extracts and stirred for 8 h to remove elemental sulfur. The extracts were filtered (Whatman 44 filter paper) to remove the copper, and the filtrates were then reduced to 1 ml under a stream of ultra pure (99.998%) nitrogen gas. Fifty ml of n-pentane (HPLC Grade) was added to the extracts and allowed to sit 8 h to precipitate asphaltenes. The extracts were filtered (Whatman 44 filter paper)

to remove the asphaltenes and the asphaltene free extract was evaporated to dryness under a stream of ultra pure nitrogen gas.

The extracts were separated into saturated (compounds with no double or triple bonds) and aromatic (compounds with one or more benzene ring) fractions by liquid chromatography using Pasteur pipettes. Silica gel (3 g) was activated by heating at 110 °C for 8 h. The activated silica gel was cooled, and 5 ml hexane (HPLC grade) was added to make a slurry. Pasteur pipettes were plugged with cotton wool and filled with the slurry. The asphaltene free extracts were dissolved in 1 ml DCM and added to the top of the column. Saturated hydrocarbons were eluted with hexane (4 ml) and aromatic hydrocarbons with hexane:DCM (1:1 v/v, 4 ml). The fractions were evaporated to dryness and dissolved in 1 ml DCM and put in autosampler vials for analysis. An extraction variability of 1.6% was determined using three samples spiked with a 5β-cholane standard.

3.4.1.3. Instrumental Analyses

3.4.1.3.1 Gas chromatography-Flame Ionization Detection (GC-FID)

GC analyses were performed on the saturated hydrocarbon fraction in order to obtain normal (n)-alkanes, pristane, and phytane data with a Hewlett Packard 5890 Series II gas chromatograph equipped with a FID and autosampler. N-alkanes are compounds consisting of carbon and hydrogen in which the carbon atoms are arranged linearly (Peters et al., 2005a) (Figure 3.3). Pristane and phytane are acyclic isoprenoid hydrocarbons (Figure 3.3) that are created by the phytyl side chain of chlorophyll a in phototrophic organisms and bacteriochlorophyll a and b in purple sulfur bacteria (Peters

et al., 2005a). Samples (1.0 µl of each) were injected in splitless mode with helium as the carrier gas onto a Zebron ZB-5 column (30 m x 0.25 mm inner diameter, 0.25 µm film thickness). The helium flow rate was set at 1.0 ml/min. The flow rate of the air and hydrogen were 300 ml/min and 30 ml/min respectively. The injector was programmed for 250 °C and the detector for 310 °C. The oven was programmed at 40°C (2 min) and heated to 310°C at 4°C/min, with a final hold time of 15 min. The amounts of n-alkanes, pristane, and phytane were determined from the integrated area of the chromatogram peak of each compound.

3.4.1.3.2 Gas Chromatography-Mass Spectroscopy-Mass Spectroscopy

Gas chromatography-mass spectroscopy-mass spectroscopy (GC-MS-MS) analyses was performed on the saturated fraction in order to obtain sterane and hopane biomarker data with a Varian Model 4000 GC/MS/MS equipped with an autosampler. Sterane is a class of tetracyclic saturated biomarkers derived from sterols in eukaryotic cells, and hopane is a class of pentacyclic saturated biomarkers derived from plasma membranes in prokaryotic cells (Peters et al., 2005a) (Figure 2.3). Parent/daughter transitions were analyzed in MS-MS mode with a collision energy of 70EV (Table 2.3). The samples (1.0 µl of each) were injected in splitless mode with helium as the carrier gas (1.0 ml/min flow rate) onto a Restek Rtx-5 column (30 m x 0.25 mm inner diameter, 0.25 µm film thickness). The GC oven was programmed at 40°C (2 min) and heated to 310°C at 4°C/min, with a final hold time of 15 min. The amounts of steranes and hopanes identified were determined from the integrated area of the chromatogram peak of each compound.

3.4.1.4 Distribution of Biomarkers Identified in the Samples

The samples analyzed were characterized based on abundance of the biomarkers identified in each. The most abundant n-alkane, most abundant sterane, and most abundant hopane were determined in each sample based on integrated peak areas of the compounds identified. Also, the most abundant n-alkane between n-C_{16} to n-C_{18} and the most abundant n-alkane between n-C_{27} to n-C_{33} were determined in each sample. The distribution of steranes identified in the samples was determined based on the percentage of each sterane (C_{27}, C_{28}, and C_{29}) making up the total of C_{27} to C_{29} steranes.

3.4.2. Thermal Maturity Interpretation

Biomarkers can be used to interpret thermal maturity based on the ratio of the chromatogram peak area of a complex biologically produced compound to the chromatogram peak area of a thermodynamically stable compound that has been produced by alteration of the less stable complex biological compound (Peters et al., 2005a). Biomarker ratios used to interpret thermal maturity are listed in Table 3.4. Ratio values were calculated using peak areas of compounds. N-alkanes, pristane, and phytane standards were run and equivalent peak areas were obtained indicating a similar response factor for each standard. Brocks et al. (2003) showed that it is suitable to use uncorrected peak areas of steranes and hopanes to calculate ratios. These ratios were chosen because they are commonly used to interpret thermal maturities from early to late oil generation (Peters et al., 2005b). The vertical distribution of thermal maturity was assessed by plotting the ratio values versus depth for all samples. The samples analyzed range over a depth interval of approximately 800 m. In previous studies (Requejo et al.,

1997; Forster et al., 2004) a depth interval of 300 to 1000 m has been shown sufficient to detect a trend in thermal maturity. The horizontal distribution of thermal maturity was assessed by contouring the average ratio values from each well.

3.4.3. Comparison with Published Interpretations

Thermal maturity interpretations using biomarker data from this investigation were compared to previous thermal maturity interpretations using R_o values (Hamilton-Smith 1993; Curtis and Faure, 1997; Repetski et al., 2008). Comparisons were made between the trend of biomarker ratios and the trend of R_o values geographically within the study area.

3.5. Results

3.5.1. Biomarkers Identified

3.5.1.1. N-alkanes and Isoprenoids

N-alkanes ranging from n-C_{10} to n-C_{31}, pristane, and phytane were identified in all samples except C3650, D5000, and D7270 (Table 3.5). The distributions based on integrated peak areas of n-alkanes and isoprenoids identified in each sample are listed in Table 3.6. The most abundant n-alkane in ten of the samples is n-C_{12}. N-C_{13}, n-C_{14}, and n-C_{16} are the most abundant n-alkane in two samples each, and n-C_{15} is the most abundant n-alkane in one sample. The aquatic range of n-alkanes is defined as n-alkanes with 16 to 18 carbon atoms because they typically originate from aquatic algae and cyanobacteria (Peters et al., 2005a). The most abundant component in the aquatic range of n-alkanes is n-C_{16} in seventeen samples. The land plant range of n-alkanes is defined as n-alkanes with 27 to 33 carbon atoms because they orginate from waxes typical of land

plants (Peters et al., 2005a). The most abundant component in the land plant range of n-alkanes is n-C_{27} in fourteen samples. Pristane is the most abundant isoprenoid in all of the samples analyzed where isoprenoids were detected.

3.5.1.2. Steranes

The ααα*R*, ααα*S*, αββ*R*, and αββ*S* isomers of cholestane (C_{27} sterane), 24-methylcholestane (C_{28} sterane), 24-ethylcholestane (C_{29} sterane), and 24-propycholestane (C_{30} sterane) were identified in all samples except C3650, D5000, and D7270 (Table 3.7). The distributions based on integrated peak areas of steranes identified in each sample are listed in Table 3.6. The isomers of cholestane are the most abundant sterane isomers comprising 28-64% of the total C_{27} to C_{29} steranes, followed by 24-ethylcholestane comprising 14-51%, and 24-methylcholestane comprising 12-44% (Table 3.6). 5α(H),14α(H),17α(H)-Cholestane-20S is the most abundant sterane isomer in eight samples (Table 3.6).

3.5.1.3. Hopanes

The following hopanes were identified in all samples except C3650, D5000, and D7270: 18α(H)-22,29,30-trisnorneohopane (Ts), 17α(H)-22,29,30-trisnorhopane (Tm), 17α(H),21β(H)-30-norhopane (C_{29}H), 18α(H)-norneohopane (C_{29}Ts), 17α(H),21β(H)-hopane (C_{30}H), 17α(H),21β(H)-homohopane-22S (C_{31}H-S), and 17α(H),21β(H)-homohopane-22R (C_{31}H-R) (Table 3.7). The distributions based on integrated peak areas of hopanes identified in each sample are listed in Table 3.6. C_{29}H is the most abundant hopane in all samples where hopanes were detected (Table 3.6).

3.5.2. Thermal Maturity Interpretations

3.5.2.1 Alkane and Isoprenoid Maturity Ratios

Thermal maturity interpretation using biomarkers is based on the thermal cracking of complex biologically produced isoprenoids to less complex n-alkanes (Tissot et al., 1971). The ratios of pristane to n-C_{17} (Pr/n-C_{17}) and phytane to n-C_{18} (Ph/n-C_{18}) decrease with increasing thermal maturity as more n-alkanes are generated by thermal cracking (Tissot et al., 1971). Correlation between decreasing Pr/n-C_{17} and Ph/n-C_{18} and increasing thermal maturity has been shown in an experiment where source rock samples were pyrolyzed at 300 °C for varying times and the change in ratios was observed over time (Alexander et al., 1981).

Pr/n-C_{17} values range from 0.40 to 0.70 in the samples analyzed (Table 3.8). The ratio values decrease with increasing depth of sample, indicating greater thermal maturity with depth (Figure 3.4A). A contour map of the average Pr/n-C_{17} values for each well in the study area shows increasing thermal maturity toward the southeast (Figure 3.5A).

Ph/n-C_{18} values range from 0.32 to 0.52 in the samples analyzed (Table 3.8). The ratio values decrease with increasing depth of sample (Figure 3.4A), indicating greater thermal maturity with depth. A contour map of the average Ph/n-C_{18} values in the study area shows increasing thermal maturity toward the east-southeast (Figure 3.5B).

3.5.2.2. Sterane Maturity Ratios

3.5.2.2.1. 20S/(20S+20R)

In the 20S/(20S+20R) ratio, only the R configuration at C-20 (20R) is found in steroid precursors in living organisms, and it gradually converts during burial and

maturation to a mixture of the R and S sterane configuration (Peters et al., 2005b). Therefore, values of 20S/(20S+20R) increase with increasing thermal maturity. The C_{27}-20S/(20S+20R), C_{28}-20S/(20S+20R), and C_{29}-20S/(20S+20R) values range from 0.14 to 0.91, 0.50 to 0.90, and 0.55 to 0.77, respectively, in the samples analyzed (Table 3.8). The C_{27}-20S/(20S+20R) ratio value in sixteen of the eighteen samples analyzed is above the reported equilibrium value of 0.55 indicating thermal maturity at or above the peak of oil generation (Peters et al., 2005b). The ratio value in sample E4060 is 0.50, which is slightly below the equilibrium value. The ratio value in sample D6030 is 0.14, which may be explained by the inversion of the C_{27}-20S/(20S+20R) ratio to lower values at higher maturities (Peters et al., 1990). The general trend of ratio values shows an increase with increasing depth, indicating greater thermal maturity with depth (Figure 3.4B). A contour map of the average C_{27}-20S/(20S+20R) ratio values for each well shows an increase in thermal maturity toward the east within the study area (Figure 3.6A).

The C_{28}-20S/(20S+20R) ratio value in thirteen of the eighteen samples analyzed is above the reported equilibrium value of 0.55 indicating thermal maturity at or above the peak of oil generation (Peters et al., 2005b). The C_{28}-20S/(20S+20R) ratio value in samples A3440, E6340, E7100, G7100, and H6600 is 0.50. The ratio values show a slight increase with increasing depth of sample, indicating greater thermal maturity with depth (Figure 3.4B). A contour map of the average C_{28}-20S/(20S+20R) ratio values for each well shows an increasing thermal maturity toward the southeast within the study

area with the exception of well D (C_{28}-20S/(20S+20R) = 0.60) in Mingo County (Figure 3.6B).

The C_{29}-20S/(20S+20R) ratio value in all of the samples analyzed is above the reported equilibrium value of 0.55 indicating thermal maturity at or above the peak of oil generation (Peters et al., 2005b). Ratio values increase with sample depth, indicating greater thermal maturity with depth (Figure 3.4B). A contour map of the average C_{29}-20S/(20S+20R) ratio values for each well shows an increasing thermal maturity toward the southeast within the study area (Figure 3.6C).

3.5.2.2.2. αββ/(αββ+ααα)

Another maturity ratio derived from the C_{28} to C_{29} steranes is the proportion of the 5α(H), 14β(H), 17β(H) isomers (αββ) to the 5α(H), 14α(H), 17α(H) isomers (ααα) expressed as the ratio αββ/(αββ+ααα). As thermal maturity increases, the ααα isomers, which are produced biologically, are converted gradually to a mixture of αββ and ααα isomers (Peters et al., 2005b). The ratio values increase with increasing thermal maturity. The C_{28}-αββ/(αββ+ααα) and C_{29}-αββ/(αββ+ααα) ratio values range from 0.19 to 0.76 and 0.46 to 0.71, respectively, in the samples analyzed (Table 3.8).

The C_{28}-αββ/(αββ+ααα) ratio value in four of the eighteen samples analyzed is above the reported equilibrium value of 0.70, indicating thermal maturity at or above the peak of oil generation (Peters et al., 2005b). The C_{28}-αββ/(αββ+ααα) ratio value of thirteen of the samples analyzed is between 0.50 and 0.69, indicating thermal maturities at the early oil generation stage. The ratio value of sample D6030 is 0.19, which may be explained by the inversion of the C_{28}-αββ/(αββ+ααα) ratio to lower values at higher

maturities (Peters et al., 1990). The ratio values show a slight trend of increasing with increasing sample depth, indicating greater thermal maturity with depth (Figure 3.4C). A contour map of the average C_{28}-αββ/(αββ+ααα) values for each well shows increasing thermal maturity toward the southeast (Figure 3.7A).

The C_{29}-αββ/(αββ+ααα) ratio value in two (D6030, F4125) of the eighteen samples analyzed is greater than the reported equilibrium value of 0.70, indicating thermal maturity at the peak of oil generation (Peters et al., 2005b). The C_{29}-αββ/(αββ+ααα) ratio value in the remaining sixteen samples is between 0.46 and 0.66, indicating thermal maturities at the early oil generation stage. The ratio values show a general trend of increasing with increasing sample depth, indicating greater thermal maturity with depth, (Figure 3.4C). The C_{29}-αββ/(αββ+ααα) values within the study area indicate increasing thermal maturity toward the southeast (Figure 3.7B).

3.5.2.3. Hopane Maturity Ratios

3.5.2.3.1. Ts/(Ts+Tm)

Tm is produced biologically and it converts during burial and maturation to Ts (Peters et al., 2005b). Therefore, Ts/(Ts+Tm) increases with increasing thermal maturity. The thermal equilibrium value of Ts/(Ts+Tm) is 1.00, which is reached at the late oil generation stage of maturity (Peters et al., 2005b). Ts/(Ts+Tm) ranges from 0.55 to 0.88 in the samples analyzed (Table 3.8). These values correspond to thermal maturities of early to peak oil generation. The ratio values show a general trend of increasing with increasing depth of sample, indicating greater thermal maturity with depth (Figure 3.4D).

The average Ts/(Ts+Tm) values for each well indicate an increasing thermal maturity toward the southeast within the study area (Figure 3.8A).

3.5.2.3.2. 22S/(22S+22R)

The R configuration at C-22 (22R) in the 22S/(22S+22R) ratio is biologically produced, and it gradually converts during burial and maturation to a mixture of 22R and 22S isomers (Peters et al., 2005b). Therefore, 22S/(22S+22R) increases with increasing thermal maturity. The thermal equilibrium value of 22S/(22S+22R) is 0.55, which is reached at the early oil generation stage of maturity (Peters et al., 2005b). The 22S/(22S+22R) values range from 0.55 to 0.84 in the samples analyzed (Table 3.8). The 22S/(22S+22R) values in all of the samples analyzed is above the reported equilibrium value of 0.55, indicating thermal maturity at or above the early oil generation stage. The ratio values show a general trend of increasing with increasing sample depth, indicating greater thermal maturity with depth (Figure 3.4D). The average 22S/(22S+22R) ratio values for each well show an increase in thermal maturity toward the southeast within the study area with the exception of well D [22S/(22S+22R) = 0.69] in Mingo County (Figure 3.8B).

3.5.3. Comparison with Published Interpretations

Contours of R_o values indicate increased thermal maturity toward the southeast within the study area (Figure 3.9) (Hamilton-Smith, 1993; Curtis and Faure, 1997; Repetski et al., 2008). An increase in this direction is expected, which corresponds to the direction of increasing maximum burial depth. Contours of current burial depth of the base of the Lower Huron Shale increase toward the southeast within the study area,

similar to the trend of maximum burial depth (Figure 3.10) (Dillman and Ettensohn, 1980; Rowan, 2006). Contours of Pristane/n-C_{17}, Phytane/n-C_{18}, C_{28}-20S/(20S+20R), C_{29}-20S/(20S+20R), C_{28}-αββ/(αββ+ααα), C_{29}-αββ/(αββ+ααα), Ts/(Ts+Tm), and 22S/(22S+22R) also indicate increased thermal maturity toward the southeast (Figures 3.5 to 3.8). Contours of C_{27}-20S/(20S+20R) (Figure 3.6A) show an increase in thermal maturity toward the east rather than southeast within the study area. This may be caused by depositional environment and organic matter source, which have been shown to influence the values of this ratio in addition to thermal maturity (Peters et al., 2005b).

Thermogenic gas generation from kerogen begins to occur within the oil generation stage of thermal maturity (Jarvie et al., 2007; Lillis et al., 2007). Minor amounts of gas can be generated during the early oil generation stage and during the peak oil generation stage of thermal maturity oil generation is accompanied by significant amounts of gas (Tissot and Welte, 1978). Biomarker data indicate that the Lower Huron Shale within the south-eastern region of the study area was buried to a great enough depth to generate significant amounts thermogenic gas. The C_{27}-20S/(20S+20R), C_{28}-20S/(20S+20R), C_{29}-20S/(20S+20R), C_{28}-αββ/(αββ+ααα), C_{29}- αββ/(αββ+ααα), and Ts/(Ts+Tm) thermal maturity ratios for the samples analyzed in this study indicate that the peak oil generation stage of thermal maturity was reached in the south-eastern region (Table 3.9). Biomarker data indicate that the Lower Huron Shale within the north-western region of the study area was not buried to a great enough depth to generate significant amounts of thermogenic gas. The C_{28}-αββ/(αββ+ααα), C_{29}- αββ/(αββ+ααα), Ts/(Ts+Tm), and 22S/(22S+22R) thermal maturity ratios for the samples analyzed

indicate that the early oil generation stage of thermal maturity was reached in the north-western region of the study area. Biomarker data suggest that gas produced from the Lower Huron Shale in the north-western region of the Big Sandy Field is biogenic or that thermogenic gas has migrated there from the more thermally mature areas to the east. R_o data (Hamilton-Smith, 1993; Curtis and Faure, 1997; Repetski et al., 2008) also indicates that the peak oil generation stage was reached in the south-eastern region of the study area but not in the north-western region. Osborn and McIntosh (2010) used chemical and isotopic tracers to investigate the origin of natural gas in Devonian black shales in the Appalachian Basin (western New York, eastern Ohio, northwestern Pennsylvania, and eastern Kentucky). They determined that the origin of the vast majority of natural gas in these shales is thermogenic. Therefore, gas produced from the areas that have not reached the peak oil generation stage may have migrated there from a more thermally mature rock to the east.

3.6. Conclusions

The following biomarkers were identified in DCM soluble extracts of Lower Huron Shale samples from eastern Kentucky and southern West Virginia: n-alkanes (C_{10} to C_{31}), pristane (Pr), phytane (Ph), steranes (αααR, αααS, ααβR, ααβS isomers of C_{27} to C_{30} steranes), and hopanes (C_{27}, C_{29}, C_{30} and C_{31} hopanes). Biomarker ratios used in interpreting thermal maturity of the samples analyzed provide consistent interpretation with each other. Thermal maturities within the early to peak oil generation stages for the samples analyzed are indicated by ratio values for C_{27}-20S/(20S+20R), C_{28}-20S/(20S+20R), C_{29}-20S/(20S+20R), C_{28}-αββ/(αββ+ααα), C_{29}- αββ/(αββ+ααα),

Ts/(Ts+Tm), and 22S/(22S+22R). Contour maps of ratio values (averaged for each well) for Pr/n-C_{17}, Ph/n-C_{18}, C_{28}-20S/(20S+20R), C_{29}-20S/(20S+20R), C_{28}-αββ/(αββ+ααα), C_{29}-αββ/(αββ+ααα), Ts/(Ts+Tm), and 22S/(22S+22R) indicate southeastward increase in thermal maturity within the study area, which corresponds to the direction of increasing maximum burial depth (Rowan, 2006). Biomarker maturity ratios indicate that samples from wells A, C, and H have reached the early oil generation stage of thermal maturity and samples from wells B, D, E, F, G in the far southeast of the study area have reached the peak oil generation stage. These biomarker maturity ratios suggest that gas produced from the Lower Huron Shale in the south-eastern region of the Big Sandy Field is thermogenic and that gas produced in the north-western region has migrated from more thermally mature strata.

3.7. References

Alexander, R., Kagi, R.I., and Woodhouse, G.W., 1981, Geochemical correlation of Windalia oil and extracts of Winning Group (Cretaceous) potential source rocks, Barrow Subbasin, Western Australia: American Association of Petroleum Geologists Bulletin, v. 65, p. 235-250.

Arfaoui, A., Montacer, M., Kamoun, F., and Rigane, A., 2007, Comparative study between Rock-Eval pyrolysis and biomarkers parameters: A case study of Ypresian source rocks in central-northern Tunisia: Marine and Petroleum Geology, v. 24, p. 566-578.

Brocks, J.J., Buick, R., Logan, G., and Summons, R.E., 2003, Composition and syngeneity of molecular fossils from the 2.78 to 2.45 billion-year-old Mount Bruce Supergroup, Pilbara Craton, Western Australia: Geochimica et Cosmochimica Acta, v. 67, p. 4289-4319.

Brown, T., and Kenig, F., 2004, Water column structure during deposition of Middle Devonian-Lower Mississippian black and green/gray shales of the Illinois and Michigan Basins: A biomarker approach: Palaeogeography, Palaeoclimatology, Palaeoecology, v. 215, p. 59-85.

Carr, A.D., 2000, Suppression and retardation of vitrinite reflectance, Part 1. Formation and significance for hydrocarbon generation: Journal of Petroleum Geology, v. 23, p. 313-343.

Curtis, J.B., and Faure, G., 1997, Accumulation of organic matter in the Rome Trough of the Appalachian Basin and its subsequent thermal history: American Association of Petroleum Geologists Bulletin, v. 81, p. 424-437.

de Witt, W., Jr., and Milici, R.C., 1989, Energy resources of the Appalachian orogen *in* Hatcher, R.D., Jr., Thomas, W.A., and Viele, G.W., eds., The Geology of North America, v. F-2, the Appalachian-Ouachita Orogen in the United States, Geological Society of America.

de Witt, W.J., Roen, J.B., and Wallace, L.G., 1993, Stratigraphy of Devonian black shales and associated rocks in the Appalachian Basin: *In* Roen, J.B. and Kepferle, R.C., eds., Petroleum Geology of the Devonian and Mississippian Black Shale of Eastern North America, volume 1909: U.S. Geological Survey Bulletin, p. B1-B57.

Dillman, S.B. and Ettensohn, F.R., 1980, Structure contour map on the base of the Lower Huron Shale Member (unit 5) of the Ohio Shale in eastern Kentucky: Morgantown Energy Technology Center-Eastern Gas Shales Project, series no. 519.

Forster, A., Sturt, H., Meyers, P.A., and the Leg 207 Shipboard Scientific Party, 2004, Molecular biogeochemistry of Cretaceous black shales from the Demerara Rise: Preliminary shipboard results from sites 1257 and 1258, Leg 207: *In* Erbacher, J., Mosher, D.C., Malone, M.J., et al., Proceedings of the Ocean Drilling Program, Initial Reports: v. 207, p. 1-22.

Hamilton-Smith, T., 1993, Gas exploration in the Devonian shales of Kentucky: Kentucky Geological Survey Bulletin, Bulletin 4, Series XI, http://kgs.uky.edu/kgsweb/PubsSearching/MoreInfo.asp?titleInput=40&map=0**,** 10/26/2009.

Harris, N.B., 2005, The deposition of organic-carbon-rich sediments: models, mechanisms, and consequences—Introduction: *In* Harris, N.B. ed, The Deposition of Organic-Carbon-Rich Sediments: Models, Mechanisms, and Consequences, Special Publication, Society for Sedimentary Geology, Tulsa, p. 1–5.

Jarvie, D.M., Hill, R.J., Ruble, T.E., and Pollastro, R.M., 2007, Unconventional shale-gas systems: The Mississippian Barnett Shale of north-central Texas as one model for thermogenic shale-gas assessment: American Association of Petroleum Geologist Bulletin, v. 91, p. 475-499.

Kepferle, R.C., 1989, A depositional model and basin analysis for the gas-bearing black shale (Devonian and Mississippian) in the Appalachian Basin: *In* Roen, J.B. and Kepferle, R.C. eds, Petroleum Geology of the Devonian and Mississippian Black Shale of eastern North America, volume 1909: U S Geological Survey Bulletin, p. F1-F23.

Lillis, P.G., Warden, A., Claypool, G.E., and Magoon, L.B., 2007, Petroleum systems of the San Joaquin Basin Province-Geochemical characteristics of gas types: *In* Scheirer A.H. ed, Petroleum Systems and Geologic Assessment of Oil and Gas in the San Joaquin Basin Province, California, U S Geological Survey Professional Paper 1713.

Milici, R.C., Ryder, R.T., Swezey, C.S., Charpentier, R.R., Cook, T.A., Crovelli, R.A., Klett, T.R., Pollastro, R.M., and Schenk, C.J., 2003, Assessment of undiscovered oil and gas resources of the Appalachian Basin Province, 2002: United States Geological Survey Fact Sheet FS-009-03.

Moody, J. R., Kemper J. R., Johnston I. M., and Elkin R. R., 1987, The geology and the drilling and production history of the Upper Devonian shale of Whitley, Knox, Bell, and Harlan counties, southeastern Kentucky: Kentucky Geological Survey, publication prepared for the Gas Research Institute, 30 p.

Nuttall, B.C., Eble, C.F., and Drahovzal, J.A, 2005, Analysis of Devonian Black Shales in Kentucky for potential carbon dioxide sequestration and enhanced natural gas production: Kentucky Geological Survey, DOE contract DE-FC26-02NT41442 Final Report.

Obermajer, M., Fowler, M.G., Goodarzi, F., and Snowdon, L.R., 1997, Organic petrology and organic geochemistry of Devonian black shales in southwestern Ontario, Canada: Organic Geochemistry, v. 26, p. 229-246.

Olcott, A.N., 2007, The utility of lipid biomarkers as paleoenvironmental indicators: Palaios, v. 22, p. 111-113.

Osborn, S.G. and McIntosh, J.C., 2010, Chemical and isotopic tracers of the contribution of microbial gas in Devonian organic-rich shales and reservoir sandstones, northern Appalachian Basin: Applied Geochemistry, v. 25, p. 456-471.

Peters, K.E., Moldowan, J.M., and Sundararaman, P., 1990, Effects of hydrous pyrolysis on biomarker thermal maturity parameters: Monterey Phosphatic and Siliceous Members: Organic Geochemistry, v. 15, p. 249-265.

Peters, K.E., Walters, C.C., Moldowan, J.M., 2005a, The Biomarker Guide: Volume 1 Biomarkers and Isotopes in the Environment and Human History: New York, Cambridge University Press.

Peters, K.E., Walters, C.C., Moldowan, J.M., 2005b, The Biomarker Guide: Volume 2 Biomarkers and Isotopes in Petroleum Exploration and Earth History: New York, Cambridge University Press.

Piper, D.Z., and Calvert, S.E., 2009, A marine biogeochemical perspective on black shale deposition: Earth Science Reviews, v. 95, p. 63-96.

Price, L.C., and Barker, C.E., 1985, Suppression of vitrinite reflectance in amorphous rich kerogen – A major unrecognized problem: Journal of Petroleum Geology, v. 8, p. 59-84.

Repetski, J.E., Ryder, R.T., Weary, D.J., Harris, A.G., and Trippi, M.H., 2008, Thermal maturity patterns (CAI and $\%R_o$) in Upper Ordovician and Devonian Rocks of the Appalachian Basin: A major revision of USGS map I–917–E using new subsurface collections: United States Geological Survey Scientific Investigation Map 3006.

Requejo, A.G., Hieshima, G.B., Hsu, C.S., McDonald, T.J., and Sassen, R., 1997, Short-chain (C21 and C22) diasteranes in petroleum and source rocks as indicators of maturity and depositional environment: Geochimica et Cosmochimica Acta, v. 61, p. 2653-2667.

Roen, J.B., 1993, Introductory review—Devonian and Mississippian black shales, eastern North America, *in* Roen, J.B. and Kepferle, R.C., eds., Petroleum Geology of the Devonian and Mississippian Black Shale of Eastern North America, volume 1909: U.S. Geological Survey Bulletin, p. A1-A8.

Rowan, E.L., 2006, Burial and thermal history of the central Appalachian Basin, based on three 2-D models of Ohio, Pennsylvania, and West Virginia: United States Geological Survey Open-File Report 2006-1019.

Sageman, B.B, Murphy, A.E, Werne, J.P., Ver Straeten, C.A., Hollander, D.J., and Lyons, T.W., 2003, A tale of shales: the relative roles of production, decomposition, and dilution in the accumulation of organic-rich strata, Middle-Upper Devonian, Appalachian basin: Chemical Geology, v. 195, p. 229-273.

Schwark, L., and Empt, P., 2006, Sterane biomarkers as indicators of Palaeozoic algal evolution and extinction events: Palaeogeography, Palaeoclimatology, Palaeoecology, v. 240, p. 225-236.

Shen, J., and Huang, W., 2007, Biomarker distributions as maturity indicators in coals, coaly shales, and shales from Taiwan: Terrestrial Atmospheric and Oceanic Sciences, v. 18, p. 739-755.

Sherman, L.S., Waldbauer, J.R., and Summons, R.E., 2007, Improved methods for isolating and validating indigenous biomarkers in Precambrian rocks: Organic Geochemistry, v. 38, p. 1987-2000.

Tissot, B., Califet-Debyser, Y., Deroo, G., and Oudin, J.L., 1971, Origin and evolution of hydrocarbons in early Toarcian Shales, Paris Basin, France: American Association of Petroleum Geologists Bulletin, v. 55, p. 2177-2193.

Tissot, B.P. and Welte, D.H., 1978, Petroleum Formation and Occurrence: Berlin, Springer-Verlag, 699 p.

Wignall, P.B., 1994, Black Shales: Oxford, Clarendon Press.

Table 3.1: Samples and depth of samples analyzed.

Well	County	Sample Number	MD[1]	TVD[2]
A	Floyd	A3440	3440 (1049)	2959 (902)
A	Floyd	A4640	4640 (1414)	2968 (905)
A	Floyd	A6100	6100 (1859)	2971 (906)
B	Pike	B4050	4050 (1234)	3923 (1196)
B	Pike	B5350	5350 (1631)	3971 (1210)
C	Perry	C3470	3470 (1058)	3372 (1028)
C	Perry	C3650	3650 (1113)	3423 (1043)
D	Mingo	D5000	5000 (1524)	4964 (1513)
D	Mingo	D6030	6030 (1838)	5169 (1576)
D	Mingo	D7270	7270 (2216)	5173 (1578)
E	Pike	E4060	4060 (1237)	3910 (1192)
E	Pike	E5160	5160 (1573)	3958 (1206)
E	Pike	E6340	6340 (1932)	3968 (1209)
E	Pike	E7100	7100 (2164)	3987 (1215)
F	Letcher	F4125	4125 (1257)	4036 (1230)
G	Logan	G4640	4640 (1414)	4513 (1376)
G	Logan	G6260	6260 (1908)	4570 (1393)
G	Logan	G7100	7100 (2164)	4566 (1392)
H	Knott	H3720	3720 (1134)	3486 (1063)
H	Knott	H5310	5310 (1618)	3519 (1073)
H	Knott	H6600	6600 (2012)	3537 (1078)

[1]Measured depth in feet (m) from ground level along length of wellbore

[2]True vertical depth in feet (m) from ground level to sample location

Table 3.2: Steps of biomarker extraction and detection from whole rock sample.

	Method	Purpose	Procedure
1	Ultrasonication	Extract organic matter	Ultrasonicate 75 g of crushed sample for 30 min in 40 ml of dichloromethane (DCM). Filter to remove crushed sample, collect extract, and repeat with additional 40 ml DCM
2	Sulfur and asphaltene removal	Remove elemental sulfur and asphaltenes	Rinse Cu pellets with 37% hydrochloric acid (HCL) until Cu reaches bright color. Then rinse with deionized (DI) water, then methanol, then DCM. Add 5 g of the activated Cu to vial containing extract and stir 8 h. After stirring filter to remove Cu. Reduce Cu free extract to 1 ml under nitrogen gas. Add 50 ml of n-pentane and allow to sit 8 h to precipitate asphaltenes. Filter extract to remove asphaltenes. Collect asphaltene free extract and reduce to 1 ml.
3	Column chromatography	Fractionate extracted organic matter	Activate silica gel by heating for 8 hours at 110°C. Mix silica gel with hexane to form slurry. Plug Pasteur pipette with cotton wool and fill with slurry. Add extract to top of column. Elute fractions of increasing polarity by sequential elution with 4 ml hexane (saturated fraction) then 2 ml hexane/2 ml DCM (aromatic fraction). Collect the eluated fractions in clean vials, evaporate to dryness, and then dissolve in 1 ml DCM.
4A	Gas chromatography (GC)/flame ionization detection (FID)	Separate and identify biomarkers	With a Phenomenex ZB-5 column (30m x 0.25mm x 0.25µm) installed in the gas chromatograph (GC), program the oven for a 2 min hold at 40°C, and then heat to 310°C at 4°C/min with a final hold time of 15 min. Use helium as the carrier gas.
4B	GC/mass spectroscopy (MS)/MS	Separate and identify biomarkers	With a Restek Rtx-5MS column (30m x 0.25mm x 0.25µm) installed in the GC, program the oven for a 2 min hold at 40°C and then heat to 310°C at 4°C/min with a final hold time of 15 min. Use helium as the carrier gas. Set transfer line at 280°C and the mass spectrophotometer (MS) source at 230°C. Acquire electron impact mass spectra at 70 eV in MS/MS mode.

Procedures modified from Sherman et al. (2007), Forster et al. (2004), and Brocks et al. (2003)

Extraction variability = ±1.6% and Detection limit = 1 ppb

Table 3.3: Parent to daughter transitions analyzed using GC/MS/MS for sterane and hopane detection in this investigation.

Biomarker	Parent Ion (m/z)	Daughter Ion (m/z)
C_{27} Steranes	372	217
C_{28} Steranes	386	217
C_{29} Steranes	400	217
C_{30} Steranes	414	217
C_{27} Hopanes	370	191
C_{29} Hopanes	398	191
C_{30} Hopanes	412	191
C_{31} Hopanes	426	191

m/z = mass to charge ratio

Table 3.4: Biomarker ratios used to interpret thermal maturity of samples in this investigation and abbreviations of each.

Biomarker Ratio	Abbreviation
Alkane and Isoprenoid Ratios	
Pristane/n-Heptadecane	Pr/n-C_{17}
Phytane/n-Dotriacontane	Ph/n-C_{18}
Sterane Ratios	
5α(H),14α(H),17α(H)-Cholestane-20S / (5α(H),14α(H),17α(H)-Cholestane-20S + 5α(H),14α(H),17α(H)-Cholestane-20R)	C_{27}-20S/(20S+20R)
5α(H), 14α(H),17α(H)-24-Methylcholestane-20S / (14α(H),17α(H)-24-Methylcholestane-20S + 14α(H),17α(H)-24-Methylcholestane-20R)	C_{28}-20S/(20S+20R)
5α(H),14α(H),17α(H)-24-Ethylcholestane-20S / (5α(H),14α(H),17α(H)-24-Ethylcholestane-20S + 5α(H),14α(H),17α(H)-24-Ethylcholestane-20R)	C_{29}-20S/(20S+20R)
5α(H),14β(H),17β(H)-24-Methylcholestane-20R + 5α(H),14β(H),17β(H)-24-Methylcholestane-20S) / (5α(H),14β(H),17β(H)-24-Methylcholestane-20R + 5α(H),14β(H),17β(H)-24-Methylcholestane-20S + 5α(H),14α(H),17α(H)-24-Methylcholestane-20S + 5α(H),14α(H),17α(H)-24-Methylcholestane-20R)	C_{28}-αββ/(αββ+ααα)
(5α(H),14β(H),17β(H)-24-Ethylcholestane-20R + 5α(H),14β(H),17β(H)-24-Ethylcholestane-20S) / (5α(H),14α(H),17α(H)-24-Ethylcholestane-20S + 5α(H),14α(H),17α(H)-24-Ethylcholestane-20R + 5α(H),14β(H),17β(H)-24-Ethylcholestane-20R + 5α(H),14β(H),17β(H)-24-Ethylcholestane-20S)	C_{29}- αββ/(αββ+ααα)
Hopane Ratios	
18α(H)-22,29,30-Trisnorneohopane / (18α(H)-22,29,30-Trisnorneohopane + 17α(H)-22,29,30-Trisnorhopane)	Ts/(Ts+Tm)
17α(H),21β(H)-Homohopane-22S / (17α(H),21β(H)-Homohopane-22S + 17α(H),21β(H)-Homohopane-22R)	22S/(22S+22R)

Table 3.5: N-alkane and isoprenoid biomarkers identified in samples analyzed with FID and characteristics of each. All biomarkers listed were identified in all samples analyzed except samples C3650, D5000, and D7270.

Biomarker	Abbreviation	Molecular Formula	Weight (amu)	*Possible Origin
n-Alkanes				
n-Decane	n-C_{10}	$C_{10}H_{22}$	142	Variable
n-Undecane	n-C_{11}	$C_{11}H_{24}$	156	Variable
n-Dodecane	n-C_{12}	$C_{12}H_{26}$	170	Variable
n-Tridecane	n-C_{13}	$C_{13}H_{28}$	184	Variable
n-Tetradecane	n-C_{14}	$C_{14}H_{30}$	198	Variable
n-Pentadecane	n-C_{15}	$C_{15}H_{32}$	212	Marine algae
n-Hexadecane	n-C_{16}	$C_{16}H_{34}$	226	Algae, Bacteria
n-Heptadecane	n-C_{17}	$C_{17}H_{36}$	240	Marine algae
n-Octadecane	n-C_{18}	$C_{18}H_{38}$	254	Algae, Bacteria
n-Nonadecane	n-C_{19}	$C_{19}H_{40}$	268	Marine algae
n-Icosane	n-C_{20}	$C_{20}H_{42}$	282	Algae, Bacteria
n-Henicosane	n-C_{21}	$C_{21}H_{44}$	296	Marine algae
n-Docosane	n-C_{22}	$C_{22}H_{46}$	310	Algae, Bacteria
n-Tricosane	n-C_{23}	$C_{23}H_{48}$	324	Nonmarine algae
n-Tetracosane	n-C_{24}	$C_{24}H_{50}$	338	Nonmarine algae
n-Pentacosane	n-C_{25}	$C_{25}H_{52}$	352	Nonmarine algae
n-Hexacosane	n-C_{26}	$C_{26}H_{54}$	366	Plant waxes
n-Heptacosane	n-C_{27}	$C_{27}H_{56}$	380	Nonmarine algae
n-Octacosane	n-C_{28}	$C_{28}H_{58}$	394	Plant waxes
n-Nonacosane	n-C_{29}	$C_{29}H_{60}$	408	Nonmarine algae
n-Triacontane	n-C_{30}	$C_{30}H_{62}$	422	Plant waxes
n-Hentriacontane	n-C_{31}	$C_{30}H_{64}$	436	Plant waxes
Isoprenoids				
Pristane	Pr	$C_{19}H_{40}$	268	Purple sulfur bacteria
Phytane	Ph	$C_{20}H_{42}$	282	Purple sulfur bacteria

*Peters et al. (2005a)
amu = atomic mass unit

Table 3.6: Characteristics of n-alkane, sterane, and hopane biomarkers identified in samples analyzed.

Sample	MAC Alkane[1]	Cmax Aquatic[2]	Cmax Waxes[3]	MAC Sterane[4]	MAC Hopane[5]	27%[6]	28%[7]	29%[8]
A3440	n-C_{13}	n-C_{16}	n-C_{28}	$C_{27}\alpha\beta\beta$-R	$C_{29}H$	41	25	34
A4640	n-C_{12}	n-C_{16}	n-C_{27}	$C_{27}\alpha\beta\beta$-S	$C_{29}H$	38	26	36
A6100	n-C_{12}	n-C_{16}	n-C_{27}	$C_{27}\alpha\beta\beta$-S	$C_{29}H$	64	21	15
B4050	n-C_{14}	n-C_{16}	n-C_{27}	$C_{27}\alpha\alpha\alpha$-S	$C_{29}H$	41	44	15
B5350	n-C_{13}	n-C_{16}	n-C_{27}	$C_{28}\alpha\beta\beta$-R	$C_{29}H$	41	40	19
C3470	n-C_{15}	n-C_{16}	n-C_{27}	$C_{28}\alpha\beta\beta$-R	$C_{29}H$	28	36	36
C3650	nd	nd	nd	nd	nd	nd	nd	nd
D5000	nd	nd	nd	nd	nd	nd	nd	nd
D6030	n-C_{21}	n-C_{17}	n-C_{27}	$C_{28}\alpha\alpha\alpha$-S	$C_{29}H$	28	43	29
D7270	nd	nd	nd	nd	nd	nd	nd	nd
E4060	n-C_{12}	n-C_{16}	n-C_{28}	$C_{27}\alpha\beta\beta$-S	$C_{29}H$	41	28	31
E5160	n-C_{12}	n-C_{16}	n-C_{27}	$C_{27}\alpha\beta\beta$-S	$C_{29}H$	49	29	22
E6340	n-C_{14}	n-C_{16}	n-C_{27}	$C_{27}\alpha\alpha\alpha$-S	$C_{29}H$	39	20	41
E7100	n-C_{12}	n-C_{16}	n-C_{27}	$C_{27}\alpha\beta\beta$-S	$C_{29}H$	46	20	34
F4125	n-C_{16}	n-C_{16}	n-C_{28}	$C_{27}\alpha\alpha\alpha$-S	$C_{29}H$	48	38	14
G4640	n-C_{16}	n-C_{16}	n-C_{27}	$C_{27}\alpha\alpha\alpha$-S	$C_{29}H$	56	17	27
G6260	n-C_{12}	n-C_{16}	n-C_{28}	$C_{27}\alpha\alpha\alpha$-S	$C_{29}H$	37	12	51
G7100	n-C_{12}	n-C_{16}	n-C_{27}	$C_{27}\alpha\alpha\alpha$-S	$C_{29}H$	42	19	39
H3720	n-C_{12}	n-C_{16}	n-C_{27}	$C_{27}\alpha\alpha\alpha$-S	$C_{29}H$	36	28	36
H5310	n-C_{12}	n-C_{16}	n-C_{27}	$C_{27}\alpha\alpha\alpha$-S	$C_{29}H$	45	41	14
H6600	n-C_{12}	n-C_{16}	n-C_{27}	$C_{29}\alpha\alpha\alpha$-R	$C_{29}H$	41	27	32

[1] Most abundant n-alkane identified in sample

[2] Most abundant n-alkane between n-C_{16} and n-C_{18} in sample

[3] Most abundant n-alkane between n-C_{27} and n-C_{33} in sample

[4] Most abundant sterane identified in sample

[5] Most abundant hopane identified in sample

[6] $(C_{27}\alpha\alpha\alpha(S+R) + C_{27}\alpha\beta\beta(S+R))/(\sum C_{27}$ to $C_{29}\ \alpha\alpha\alpha(S+R) + \alpha\beta\beta(S+R))$

[7] $(C_{28}\alpha\alpha\alpha(S+R) + C_{28}\alpha\beta\beta(S+R))/(\sum C_{27}$ to $C_{29}\ \alpha\alpha\alpha(S+R) + \alpha\beta\beta(S+R))$

[8] $(C_{29}\alpha\alpha\alpha(S+R) + C_{29}\alpha\beta\beta(S+R))/(\sum C_{27}$ to $C_{29}\ \alpha\alpha\alpha(S+R) + \alpha\beta\beta(S+R))$

nd = not detected (below detection limit)

Table 3.7: Sterane and hopane biomarkers identified in samples analyzed with GC/MS/MS and characteristics of each. All biomarkers listed were identified in all samples analyzed except samples C3650, D5000, and D7270.

Biomarker	Abbreviation	Molecular Formula	Weight (amu)	*Source
C_{27} Steranes				
5α(H),14α(H),17α(H)-Cholestane-20S	C_{27}ααα-S	$C_{27}H_{48}$	372	Marine algae
5α(H),14β(H),17β(H)-Cholestane-20R	C_{27}αββ-R	$C_{27}H_{48}$	372	Marine algae
5α(H),14β(H),17β(H)-Cholestane-20S	C_{27}αββ-S	$C_{27}H_{48}$	372	Marine algae
5α(H),14α(H),17α(H)-Cholestane-20R	C_{27}ααα-R	$C_{27}H_{48}$	372	Marine algae
C_{28} Steranes				
5α(H),14α(H),17α(H)-24-Methylcholestane-20S	C_{28}ααα-S	$C_{28}H_{50}$	386	Bacterial plankton and algae
5α(H),14β(H),17β(H)-24-Methylcholestane-20R	C_{28}αββ-R	$C_{28}H_{50}$	386	Bacterial plankton and algae
5α(H),14β(H),17β(H)-24-Methylcholestane-20S	C_{28}αββ-S	$C_{28}H_{50}$	386	Bacterial plankton and algae
5α(H),14α(H),17α(H)-24-Methylcholestane-20R	C_{28}ααα-R	$C_{28}H_{50}$	386	Bacterial plankton and algae
C_{29} Steranes				
5α(H),14α(H),17α(H)-24-Ethylcholestane-20S	C_{29}ααα-S	$C_{29}H_{52}$	400	Land plants
5α(H),14β(H),17β(H)-24-Ethylcholestane-20R	C_{29}αββ-R	$C_{29}H_{52}$	400	Land plants
5α(H),14β(H),17β(H)-24-Ethylcholestane-20S	C_{29}αββ-S	$C_{29}H_{52}$	400	Land plants
5α(H),14α(H),17α(H)-24-Ethylcholestane-20R	C_{29}ααα-R	$C_{29}H_{52}$	400	Land plants
C_{30} Steranes				
5α(H),14α(H),17α(H)-24-Propylcholestane-20S	C_{30}ααα-S	$C_{30}H_{54}$	414	Marine algae
5α(H),14β(H),17β(H)-24-Propylcholestane-20R	C_{30}αββ-R	$C_{30}H_{54}$	414	Marine algae

Table 3.7 continued

5α(H),14β(H),17β(H)-24-Propylcholestane-20S	C_{30}αββ-S	$C_{30}H_{54}$	414	Marine algae
5α(H),14α(H),17α(H)-24-Propylcholestane-20R	C_{30}ααα-R	$C_{30}H_{54}$	414	Marine algae
C_{27} Hopanes				
18α(H)-22,29,30-Trisnorneohopane	Ts	$C_{27}H_{46}$	370	Cyanobacteria, Proteobacteria
17α(H)-22,29,30-Trisnorhopane	Tm	$C_{27}H_{46}$	370	Cyanobacteria, Proteobacteria
C_{29} Hopane				
17α(H),21β(H)-30-Norhopane	C_{29}H	$C_{29}H_{50}$	398	Cyanobacteria, Proteobacteria
18α(H)-Norneohopane	C_{29}Ts	$C_{29}H_{50}$	398	Cyanobacteria, Proteobacteria
C_{30} Hopane				
17α(H),21β(H)-Hopane	C_{30}H	$C_{30}H_{52}$	400	Cyanobacteria, Proteobacteria
C_{31} Hopane				
17α(H),21β(H)-Homohopane-22S	C_{31}H-S	$C_{31}H_{54}$	426	Cyanobacteria, Proteobacteria
17α(H),21β(H)-Homohopane-22R	C_{31}H-R	$C_{31}H_{54}$	426	Cyanobacteria, Proteobacteria

*Peters et al. (2005 a and b)
amu = atomic mass unit

Table 3.8: Biomarker maturity ratios of samples analyzed.

	Alkanes		Steranes					Hopanes	
Sample	Pr/n-C_{17}	Ph/n-C_{18}	C_{27} 20S(20S+20R)	C_{28} 20S(20S+20R)	C_{29} 20S(20S+20R)	C_{28} ββ/(ββ+αα)	C_{29} ββ/(ββ+αα)	Ts/(Ts+Tm)	22S/(22S+2
A3440	0.70	0.52	0.64	0.50	0.55	0.55	0.46	0.55	0.67
A4640	0.68	0.51	0.65	0.60	0.61	0.60	0.57	0.62	0.71
A6100	0.58	0.45	0.60	0.68	0.67	0.68	0.66	0.6	0.58
B4050	0.49	0.49	0.65	0.62	0.65	0.73	0.66	0.75	0.63
B5350	0.44	0.44	0.71	0.69	0.69	0.72	0.61	0.79	0.69
C3470	0.59	0.49	0.67	0.63	0.67	0.61	0.65	0.64	0.67
C3650	nd	nd	nd	nd	nd	nd	nd	nd	nd
D5000	nd	nd	nd	nd	nd	nd	nd	nd	nd
D6030	0.40	0.32	0.14	0.60	0.77	0.19	0.71	0.88	0.69
D7270	nd	nd	nd	nd	nd	nd	nd	nd	nd
E4060	0.49	0.47	0.50	0.63	0.66	0.68	0.66	0.59	0.69
E5160	0.47	0.45	0.70	0.59	0.71	0.76	0.62	0.78	0.69
E6340	0.45	0.43	0.81	0.50	0.77	0.65	0.63	0.55	0.55
E7100	0.45	0.47	0.74	0.50	0.64	0.68	0.64	0.64	0.65
F4125	0.43	0.46	0.63	0.67	0.75	0.71	0.70	0.65	0.73
G4640	0.42	0.35	0.76	0.90	0.72	0.69	0.62	0.58	0.55
G6260	0.41	0.36	0.91	0.56	0.71	0.68	0.66	0.76	0.74
G7100	0.42	0.35	0.61	0.50	0.68	0.69	0.62	0.73	0.81
H3720	0.51	0.50	0.65	0.64	0.67	0.50	0.64	0.58	0.55
H5310	0.52	0.50	0.55	0.65	0.70	0.60	0.65	0.65	0.74
H6600	0.50	0.44	0.56	0.50	0.68	0.60	0.65	0.69	0.84

nd = below detection limit

Table 3.9: Thermal maturities represented by the samples analyzed for biomarker maturity ratios.

Ratio	Values	Thermal Maturity
C_{27}-20S/(20S+20R)	0.14 – 0.91	At or above peak oil generation
C_{28}-20S/(20S+20R)	0.50 – 0.90	Early to peak oil generation
C_{29}-20S/(20S+20R)	0.55 – 0.77	At or above peak oil generation
C_{28}-αββ/(αββ+ααα)	0.19 – 0.79	Early to peak oil generation
C_{29}- αββ/(αββ+ααα)	0.46 – 0.71	Early to peak oil generation
Ts/(Ts+Tm)	0.55 – 0.88	Early to peak oil generation
22S/(22S+22R)	0.55 – 0.84	At or above early oil generation

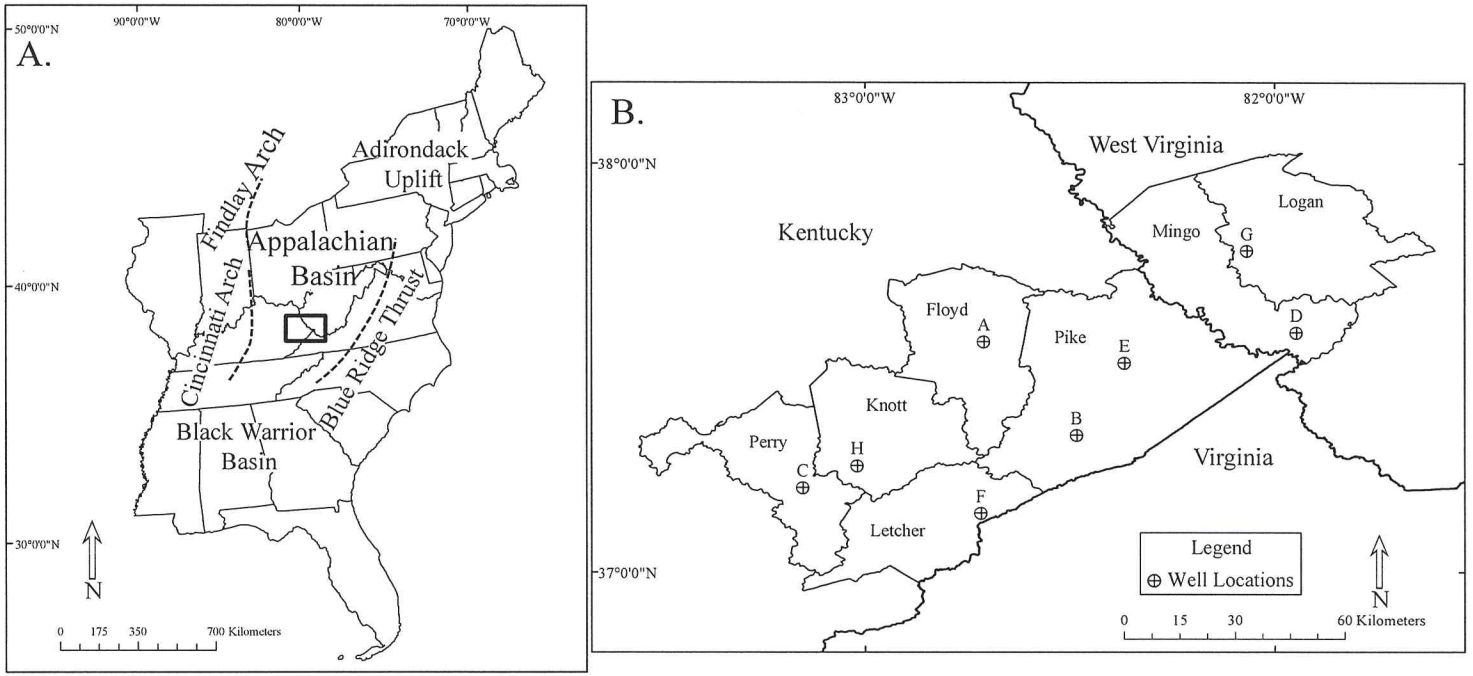

Figure 3.1: A = Major structural features of eastern United States (modified from Roen, 1993) and location of study area map. B = Sample locations with states and counties labeled.

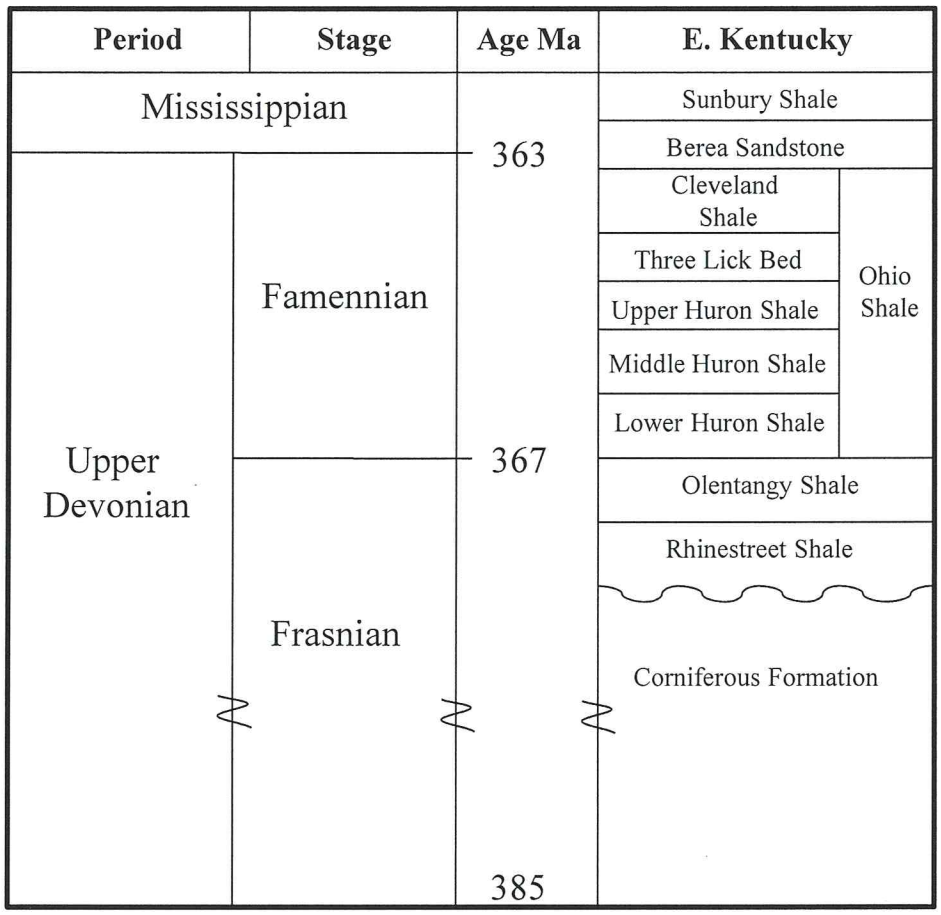

Figure 3.2: Upper Devonian and Lower Mississippian stratigraphy of eastern Kentucky and southern West Virginia (modified from Hamilton-Smith, 1993 and de Witt et al., 1993).

n-pentadecane (n-C_{15})

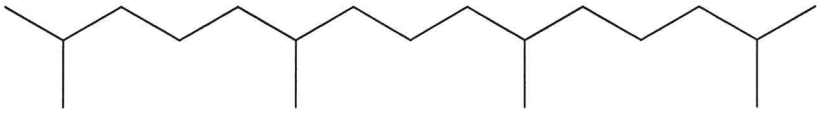

Pristane (Pr)

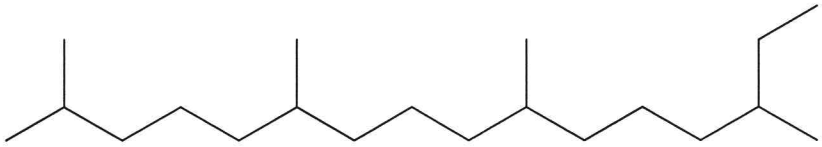

Phytane (Ph)

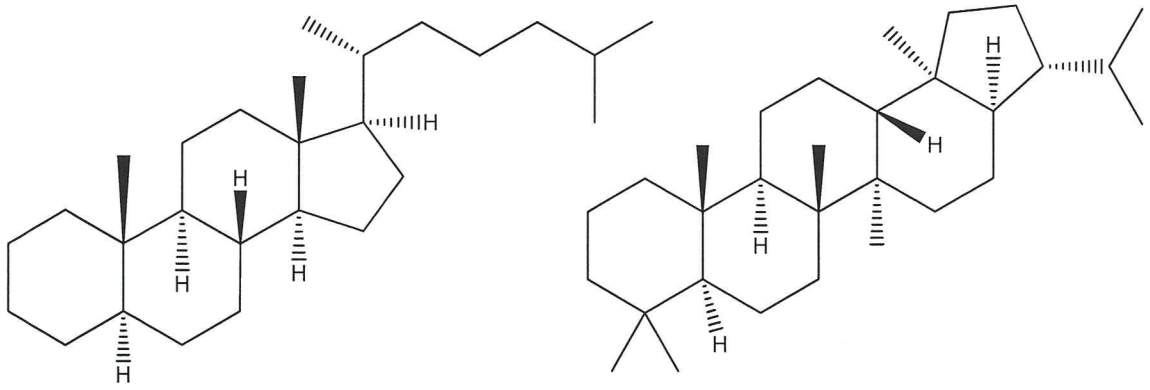

C_{27} Sterane C_{30} Hopane

Figure 3.3: General structures of biomarkers identified in samples. N-pentadecane structure represents structure of n-alkanes.

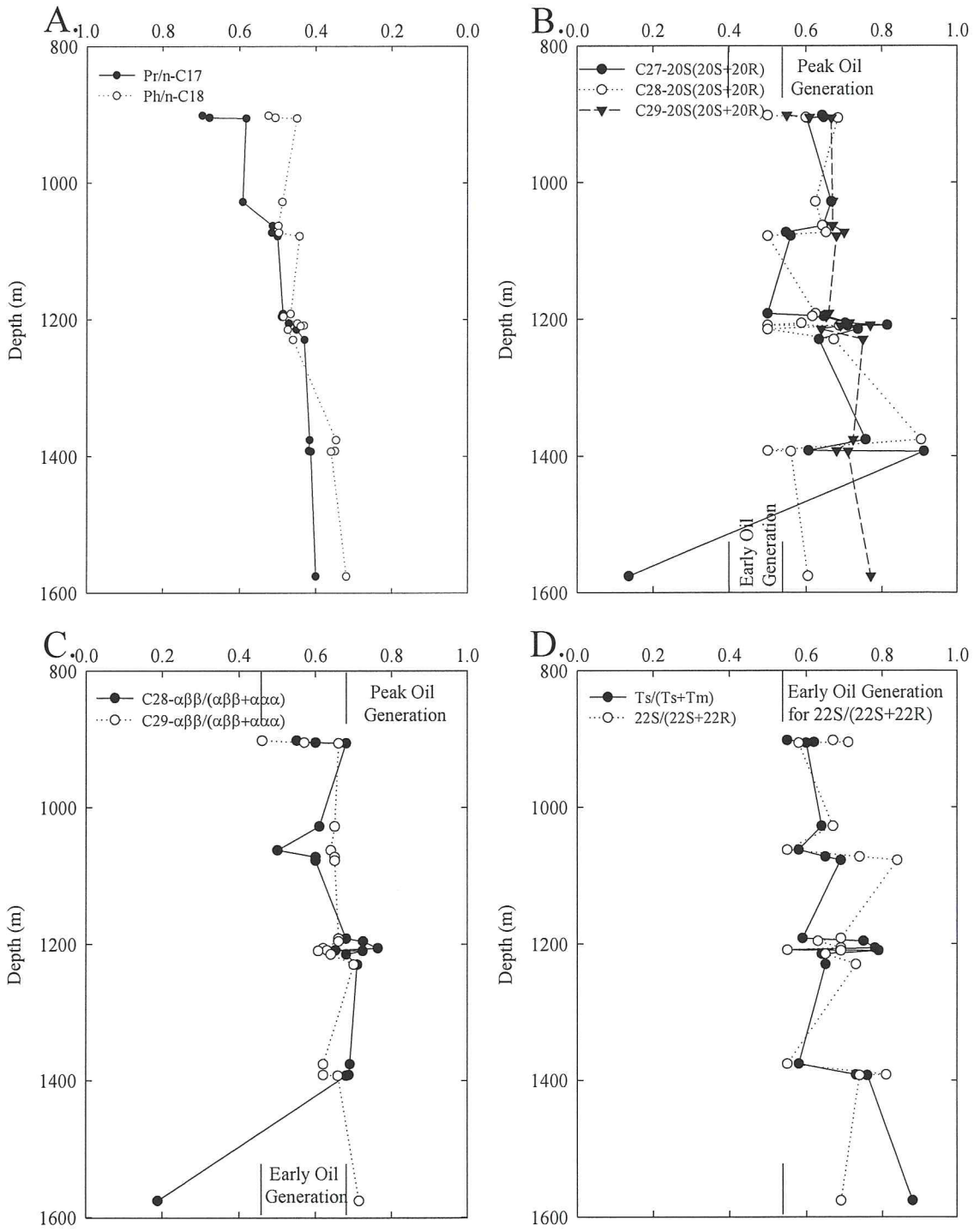

Figure 3.4: Biomarker maturity ratios versus depth for samples analyzed. Thermal maturity increases to the right on each graph. A = Pr/n-C_{17} and Ph/n-C_{18} maturity ratios. B = C_{27}-20S/(20S+20R), C_{28}-20S/(20S+20R), and C_{29}-20S/(20S+20R) maturity ratios. Early oil generation stage 0.40 to 0.55 and peak oil generation stage greater than 0.55

(Peters et al., 2005b). C = C_{28}-αββ/(αββ+ααα) and C_{29}-αββ/(αββ+ααα) maturity ratios. Early oil generation stage 0.45 to 0.70 and peak oil generation stage greater than 0.70 (Peters et al., 2005b). D = Ts/(Ts+Tm) and 22S/(22S+22R) maturity ratios. Early oil generation stage greater than 0.55 for 22S/(22S+22R) ratio (Peters et al., 2005b). Ts/(Ts+Tm) values greater than 1.00 represent late oil generation stage (Peters et al., 2005b).

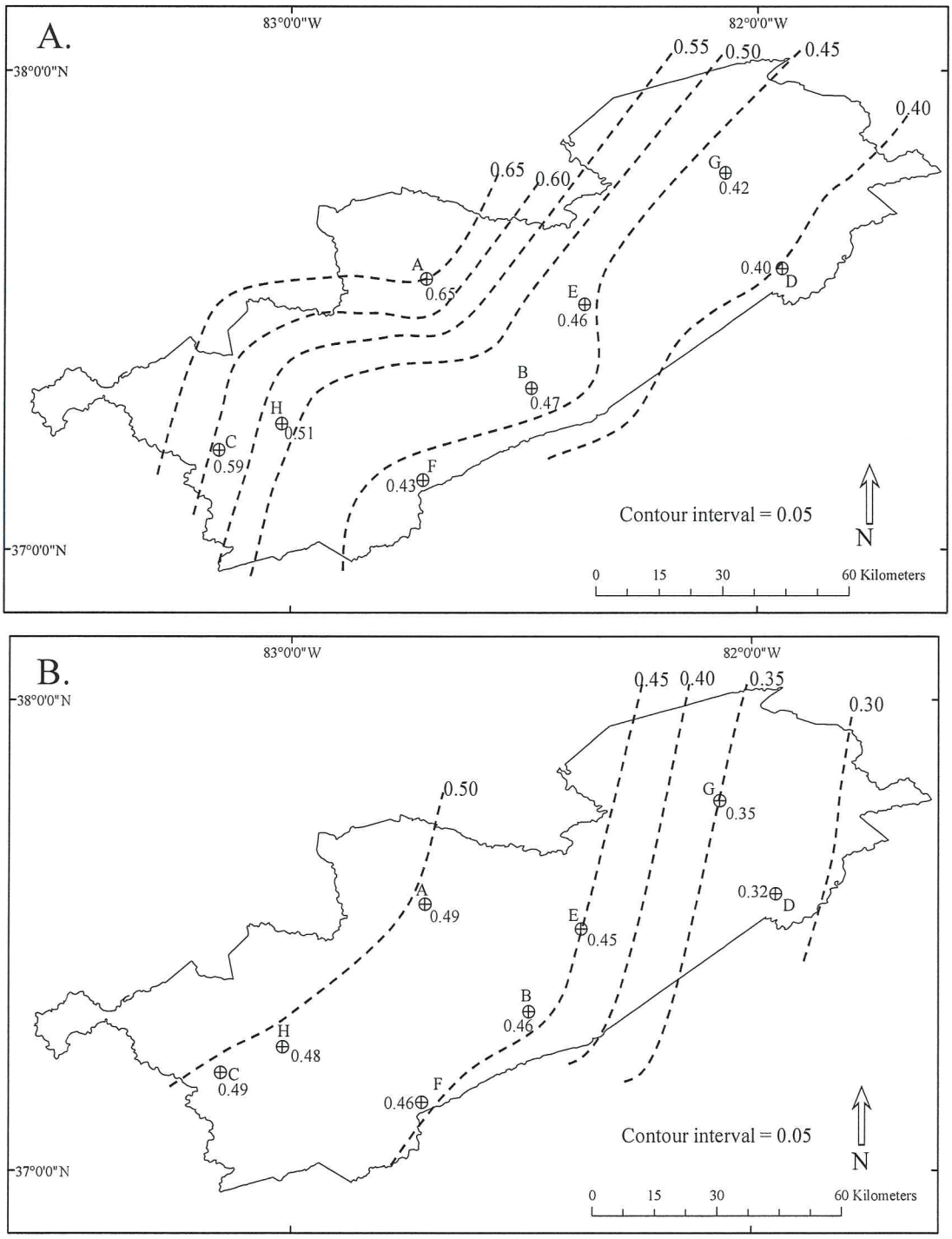

Figure 3.5: Contour maps of n-alkane and isoprenoid thermal maturity ratios. Mapped value for each well is the average for all samples analyzed from that well. A = Contour map of Pr/n-C_{17} values indicating increase in thermal maturity toward the southeast. B = Contour map of Ph/n-C_{18} values indicating increase in thermal maturity toward the southeast.

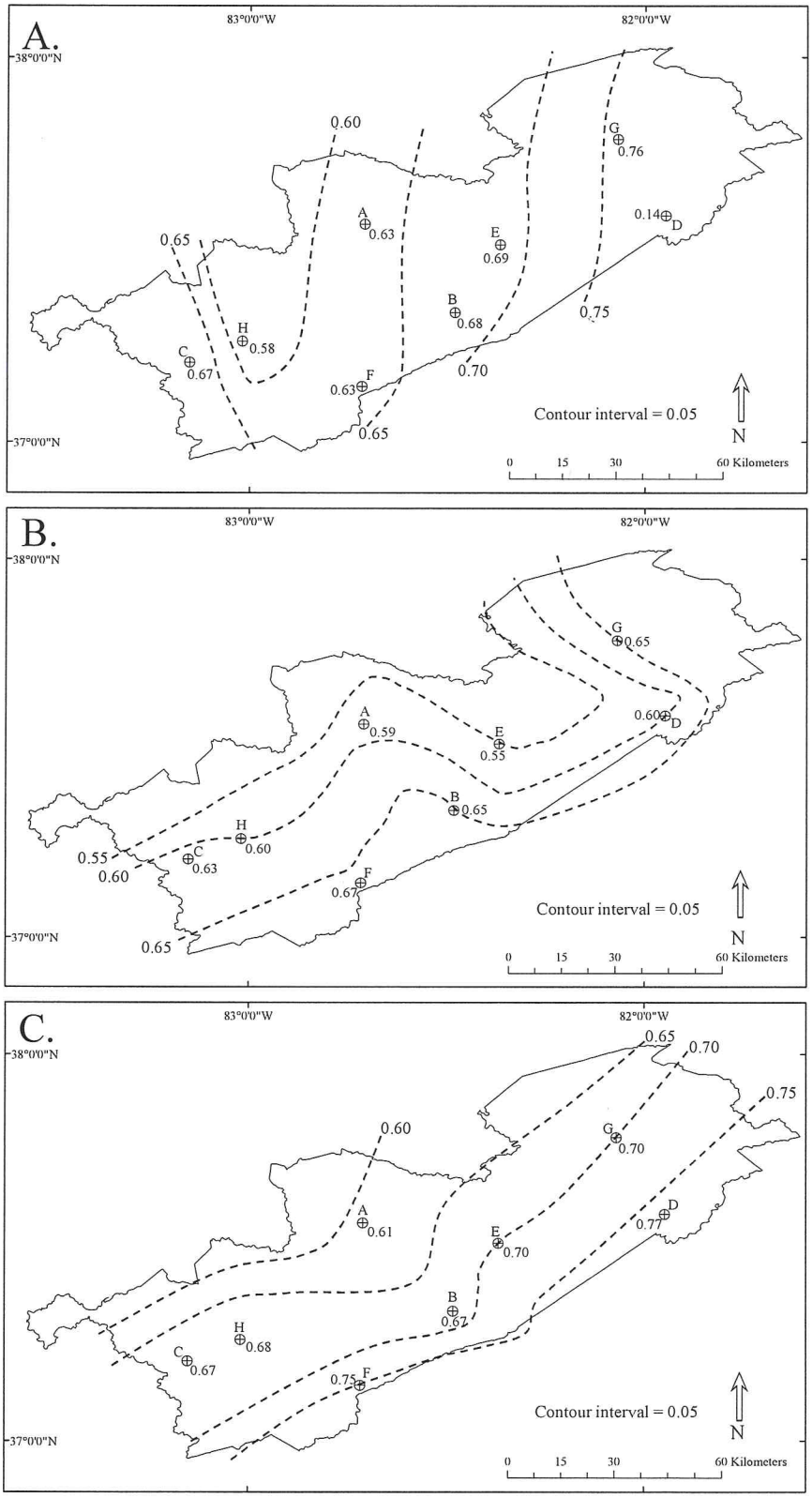

Figure 3.6: Contour maps of sterane thermal maturity ratios. Mapped value for each

well is the average for all samples analyzed from that well. A = Contour map of C_{27}-20S/(20S+20R) values indicating increase in thermal maturity toward the east. The 0.14 value at well D may be caused by inversion of the ratio due to high thermal maturity (Peters et al., 2005b). B = Contour map of C_{28}-20S/(20S+20R) values indicating increase in thermal maturity toward the southeast. C = Contour map of C_{29}-20S/(20S+20R) values indicating increase in thermal maturity toward the southeast.

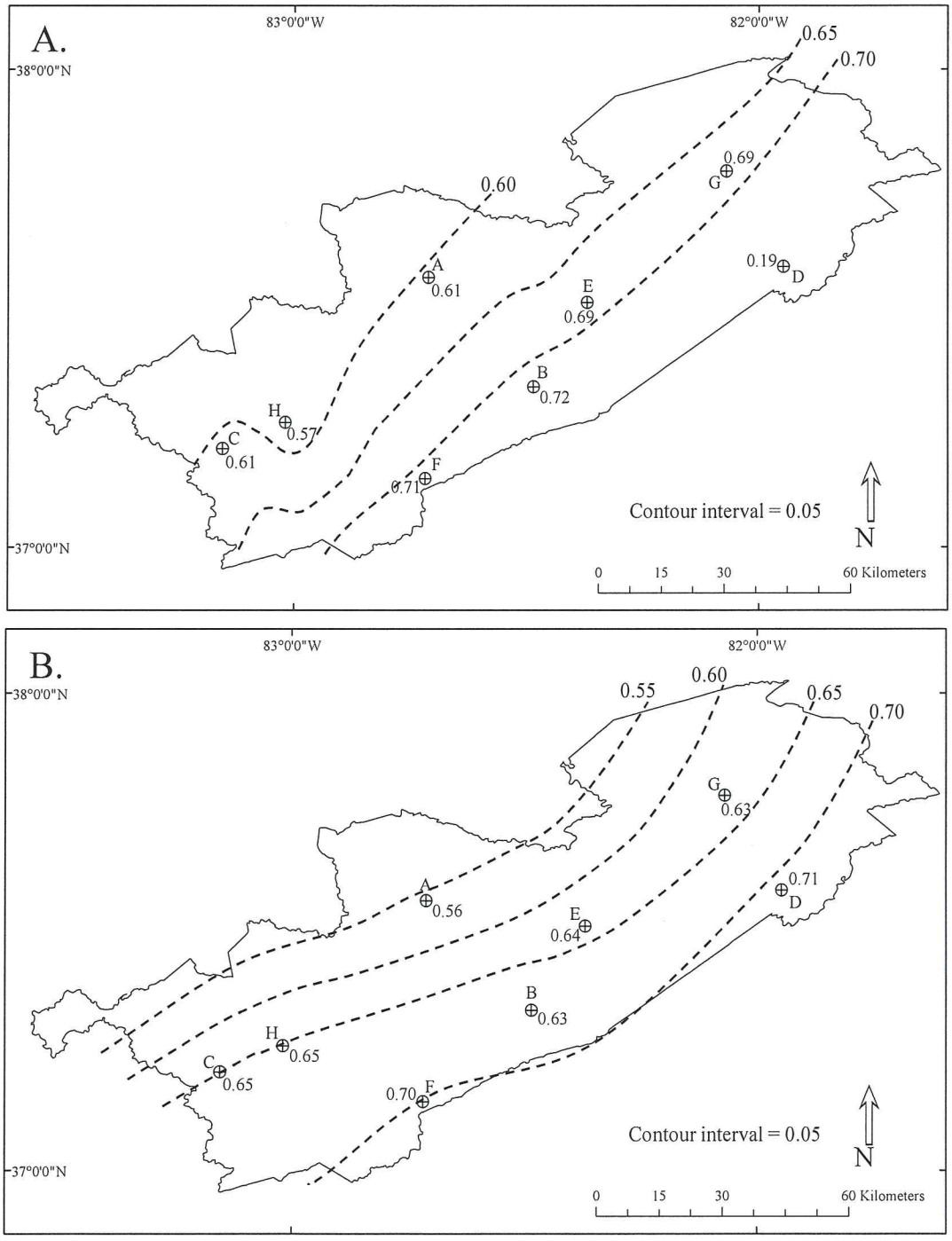

Figure 3.7: Contour maps of sterane thermal maturity ratios. Mapped value for each well is the average for all samples analyzed from that well. A = Contour map of C_{28}-αββ/(αββ+ααα) values indicating increase in thermal maturity toward the southeast. The 0.19 value at well D may be caused by inversion of the ratio due to high thermal maturity (Peters et al., 2005b). B = C_{29}-αββ/(αββ+ααα) values increase in thermal maturity toward the southeast.

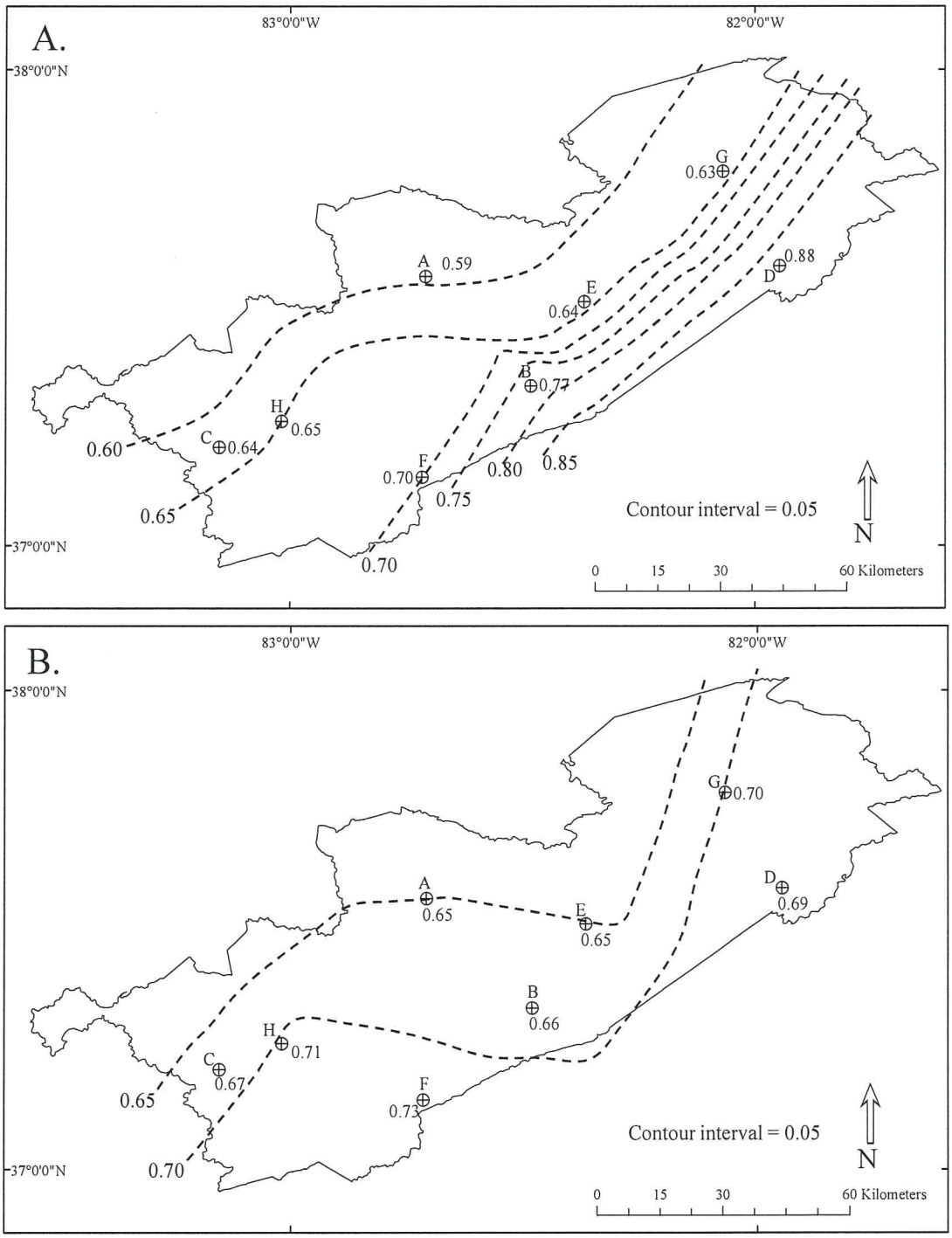

Figure 3.8: Contour maps of hopane thermal maturity ratios. Mapped value for each well is the average for all samples analyzed from that well. A = Contour map of Ts/(Ts+Tm) values indicating increase in thermal maturity toward the southeast. B = Contour map of 22S/(22S+22R) values indicating increase in thermal maturity toward the southeast.

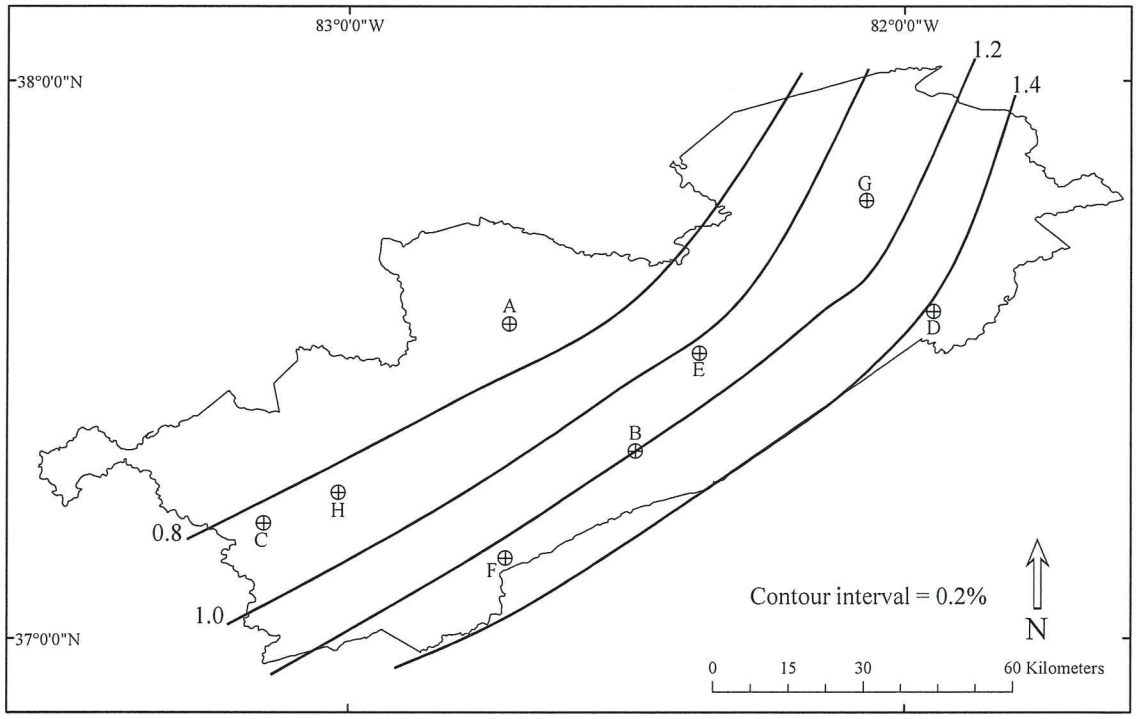

Figure 3.9: Contours of R_o (%) values indicating increase in thermal maturity toward the southeast. Modified from Hamilton-Smith (1993), Curtis and Faure (1997), and Repetski et al., (2008).

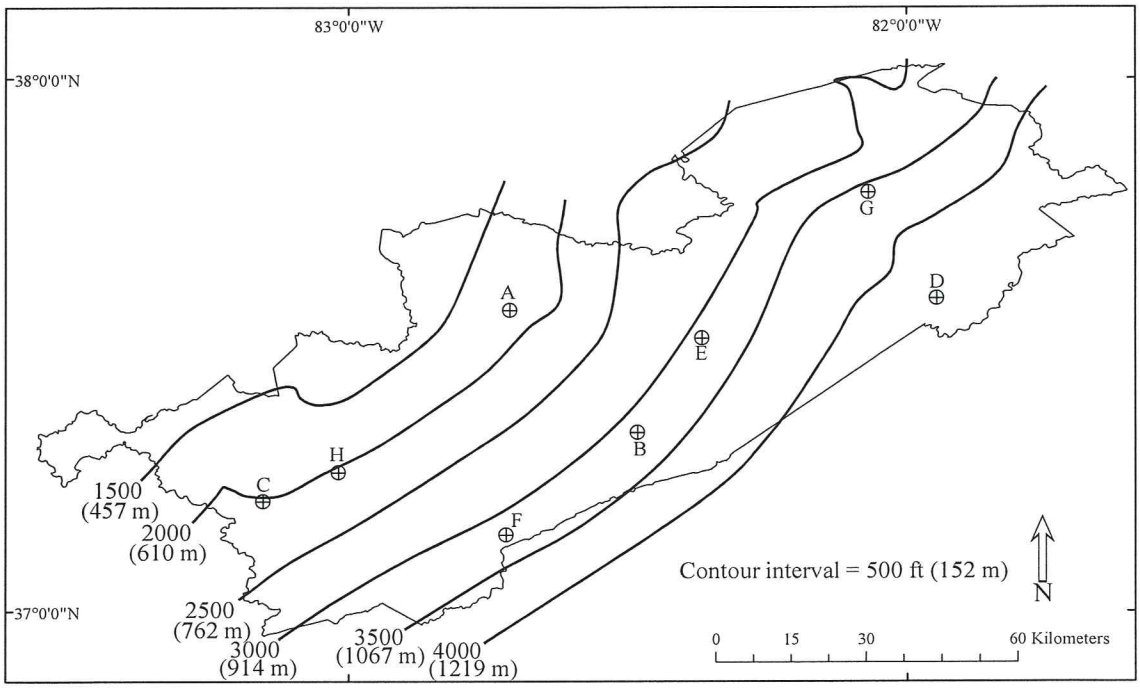

Figure 3.10: Structure contour map on base of Ohio Shale (base Lower Huron Shale) for the study area (from Dillman and Ettensohn, 1980). Structural trend follows trend of maximum burial depth (Rowan, 2006).

CHAPTER FOUR

CONCLUSIONS

The following biomarkers were identified in Lower Huron Shale (Upper Devonian) samples from eight wells located in eastern Kentucky and southern West Virginia: n-alkanes (C_{15} to C_{35}), pristane (Pr), phytane (Ph), steranes (ααα*R*, ααα*S*, αα*β*R, αα*β*S isomers of C_{27} to C_{30} steranes), and hopanes (C_{27}, C_{29}, C_{30} and C_{31} hopanes). The TAR (terrigenous versus aquatic n-alkanes ratio), n-C_{17}/n-C_{31}, Pr/n-C_{17}, Ph/n-C_{18}, and sterane distribution indicate the biological source of preserved organic matter in the Lower Huron Shale is predominately marine algae and bacteria. Pr/n-C_{17} and Ph/n-C_{18} indicate kerogen in the samples analyzed is type II, which can be the source of both oil and natural gas. The Pr/Ph, n-C_{17}/n-C_{31}, Pr/n-C_{17}, and Ts/Tm ratios in the samples analyzed indicate the Lower Huron Shale was deposited in alternating oxic and anoxic conditions. Sterane distributions in the samples analyzed indicate the Lower Huron Shale was deposited in deep waters (> 150 m).

The biomarker data coupled with published paleogeographical interpretations support establishment and breakdown of a seasonal thermocline during deposition of sediments represented by the Lower Huron Shale. During the warm season of a subtropical climate anoxic bottom waters persisted and allowed accumulation of phosphorus and nitrogen due to anaerobic decomposition of organic matter. As the climate cooled the thermocline was broken down resulting in mixing of the shallow and deep waters, which allowed the bottom waters to become oxic and increased primary productivity due to the upwelling of phosphorus and nitrogen.

Biomarker maturity ratios indicate that the samples analyzed have reached the early to late oil generation stages. Contour maps of the biomarker maturity ratio values indicate increasing thermal maturity toward the southeast within the study area, which corresponds to the direction of increasing maximum burial depth. Biomarker data suggest that gas produced from the Lower Huron Shale in the south-eastern region of the Big Sandy Field is thermogenic and that gas produced in the north-western region has migrated from more thermally mature areas to the east.

Appalachian Basin Devonian shales are a major shale gas play in the United States. This study was the first published study to identify biomarkers in the Lower Huron Shale to interpret organic matter source, depositional environment, and thermal maturity. A thorough geologic understanding of shale gas can aid in exploration of these plays. The availability of large amounts of shale gas will allow the United States to consume predominately a domestic supply of gas. By consuming gas produced domestically the supply is not dependent on foreign producers and the delivery system is less subject to interruption.

APPENDICES

Appendix A

Representative Chromatograms of Samples Analyzed and Standards

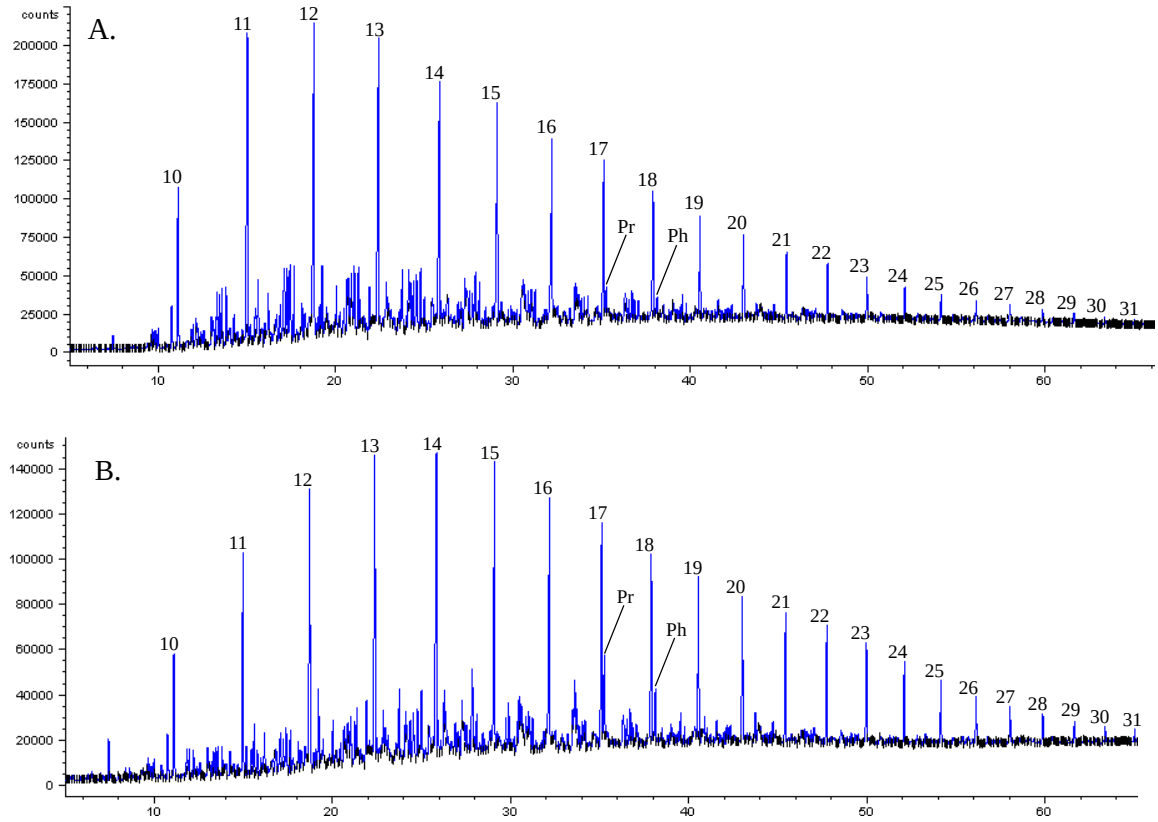

Figure A.1: Chromatograms showing n-alkanes, pristane (Pr), and phytane (Ph) of two representative samples. Numbers by the peaks give the number of carbon atoms in n-alkanes. Time in minutes on x-axis and ion count on y-axis. A. Sample G7100. B. Sample C3470.

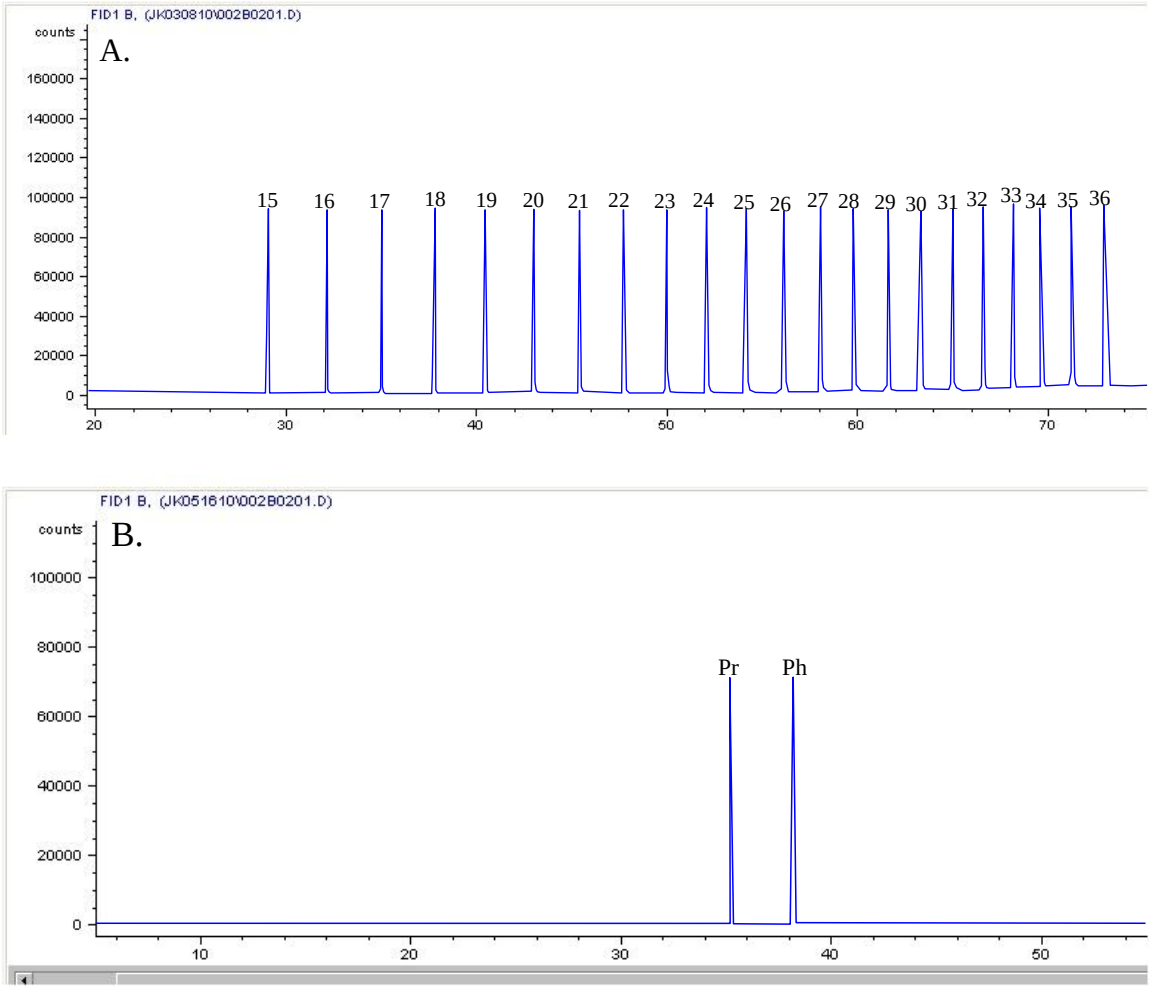

Figure A.2: Chromatograms showing n-alkanes, pristane (Pr), and phytane (Ph) standards. Numbers by the peaks give the number of carbon atoms in n-alkanes. Time in minutes on x-axis and ion count on y-axis.

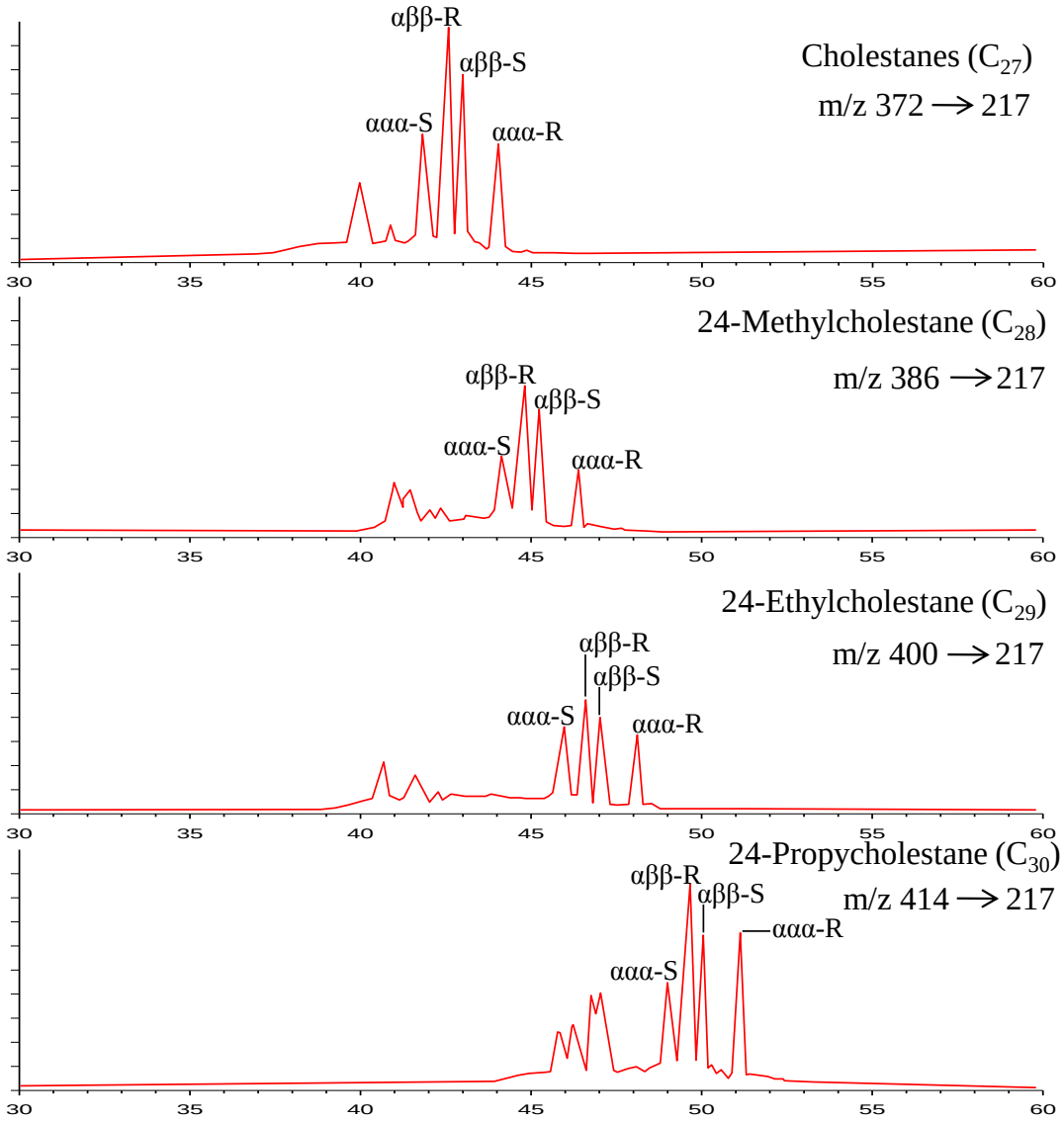

Figure A.3: Chromatograms showing isomers of C_{27} to C_{30} steranes identified in a representative sample (A6100). Parent to daughter ion transitions are labeled on each chromatogram. Time in minutes on x-axis and ion count on y-axis.

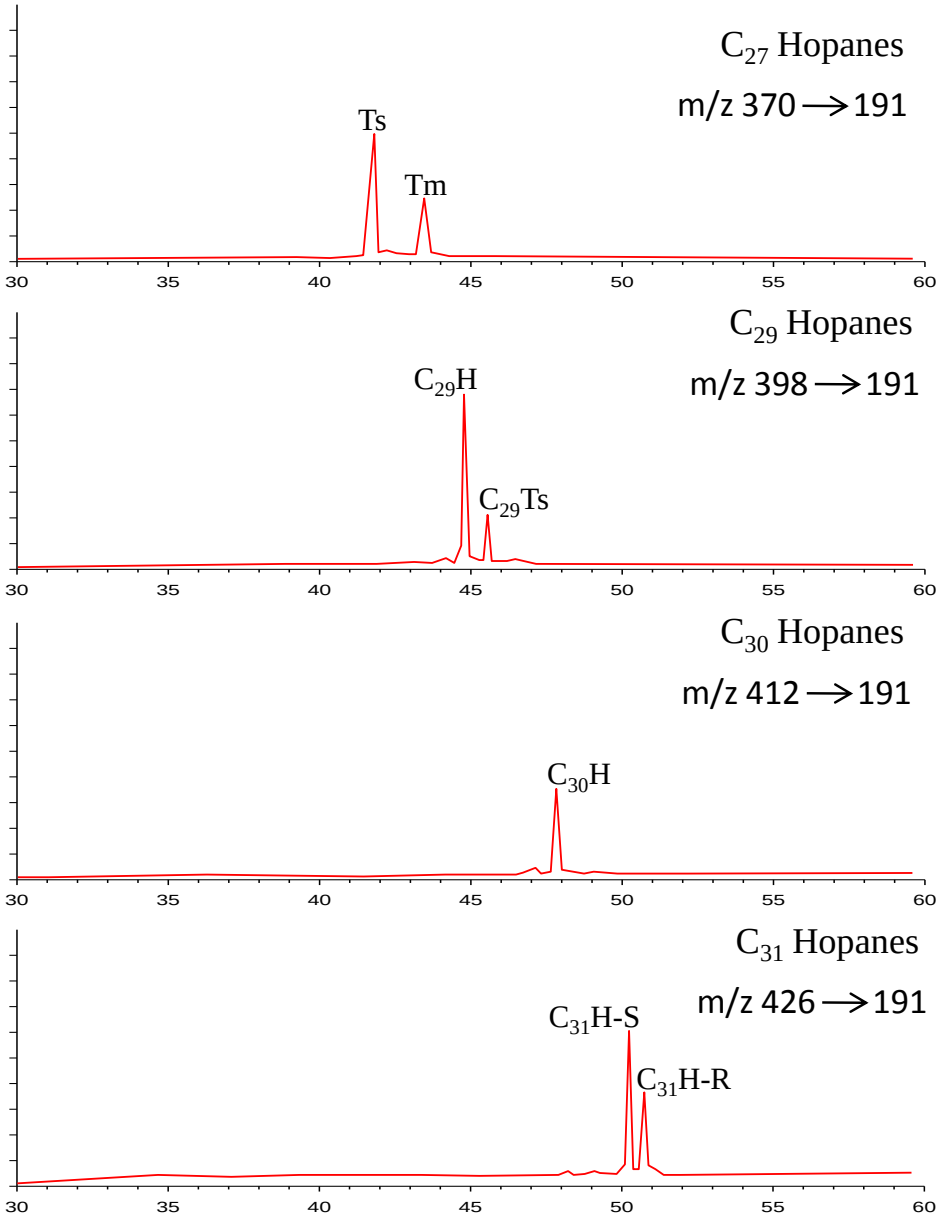

Figure A.4: Chromatograms showing isomers identified of C_{27}, C_{29}, C_{30}, and C_{31} hopanes in a representative sample (A6100). Parent to daughter ion transitions are labeled on each chromatogram. Time in minutes on x-axis and ion count on y-axis. Ts = 18α(H)-22,29,30-Trisnorneohopane, Tm = 17α(H)-22,29,30-Trisnorhopane, C_{29}H = 17α(H),21β(H)-30-Norhopane, C_{29}Ts = 18α(H)-Norneohopane, C_{30}H = 17α(H),21β(H)-Hopane, C_{31}H-S = 17α(H),21β(H)-Homohopane-22S, C_{31}H-R = 17α(H),21β(H)-Homohopane-22R.

Appendix B

Standard Operating Procedures for Biomarker Analysis

The standard operating procedures used to analyze rock samples for biomarkers are listed below and found on the pages indicated.

METHOD FOR EXTRACTING BIOMARKERS FROM ROCK SAMPLES

John Kroon and James W. Castle

1.0 OBJECTIVE

Biomarkers are preserved remnants of molecules originally synthesized by organisms with distinctive chemical structures closely related to the biological precursor molecule (Peters et al., 2005 and Olcott, 2007). Biomarkers can be present in organic matter preserved in sedimentary rocks. The objective of this method is to detail the procedure used to extract biomarkers from rock samples for the subsequent separation and detection of the biomarkers present in the samples using analytical instruments. The sequential extraction procedure for the samples and instrumental analysis of extract for biomarker detection follows the methodology of Brocks et al. (2003), Forster et al. (2004), and Sherman et al. (2007).

2.0 HEALTH AND SAFETY

Proper lab attire, including scrubs, lab coat, gloves, and safety glasses must be worn at all times.

3.0 PERSONNEL/TRAINING/RESPONSIBILITIES

Any graduate research assistant familiar with the equipment and laboratory techniques and trained in this SOP may perform this procedure.

4.0 REQUIRED AND RECOMMENDED MATERIALS

4.1 Reagents

Deionized (DI) water
Dichloromethane (DCM)
37% Hydrochloric acid (HCL)
Methanol (MeOH)
N-pentane
Hexane

4.2 Supplies

Whatman 44 filter paper
Copper (Cu) pellets
Silica gel
Pasteur pipette
Cotton wool
Whole rock samples

4.3 Equipment

Bottle top vacuum filter

Ceramic mortar and pestle
Magnetic stirrer
Drying oven
Ultrasonicator

5.0 PROCEDURE

Grind whole rock samples to a fine powder using a ceramic mortar and pestle. Between samples clean the mortar and pestle with hot tap water and rinse with DI water, then MeOH, and then DCM. Ultrasonicate (Fisher Sonic Dismembrator Model 300) 75 g of powdered sample for 30 min in 40 ml of DCM. Filter to remove powdered sample using a bottle top vacuum filter with Whatman 44 filter paper, collect extract, and repeat ultrasonication of powdered sample with additional 40 ml DCM. Again using bottle top vacuum filter and Whatman 44 filter paper collect extract and combine with the first extract collected. Powdered sample can now be discarded.

Rinse Cu pellets (Fisher Scientific C-430 Copper Metal) with 37% HCL until Cu reaches bright color. Then rinse with DI water, then methanol, then DCM. Add small amount of Cu to vial containing extract and stir 8 h with magnetic stirrer, after stirring filter using a bottle top vacuum filter with Whatman 44 filter paper to remove Cu. Reduce Cu free extract to 1 ml under ultra pure (99.998%) nitrogen gas. Add 50 ml of n-pentane to reduced extract and allow to sit 8 h to precipitate asphaltenes. Filter extract using a bottle top vacuum filter with Whatman 44 filter paper to remove asphaltenes. Collect asphaltene free extract and evaporate to dryness under ultra pure (99.998%) nitrogen gas. Dissolve dried asphaltenes free extract in 1 ml DCM.

Activate silica gel by heating for 8 hours at 110°C. Mix 3 g silica gel with 5 ml hexane to form slurry. Plug Pasteur pipette with cotton wool and fill with slurry. Add extract in 1 ml DCM to top of column. Elute fractions of increasing polarity by sequential elution with 4 ml hexane (saturated fraction) then 2 ml hexane/2 ml DCM (aromatic fraction). Collect the eluated fractions in clean vials, evaporate to dryness, and then dissolve in 1 ml DCM.

6.0 QUALITY CONTROL CHECKS AND ACCEPTANCE CRITERIA

All procedures are subject to review by the Quality Assurance Unit

7.0 REFERENCES

Brocks, J.J., Buick, R., Logan, G., and Summons, R.E., 2003, Composition and syngeneity of molecular fossils from the 2.78 to 2.45 billion-year-old Mount Bruce Supergroup, Pilbara Craton, Western Australia: Geochimica et Cosmochimica Acta, v. 67, p. 4289-4319.

Forster, A., Sturt, H., Meyers, P.A., and the Leg 207 Shipboard Scientific Party, 2004, Molecular biogeochemistry of Cretaceous black shales from the Demerara Rise: Preliminary shipboard results from sites 1257 and 1258, Leg 207: *In* Erbacher, J.,

Mosher, D.C., Malone, M.J., et al., Proceedings of the Ocean Drilling Program, Initial Reports: v. 207, p. 1-22.

Olcott, A.N., 2007, The utility of lipid biomarkers as paleoenvironmental indicators: Palaios, v. 22, p. 111-113.

Peters, K.E., Walters, C.C., Moldowan, J.M., 2005, The Biomarker Guide: Volume 1 Biomarkers and Isotopes in the Environment and Human History: New York, Cambridge University Press.

Sherman, L.S., Waldbauer, J.R., and Summons, R.E., 2007, Improved methods for isolating and validating indigenous biomarkers in Precambrian rocks: Organic Geochemistry, v. 38, p. 1987-2000.

METHOD FOR IDENTIFYING BIOMARKERS IN A ROCK EXTRACT WITH GAS CHROMATOGRPAHY/FLAME IONIZATION DETECTION (GC/FID)

John Kroon and James W. Castle

1.0 OBJECTIVE

Gas chromatography (GC) can be used to separate complex mixtures of biomarkers in solvent extracts from rock samples and a flame ionization detector (FID) can be used to detect those biomarkers. The objective of this method is to detail the procedure used to separate and detect normal (n)-alkanes, pristane, and phytane biomarkers present in rock sample extracts using GC/FID. The instrumental analysis for biomarker detection follows the methodology of Brocks et al. (2003), Forster et al. (2004), and Sherman et al. (2007).

2.0 HEALTH AND SAFETY

Proper lab attire, including scrubs, lab coat, gloves, and safety glasses must be worn at all times.

3.0 PERSONNEL/TRAINING/RESPONSIBILITIES

Any graduate research assistant familiar with the equipment and laboratory techniques and trained in this SOP may perform this procedure.

4.0 REQUIRED AND RECOMMENDED MATERIALS

4.1 Supplies

Autosampler vials and caps

4.2 Equipment

Gas chromatograph equipped with a flame ionization detector and autosampler

5.0 PROCEDURE

Place 1 ml of rock sample extract in autosampler vials. With a Zebron ZB-5 column (30 m x 0.25 mm inner diameter x 0.25 µm film thickness) installed in the GC (Hewlett Packard 5890 Series II), program the oven for a 2 min hold at 40°C and then heat to 310°C at 4°C/min with a final hold time of 15 min. Set the flow rate on the air and hydrogen at 300 ml/min and 30 ml/min respectively. Program the injector for 250 °C and the detector for 310 °C. Inject 1.0 µl of each sample in splitless mode with helium as the carrier gas at a flow rate of 1.0 ml/min. Retention times for compounds interested in can be determined by running standards of those compounds with the same procedure. The amount of n-alkanes, pristane, and phytane can be determined from the integrated chromatogram peak area of each compound.

6.0 QUALITY CONTROL CHECKS AND ACCEPTANCE CRITERIA

All procedures are subject to review by the Quality Assurance Unit

7.0 REFERENCES

Brocks, J.J., Buick, R., Logan, G., and Summons, R.E., 2003, Composition and syngeneity of molecular fossils from the 2.78 to 2.45 billion-year-old Mount Bruce Supergroup, Pilbara Craton, Western Australia: Geochimica et Cosmochimica Acta, v. 67, p. 4289-4319.

Forster, A., Sturt, H., Meyers, P.A., and the Leg 207 Shipboard Scientific Party, 2004, Molecular biogeochemistry of Cretaceous black shales from the Demerara Rise: Preliminary shipboard results from sites 1257 and 1258, Leg 207: *In* Erbacher, J., Mosher, D.C., Malone, M.J., et al., Proceedings of the Ocean Drilling Program, Initial Reports: v. 207, p. 1-22.

Sherman, L.S., Waldbauer, J.R., and Summons, R.E., 2007, Improved methods for isolating and validating indigenous biomarkers in Precambrian rocks: Organic Geochemistry, v. 38, p. 1987-2000.

METHOD FOR IDENTIFYING BIOMARKERS IN A ROCK EXTRACT WITH GAS CHROMATOGRPAHY/MASS SPECTROSCOPY/MASS SPECTROSCOPY (GC/MS/MS)

John Kroon and James W. Castle

1.0 OBJECTIVE

Gas chromatography (GC) can be used to separate complex mixtures of biomarkers in solvent extracts from rock samples and a mass spectrometer (MS) can be used to detect those biomarkers. The objective of this method is to detail the procedure used to separate and detect sterane and hopane biomarkers present in rock sample extracts using GC/MS/MS. The instrumental analysis for biomarker detection follows the methodology of Brocks et al. (2003), Forster et al. (2004), and Sherman et al. (2007).

2.0 HEALTH AND SAFETY

Proper lab attire, including scrubs, lab coat, gloves, and safety glasses must be worn at all times.

3.0 PERSONNEL/TRAINING/RESPONSIBILITIES

Any graduate research assistant familiar with the equipment and laboratory techniques and trained in this SOP may perform this procedure.

4.0 REQUIRED AND RECOMMENDED MATERIALS

4.1 Supplies

Autosampler vials and caps

4.2 Equipment

Gas chromatograph equipped with a mass spectrophotometer and autosampler

5.0 PROCEDURE

Place 1 ml of rock sample extract in autosampler vials. With a Restek Rtx-5 column (30 m x 0.25 mm inner diameter, 0.25 µm film thickness) installed in the GC (Varian Model 4000 GC/MS/MS) program the over for a 2 min hold at 40°C and then heat to 310°C at 4°C/min with a final hold time of 15 min. Set transfer line at 280°C, the mass spectrophotometer (MS) source at 230°C, and electron impact at 70 eV. The MS is set to MS/MS mode so that chosen parent mass fragments are detected in the first MS step and daughter mass fragments are detected in the second MS step. C_{27} to C_{30} steranes are identified with 372, 386, 400, 414 as the parent mass fragments, respectively, and 217 as the daughter mass fragment for each. C_{27} hopanes are identified with 370 as the parent mass fragment and 191 as the daughter mass fragment. C_{29} to C_{31} hopanes are identified with 398, 412, and 426 as the parent mass fragments, respectively, and 191 as the

daughter mass fragment for each. Inject 1.0 µl of each sample in splitless mode with helium as the carrier gas at a flow rate of 1.0 ml/min. Retention times for compounds interested in can be determined by running standards of those compounds with the same procedure. The amount of steranes and hopanes in samples can be determined from the integrated area of the chromatogram peak of each compound.

6.0 QUALITY CONTROL CHECKS AND ACCEPTANCE CRITERIA

All procedures are subject to review by the Quality Assurance Unit

7.0 REFERENCES

Brocks, J.J., Buick, R., Logan, G., and Summons, R.E., 2003, Composition and syngeneity of molecular fossils from the 2.78 to 2.45 billion-year-old Mount Bruce Supergroup, Pilbara Craton, Western Australia: Geochimica et Cosmochimica Acta, v. 67, p. 4289-4319.

Forster, A., Sturt, H., Meyers, P.A., and the Leg 207 Shipboard Scientific Party, 2004, Molecular biogeochemistry of Cretaceous black shales from the Demerara Rise: Preliminary shipboard results from sites 1257 and 1258, Leg 207: *In* Erbacher, J., Mosher, D.C., Malone, M.J., et al., Proceedings of the Ocean Drilling Program, Initial Reports: v. 207, p. 1-22.

Sherman, L.S., Waldbauer, J.R., and Summons, R.E., 2007, Improved methods for isolating and validating indigenous biomarkers in Precambrian rocks: Organic Geochemistry, v. 38, p. 1987-2000.